AD-A093 792 ARMY MILITARY PERSONNEL CENTER ALEXANDRIA VA F/G 17/9
FOURIER TRANSFORMATION THEORY FOR AVERAGED FUNCTIONS, WITH APPL--ETC(U)
FEB 81 R J BONOMETTI

UNCLASSIFIED NL

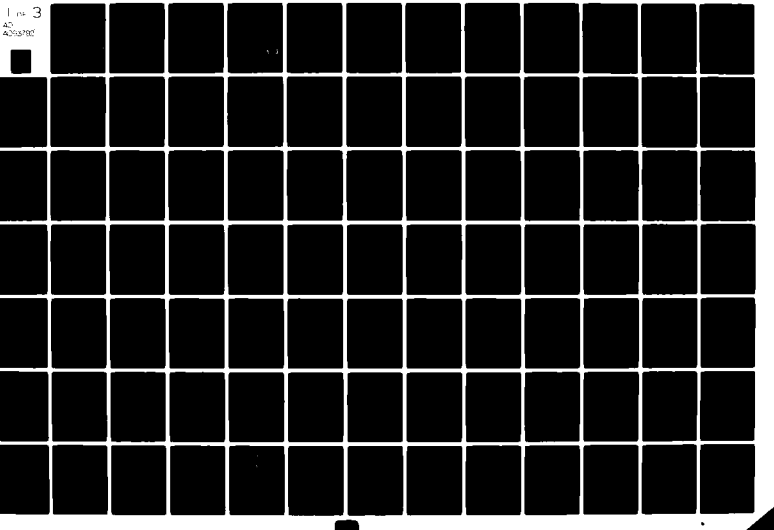

FOURIER TRANSFORMATION THEORY FOR AVERAGED FUNCTIONS, WITH APPLICATION TO VERY LONG BASELINE RADIO INTERFEROMETRY

BY

ROBERT JOHN BONOMETTI

B.S., United States Military Academy
(1975)

SUBMITTED IN PARTIAL FULFILLMENT
OF THE REQUIREMENTS OF THE
DEGREE OF

MASTER OF SCIENCE IN PHYSICS

At the

MASSACHUSETTS INSTITUTE OF TECHNOLOGY

February 1981

Signature of Author Robert J. Bonometti
Department of Physics, December 12, 1980

Certified by
Irwin I. Shapiro, Thesis Supervisor

Accepted by
George F. Koster, Chairman
Physics Graduate Committee

SECURITY CLASSIFICATION OF THIS PAGE *(When Data Entered)*

REPORT DOCUMENTATION PAGE		READ INSTRUCTIONS BEFORE COMPLETING FORM
1. REPORT NUMBER	2. GOVT ACCESSION NO. AD-A092 792	3. RECIPIENT'S CATALOG NUMBER
4. TITLE *(and Subtitle)* Fourier Transformation Theory for Averaged Functions, with Application to Very Long Baseline Radio Interferometry		5. TYPE OF REPORT & PERIOD COVERED Grade: A 5 Dec 1980
		6. PERFORMING ORG. REPORT NUMBER
7. AUTHOR(s) CPT Robert John Bonometti		8. CONTRACT OR GRANT NUMBER(s)
9. PERFORMING ORGANIZATION NAME AND ADDRESS Student, HQDA, MILPERCEN (DAPC-OPP-E) 200 Stovall St. Alexandria, VA 22332		10. PROGRAM ELEMENT, PROJECT, TASK AREA & WORK UNIT NUMBERS
11. CONTROLLING OFFICE NAME AND ADDRESS HQDA, MILPERCEN ATTN: DAPC-OPP-E 200 Stovall St. Alexandria, VA 22332		12. REPORT DATE 5Dec 1980
		13. NUMBER OF PAGES 203
14. MONITORING AGENCY NAME & ADDRESS *(if different from Controlling Office)*		15. SECURITY CLASS. *(of this report)* UNCLAS
		15a. DECLASSIFICATION/DOWNGRADING SCHEDULE

16. DISTRIBUTION STATEMENT *(of this Report)*

Approved for public release;distribution unlimited

17. DISTRIBUTION STATEMENT *(of the abstract entered in Block 20, if different from Report)*

18. SUPPLEMENTARY NOTES

M.S. thesis at M.I.T.

19. KEY WORDS *(Continue on reverse side if necessary and identify by block number)*

VLBI
Fourier Transforms
Averaged functions
Satellite VLBI systems
Image resolution

20. ABSTRACT *(Continue on reverse side if necessary and identify by block number)*

This thesis investigates the effects on brightness function resolution when the visibility function is truncated and averaged. The causes of truncation and averaging (which arise in cases where satellites are incorporated as interferometer elements) are presented, and the basic Fourier transform relation between the visibility and brightness functions is reviewed. The standard Fourier transform method, which is based on a generalization of the Sampling (or Nyquist) theorem and does not account for the effects of truncation and averaging, is presented. The effects of truncation and averaging are illustrated for a

DD FORM 1 JAN 73 1473 EDITION OF 1 NOV 65 IS OBSOLETE

SECURITY CLASSIFICATION OF THIS PAGE *(When Data Entered)*

20. Continued

double Gaussian model source using the standard Fourier inversion method. Theprems concerning the Fourier transformation of a truncated and/or averaged visibility function are then developed, and an algorithm based on this study is developed. This algorithm attempts to enhance resolution by using a derived relationship between an average value of the visibility function and the true source brightness function. The algorithm is applied to several one-dimensional test dases to illustrate its potential.

Fourier Transformation Theory for Averaged Functions, with Application to Very Long Baseline Radio Interferometry

CPT Robert John Bonometti
HQDA,MILPERCEN (DAPC-OPP-E)
200 Stovall St.
Alexandria, VA 22332

Grade: A 5 December 1980

Approved for public release, distribution unlimited

A thesis submitted to the Department of Physics, M.I.T., Cambridge, MA, in partial fulfillment of the requirements of the degree of Master of Science in Physics.

FOURIER TRANSFORMATION THEORY FOR AVERAGED FUNCTIONS, WITH APPLICATION TO VERY LONG BASELINE RADIO INTERFEROMETRY

BY

ROBERT JOHN BONOMETTI

B.S., United States Military Academy
(1975)

SUBMITTED IN PARTIAL FULFILLMENT
OF THE REQUIREMENTS OF THE
DEGREE OF

MASTER OF SCIENCE IN PHYSICS

At the

MASSACHUSETTS INSTITUTE OF TECHNOLOGY

February 1981

Signature of Author Robert J. Bonometti
Department of Physics, December 12, 1980

Certified by _____
Irwin I. Shapiro, Thesis Supervisor

Accepted by _____
George F. Koster, Chairman
Physics Graduate Committee

FOURIER TRANSFORMATION THEORY FOR AVERAGED FUNCTIONS, WITH APPLICATION TO VERY LONG BASELINE RADIO INTERFEROMETRY

by

Robert John Bonometti

Submitted to the Department of Physics on December 12, 1980 in partial fulfillment of the requirements for the Degree of Master of Science in Physics.

ABSTRACT

The resolution of a two-element interferometer increases in proportion to the element separation distance, so that incorporation of interferometer elements on satellites will enable very long baseline interferometry (VLBI) arrays to achieve greater resolution of celestial sources than has been possible using elements on the earth. The interferometric response is the visibility function, which is the Fourier transform of the source's brightness distribution function. Since a satellite typically moves faster in its orbit than does a point on the rotating earth, and since the integration time period for cross-correlating the received signals will generally be larger for a system which includes satellites, the interferometric response will actually be an averaged visibility function as opposed to a point-wise sampled visibility function. Since the baseline magnitude is finite, the visibility function is not known throughout its domain and is therefore effectively truncated. Truncating and averaging the visibility function adversely affects the brightness function resolution, and understanding these effects is therefore necessary to more fully realize the source resolution capabilities of an interferometer incorporating elements on satellites.

This thesis investigates the effects on brightness function resolution when the visibility function is truncated and averaged. The causes of truncation and averaging are presented, and the basic Fourier transform relation between the visibility and brightness functions is reviewed. Basic properties of the two-dimensional Fourier transform are reviewed, and the standard Fourier inversion method is presented. This method is based on a generalization of the Sampling Theorem and does not account for truncation or averaging effects. The effects of truncation and averaging are illustrated for a double Gaussian model source using the standard Fourier inversion method. Theorems concerning the Fourier transformation of a truncated and/or averaged function are then developed,

and an algorithm based on this study is presented. This algorithm attempts to enhance resolution by using a derived relationship between an average value of the visibility function and the true source brightness function. The algorithm is applied to several one-dimensional test cases to illustrate its potential.

Thesis Supervisor: IRWIN I. SHAPIRO

Title: Professor of Physics

ACKNOWLEDGEMENTS

I would like to thank the faculty, staff and my fellow students at M.I.T. for a very challenging , but ultimately enjoyable and memorable experience as part of the M.I.T. Community. To cite the many kind and helpful people whom I have studied under and worked with is far beyond the space available here, and I therefore offer a collective statement of sincere gratitude to these members of this vibrant international microcosm.

Specifically, I would like to express my sincere gratitude to Professor Irwin I. Shapiro for proposing the research work undertaken in this thesis, for his guidance and supervision during its conduct, and for his helpful critique of the major portions of the final manuscript. It has indeed been an honor and a privilege to have worked for Professor Shapiro.

I would like to thank my office mates, Javad Heshmati and Martin Weinberg for their friendship and for their help with the computer work, and I thank Emilio Falco for his generous assistance with the computer graphics.

I wish to thank Terry Crossley for her perennial good cheer and for the excellent typing of this thesis.

I would also like to take this opportunity to thank my parents for an upbringing based on love and sound values which has led me to admire and respect mankind's scientific heritage and to

endeavor to contribute to it.

Finally, but most importantly, I wish to thank my wife Janice for the love and constant support which has enabled me to persevere under the rigorous demands of this great institution.

TABLE OF CONTENTS

TABLE OF CONTENTS (cont'd.)

CHAPTER I

INTRODUCTION

1.1 Problem Statement and Purpose of This Study

1.1.1: The Role of VLBI

Interferometric techniques in the radio region of the electromagnetic spectrum have been developed to the present state at which this technology provides the most accurate means of determining positional and structural information on extragalactic objects that are emitters in this part of the spectrum. An interferometer is an instrument consisting of two or more receiving terminals (or "elements") which compares signals received at each element from a common source in order to obtain information on the nature and position of the source. As will be shown later, the resolution of an interferometer exceeds that possible with a single element, and the maximum resolution is directly proportional to the greatest separation distance between elements. Present technology has enabled systems with element separations on the order of intercontinental distances to be used, resulting in angular resolutions on the order of milliarcseconds. These systems, in which the widely-separated elements are not in communication with one another during the actual conduct of an experiment, are known as Very Long Baseline Interferometry (VLBI) systems.

The importance and utility of VLBI as a research tool is

immediately realized by a consideration of the diverse applications which it serves. Highly accurate source position measurements and capabilities for high resolution of source structure are of great value in astrometry and astrophysics. Enhanced knowledge of the kinematics of celestial bodies and of diffuse objects, such as HI and HII regions and molecular clouds, can be used for refined testing of dynamical theories and to achieve greater understanding of astrophysical processes and source parameters (mass, angular momentum, etc.). Examples of some applications of VLBI along these lines include resolution of close but discrete water-vapor masers in our own galaxy, accurate positional determinations for ALSEP transmitters on the moon yielding information on lunar kinematics, and tests of general relativity by measuring changes in relative quasar positions by deflection of radio waves in the sun's gravitational field [Shapiro (1976)]. Additionally, VLBI may become an important tool in accurate spacecraft tracking [Addleman (1978), Treinish (1978)].

VLBI can also be applied to geodesy and to studies of dynamics of the earth's crust [Counselman (1976), Whitney (1974)]. Shapiro and Knight (1970) enumerate and discuss the geophysical applications of VLBI and indicate the attainable levels of accuracy for determinations of various geophysical parameters.

If a point source is observed with a two-element interferometer, accurate determination of the source position is predicated on

accurate knowledge of the baseline vector, which is the vector between the two elements. We can therefore see that accurate knowledge of a point source's location can in turn be used to provide information on the baseline vector. In actual practice, by using one or more different baselines and observing a number of different sources, both source positions and baseline lengths may be treated as unknowns and solved for by using the interferometry data. (See Whitney 74 for more details on this method.) In this way, distances between points on the earth's surface will be ascertained to the centimeter level of accuracy, and hence provide geodetic information and insight into associated dynamical processes.

We have illustrated the importance of VLBI as a research instrument, and seen the order-of-magnitude resolution capable with present baseline lengths. Given that interferometer resolution improves with increasing baseline length, a natural improvement on existing systems would be to incorporate elements on satellites thereby greatly increasing baseline length and enhancing resolving power. However, there are some disadvantages incurred when a satellite is used as an interferometer element. In this thesis, we shall be concerned with one aspect of these inherent problems.

1.1.2 Purpose and Scope

The purpose and scope of this thesis will be an examination of the adverse effects of truncating and averaging a function on the

resolution of its conjugate Fourier transform. We will examine these effects, and then develop theorems which relate the truncated, and/or averaged function to its exact Fourier transform. We will then develop an algorithm based on these theorems which attempts to achieve at least partial compensation for the effects of truncating and averaging V(u,v) and possibly giving a better approximation to the true brightness distribution function than does the standard Fourier inversion method.

1.1.3 Adverse Effects on Resolution

Antenna gain is proportional to the physical aperture of an antenna. [Kraus (1966)] Since the radio signals from celestial sources are generally quite weak, large physical apertures are normally employed in the radio telescope antennas which serve as elements in an interferometer array. To yield intelligible information from a celestial signal, the signal must not be less than the fluctuations of the noise which is present. The noise results not only from instrumental sources which may be reduced, but also from fundamental causes such as background noise in the sky and quantum-statistical limitations which cannot be circumvented. A large physical aperture providing high antenna gain is therefore an important factor in achieving an acceptable ratio of signal to rms noise (signal to noise ratio, or SNR) for the system. The SNR is enhanced when the received signals are integrated during the process of cross correlation. Increasing the integration time period

by a factor of N results in enhancing the SNR by the factor $\sqrt{N}$. [Kraus (1966)].

We have seen that antenna size and integration time are two primary parameters affecting the SNR. For an earth-based interferometer, the physical aperture may usually be constructed adequately large to keep the required integration time period relatively small while maintaining adequate SNR's. The integration time period here is considered small relative to the time required for the projection of the baseline vector $\vec{b}$ normal to the source vector $\hat{s}_o$ (a unit vector towards the source, which will here be considered infinitely distant) to change by an appreciable amount. (We shall presently clarify the term "appreciable".) The maximum interferometer resolution occurs when the source vector is perpendicular to the baseline vector and is directly proportional to baseline length $|\vec{b}|$; however, the resolution for a typical case in which the source vector is not perpendicular to the baseline vector depends upon the projection of $\vec{b}$ normal to $\hat{s}_o$. What we have heretofore ignored is the fact that $\vec{b}$ and $\hat{s}_o$ are in relative motion due to the earth's rotation (other motions such as the earth's orbital motion, the motion of the solar system barycenter, etc., can be ignored for the infinitely distant source which we are idealistically considering here). Therefore, the resolution of the interferometer is really a time-dependent function.

The brightness distribution function, B(x,y), characterizing

a source can be conceived as the function which specifies the radiation intensity distribution as a function of positional coordinates x and y on the plane of the sky. (In general, B(x,y) is a frequency dependent function; however, we will consider it to be independent of frequency in this thesis.) Since B(x,y) is an intensity, it is constant along a ray path in free space and hence the brightness function measured at the earth is identical to the brightness function at the surface of the source, and for this reason the brightness function provides important information on the physical parameters characterizing the source. As we will show later, the interferometer response is a function V, known as the visibility function, which is the fourier transform of the brightness distribution function. The visibility is a function of the interferometric resolution, and we shall see that the arguments of V are in fact two orthogonal resolution components, designated u and v. As mentioned above, the interferometric resolution is time dependent; hence, u and v are time dependent parameters. The domain of the visibility function is the u-v plane, in which u and v serve as orthogonal coordinates. As the baseline vector $\vec{b}$ moves relative to the source vector $\hat{s}_o$, we know that the interferometric resolution varies, and hence we must be moving along a path in the u-v plane. We will see that these paths are generally ellipses in the u-v plane. As $\vec{b}$ moves relative to $\hat{s}_o$, the interferometer is measuring the visibility function V[u(t), v(t)] (implicitly a function of time t) by recording values of V along the track in the u-v plane which is given by the locus of points [u(t), v(t)].

We can now see why it was important to have integration times relatively short compared to the time required for $|\vec{b}x\hat{s}_0|$ to vary appreciably. In the limit of zero integration time, the interferometer measures V(u,v) along the relevant track in the u-v plane. However, when we integrate, the interferometer records the average value of V(u,v) over that segment of the track which is traversed during the integration time period t_0. Because B(x,y) is the Fourier transform of V(u,v), it is immediately discernible that the brightness distribution function is distorted when observations with $t_0 \neq 0$ are made. If t_0 is non-zero but small, then the segment traversed in time t_0 is small and we are almost measuring V(u,v), since

$$V\left[u\left(\frac{t_0}{2}\right), v\left(\frac{t_0}{2}\right)\right] \approx \frac{1}{t_0}\int_{u(0),v(0)}^{u(t_0),v(t_0)} du\, dv\, V(u,v)$$

This case generally applies to earth-based VLBI systems, and averaging effects have previously been ignored. Fomalont (1973) states the criterion for short averaging intervals as being those cases in which $|\vec{b}x\hat{s}_0|$ changes by an amount less than the antenna radius during the integration time period. However, a satellite in a typical orbit about the earth moves roughly ten times faster than a point on the surface of the earth, and therefore $|\vec{b}x\hat{s}_0|$ undergoes a greater change in the time period than it would for an earth-based VLBI system.

Although there is no physical limitation on the aperture

size for a satellite element, practical limitations will require that the antenna aperture sizes be considerably smaller (at least for initial experiments) than earth-based elements. Consequently, we realize that integration times will have to be correspondingly increased to achieve an acceptable SNR, which has the adverse effect of making the averaging considerations for V(u,v) discussed above a more significant problem.

To get an order-of-magnitude "feel" for the impact of this effect, let us suppose that, all other factors being equal, the satellite's aperture is 1% of that of a typical earth-based antenna. The interferometer's aperture is the geometric mean of the two individual antenna apertures, or $\sqrt{A(.01A)} = .1\ A$, where A is the area of the antenna on the earth. The signal gain from the interferometer therefore decreases by a factor of 10. The interferometer system sensitivity is (ideally) related to the integration time t_o by [Kraus (1966)]

$$\text{sensitivity} \propto \sqrt{t_o} \ .$$

If t_e is the integration time period for an earth-based VLBI system and t_s the corresponding period for our satellite system, then to increase the sensitivity by a factor of 10 to compensate for the decreased antenna gain implies $t_s = 100 t_e$. In practice, one would not approach the sensitivity limit of the interferometer because the corresponding integration time period could well be of the order of an orbital period for the satellite. Thus, only relatively strong

sources would be chosen for observation.

Another problem which we have not yet addressed concerns itself with the fact that practical limitations prevent the measurement of V(u,v) throughtout the entire u-v plane. This problem is independent of the averaging problem and is present in earth-based systems also. Now, from the basic uncertainty relation for conjugate functions B(x) and V(u) in a one dimensional Fourier transform pair, we know that as we decrease the domain of the function B(x), the corresponding domain of the transform function V(u) necessarily increases. The implication here is that as we probe into smaller regions of the x-y plane, i.e., as we examine smaller sources (or extended sources in greater detail) by using our satellite VLBI system with large $|\vec{b}|$, then the associated visibility function V(u,v) "spreads-out" in the u-v plane. Limitations on the extend of the u-v plane examined during the VLBI experiment then present more acute problems, because we are now truncating V(u,v)into a restricted domain which is significantly less than its true domain of definition. To see this more tangibly, we need only consider that a point source has a Fourier transform of infinite extent, and hence any truncation of V(u,v) due to practical limitations will distort the brightness function deduced from the measured V(u,v). This is equivalent to saying that infinite resolution is required to resolve a point source.

Since all celestial sources are of a finite, "region-limited" extent in the plane of the sky, a generalization of the

sampling (or Nyquist) theorem to two dimensions is beneficial to consider. We will later see that this theorem allows us to merely sample V(u,v) at distinct points in a 2-D lattice extending throughout the u-v plane, and nevertheless reproduce B(x,y) exactly. The Sampling Theorem is the basis for the technique of aperture synthesis, whereby it is possible to synthetically produce information equivalent to that obtainable from an aperture of very large extent by using smaller physical antennas. Essentially, the concept here is that if the small antennas are located at properly spaced points on a 2-D lattice, then their correllated information is equivalent to one hugh antenna whose physical aperture would be the same as the area encompassed by the 2-D lattice of antennas. In fact, it is sufficient to successively move a few antennas throughout the lattice and subsequently combine individual recorded results at a later time to produce the aperture synthesis result (if the signal from the source is not time dependent). Earth-rotation aperture synthesis uses array elements at fixed points on the earth, so that the earth's rotation causes the array elements to move in some fashion with respect to the source. If some of the properly spaced lattice points are not occupied by an array element during the observation period, an approximation to the brightness function can be obtained from the data obtained along the tracks in the u-v plane generated by the element pairs. Interferometer arrays having enough elements to provide good coverage of the u-v plane can therefore be used to obtain reasonable approximations to the brightness function. If an

array includes elements on satellites, then the averaging problems discussed above must be considered. However, the sampling theorem alone cannot fully compensate for the effects of averaging and truncation (which in realistic experiments means not only restricting the extent of the u-v plane examined, but also restricting measurements of V(u,v) to tracks in the u-v plane which do not for a simple 2-D lattice).

1.2 Thesis Outline

In Chapter 2, a sample calculation for a track in the u-v plane for a two-element, earth-satellite interferometer will be presented. Basic VLBI concepts for a two element interferometer will be reviewed. Basic Fourier transform theorems in 2-D will be reviewed, and some examples of exact transforms given. Truncation effects are discussed and summarized by a theorem. The representation of an averaged function is considered, and the standard Fourier transform for averaged functions is presented. We then examine the sampling theorem and its relevance to the 2-D visibility-brightness function pair. Aliasing effects and the effects of the epoch of sampling intervals are considered. In Chapter 3, we apply the standard transform method to a typical model of a truncated and averaged visibility function. In Chapter 4, we derive theorems for truncation and averaging effects and develop a matrix algorithm for the implementation of the basic theorem for these effects. The matrix algorithm is applied in Chapter 5 to several one-dimensional test cases, and these results are compared with the results obtained

from the standard Fourier inversion method applied to the same data sets of average values of the visibility function. Chapter 6 presents a summary and the conclusions of the study. A definite conclusion as to whether the standard Fourier inversion method or the matrix algorithm is the better technique to obtain the highest resolution from a given set of data requires further analysis than has been possible to perform here. Therefore, the conclusions presented here concerning the comparison between the two techniques should be considered preliminary conclusions, subject to more extensive investigation.

CHAPTER 2

BACKGROUND AND PRELIMINARY CONCEPTS

In this chapter, we will present a brief background discussion on VLBI which includes a derivation for the baseline vector of an earth-station satellite-station two element interferometer. We then consider the two dimensional Fourier transform and prove some fundamental theorems relevant to our work here. The standard Fourier transform method for an averaged function is presented. The Sampling Theorem is derived for the two-dimensional case and its implications are discussed.

2.1 Baseline Vector for the Earth-Satellite Two-Element Interferometer

The baseline vector for the earth-satellite interferometer will be taken as the vector from the earth station to the satellite station. We calculate the position vector as a function of time for each station separately, and take their vector difference to obtain the baseline vector.

We choose a rectangular frame of reference based on the standard equatorial coordinate system. The origin of coordinates is at the center of the earth with the z axis along the spin axis of the earth, the x axis in the direction of the true vernal equinox of date, and the y axis completing a right-handed triad. We will consider this earth-centered system as being inertial over the time periods of interest to us.

Let the earth station have latitude ϕ_E and longitude ψ_E and have a radial distance from the center of the earth of r_E. Define the vector $\hat{G}$ as a unit vector along the line connecting the center of the earth to the point where the Greenwich meridian intersects the x-y plane. Let g_o be the angle between $\hat{G}$ and $\hat{x}$ at the time t=0. From Figure 2.1, it is easy to see that the position vector $\vec{R}_E(t)$ for the earth station at time t is given by

$$\vec{R}_E(t) = \hat{i}\,|r_E \cos\phi_E|\cos(\omega t+g_o+\psi_E) + \hat{j}\,|r_E \cos\phi_E|\cos(\omega t+g_o+\psi_E) + \hat{k}\; r_E \sin\phi_E$$

where ω is the angular velocity of the earth.

We consider the position vector for the satellite. Viewed simplistically (i.e., neglecting effects of perturbing bodies, non-sphericity of the earth, tidal effects, effects of general relativity, etc.) the satellite travels about the earth in a plane Keplerian orbit. Define a primed coordinate system with origin at the center of the earth and with z' normal to the plane of the orbit, x' along the line from the center of the earth to perogee, and y' completing a right-handed triad. (See Figure 2.2.) Let the direction cosines of the primed axes in the unprimed system be $(\alpha_{x',x}, \beta_{x',y}, \gamma_{x',z})$, $(\alpha_{y',x}, \beta_{y',y}, \gamma_{y',z})$, and $(\alpha_{z'x}, \beta_{z',y}, \gamma_{z',z})$ for x', y', and z', respectively. Given an initial position and an initial velocity for the satellite at time t=0, one may compute the position vector $\vec{R}'_S(t)$ for the satellite at any time to. (This is a standard well-documented problem in astro-

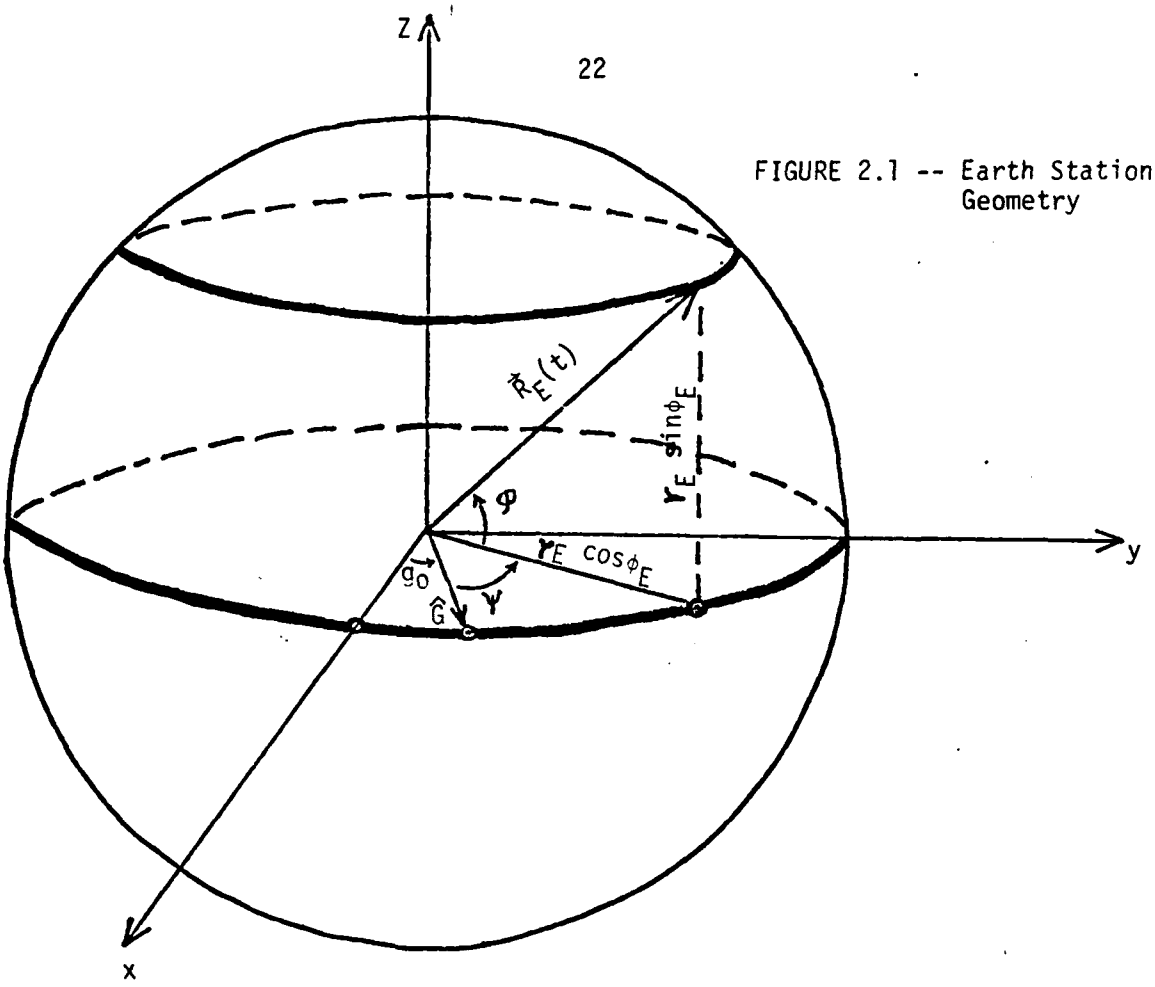

FIGURE 2.1 -- Earth Station Geometry

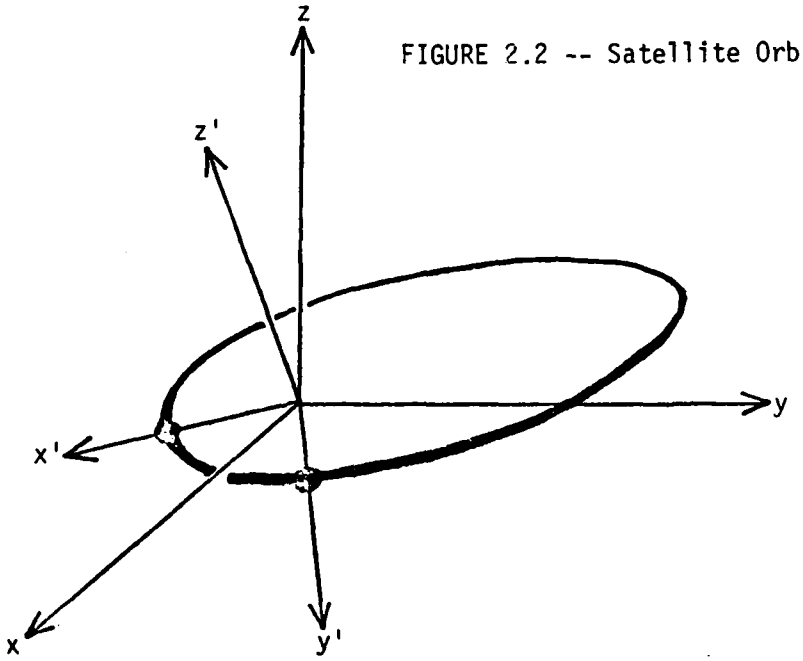

FIGURE 2.2 -- Satellite Orbit Plane

dynamics and we will not present the full general solution here. The Fortran algorithm which was used to solve for $\vec{R}'_S(t)$ on the computer was based on a similar algorithm written by T. Herring.) The conversion of $\vec{R}'_S(t)$ to our unprimed system is given by

$$\vec{R}_S(t) = \hat{i}\left(R_{x'}\alpha_{x',x} + R_{y'}\alpha_{y',x} + R_{z'}\alpha_{z',x}\right)$$

$$+ \hat{j}\left(R_{x'}\beta_{x',x} + R_{y'}\beta_{y',y} + R_{z'}\beta_{z',y}\right) + \hat{k}\left(R_{x'}\gamma_{x',z} + R_{y'}\gamma_{y',z} + R_{z'}\gamma_{z',z}\right)$$

where $\vec{R}'_S(t) \equiv [R_{x'}, R_{y'}, R_{z'}]$.

The baseline vector as a function of time is then given by

$$\vec{b}(t) = \vec{R}_S(t) - \vec{R}_E(t)$$

2.2 Basic VLBI Concepts

A detailed description and analysis of a VLBI system would involve a far more extensive study than is possible here and, in any event, there are extensive references in the literature discussing the intricacies of VLBI. We, therefore, present a simplified view of VLBI which will be sufficient as background and motivation for the specific problem studied in this thesis.

The two element interferometer, which is the building block for multi-element arrays, consists of two receiving antennas and equipment to process and correlate their received signals. If a real-time link such as a cable is used to connect the two elements, then real-time data analysis is possible and, more significantly, if the electrical path lengths are properly set then the relative phase information for the received signals is directly input to the correlator. In VLBI, a real-time link between elements is usually not possible due to the very large baseline distance. Therefore, real-time data analysis is not carried out, and instead the data are recorded for later processing. To preserve the relative phase information, which is essential for correlation, to an acceptable level of accuracy commensurate with the desired level of accuracy expected for the parameters of interest now requires highly accurate timekeeping during the conduct of the independent observations. The advent of hydrogen maser frequency standards provided the time-keeping accuracy required to enable VLBI to exceed the accuracy levels attainable by connected element interferometry [Whitney (1974)]. With accurate time-keeping at each element, the received signals can be recorded on magnetic tape for later processing. In fact, when the data are correlated, it is possible to ascertain the error in original clock synchronization between the two elements and thereby provide a technique for unprecedented accuracy (to about .1 nanosecond) in clock synchronization over intercontinental distances [Shapiro and Knight (1970)]. The actual reduction and processing of data from a VLBI experiment is an extensive subject

in itself and cannot be discussed here. There are several different algorithmic approaches to the problem of data analysis, and ample references may be found in the literature [see, for instance, Whitney (1974), and Moran (1976)].

The basic geometry for a two-element interferometer is illustrated in Figure 2.3. We assume an infinitely distant point source so that plane waves are received by the interferometer elements, which therefore point in the same direction at angle ϕ with respect to the baseline vector $\vec{b}$ (i.e., we neglect parallax effects which would have to be accounted for if the source were sufficiently close to the interferometer to cause different antenna orientations). The baseline vector $\vec{b}$ points from the reference station to the remote station, where the reference station receives any given wavefront earlier than the remote station by a time factor known as the group delay $\tau_g = \frac{1}{c}\vec{b}\cdot\hat{s}_o$. The projection of the baseline normal to the source is just $|b x \hat{s}_o|$, and will be seen to be related to the interferometric resolution.

Our aim at this stage is to demonstrate that the response of the interferometer is the visibility function, which is the Fourier transform of the source brightness distribution function. A detailed derivation requires the application of coherence theory to the two element interferometer [see, for instance, Swenson and Mathur (1968)]. However, a less sophisticated development will suffice for our purposes here. We will base our discussion on the treatments presented by Moran (1976), Fomalont (1973), and

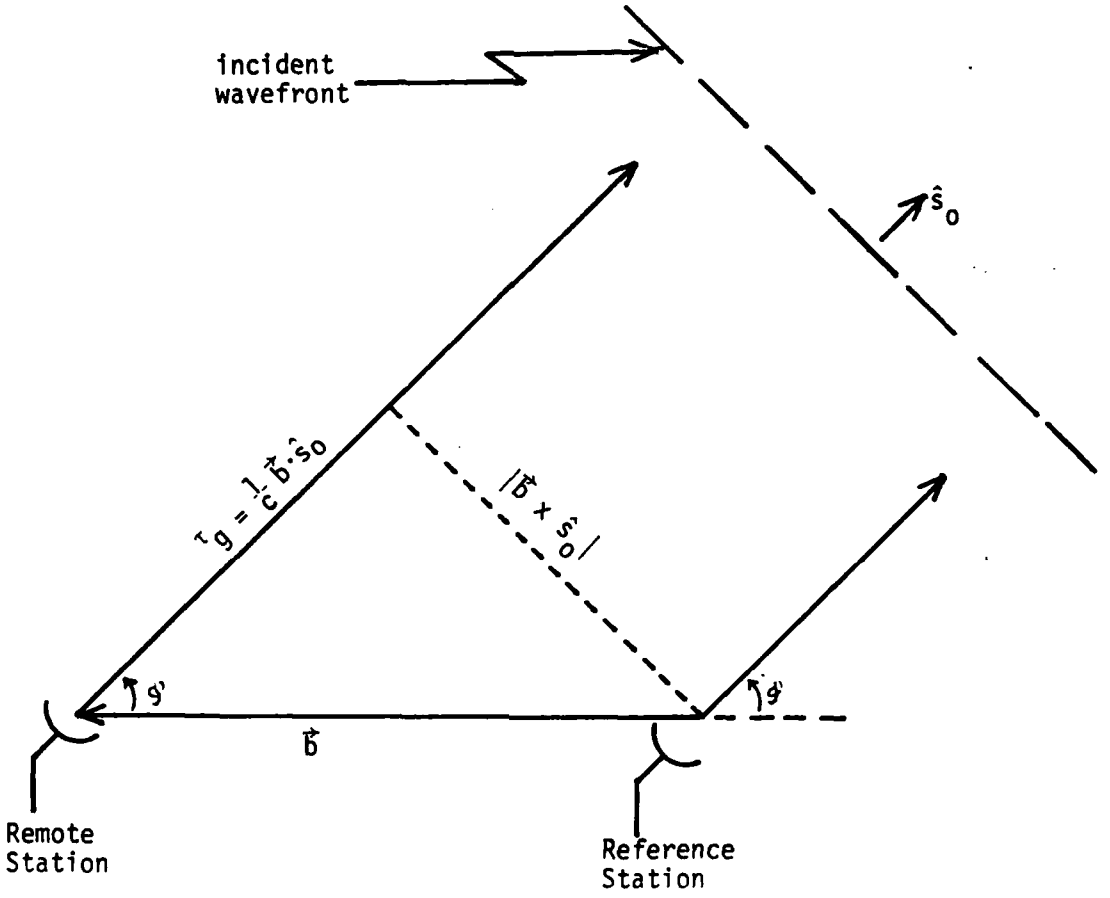

FIGURE 2.3 -- Basic Interferometer Geometry

Whitney (1974). Partial coherence theory establishes that all characteristics of a source's radiation power idstribution (i.e., angular distribution, frequency distribution, and polarization) are related to spatial, temporal, and polarization cross correlations of the received signals at the two interferometer elements. We will primarily deal only with the spatial correlation aspects here, which assumes monochromatic plane polarized radiation from our infinitely distant point source.

Let the point source emit a sinusoidal signal at frequency ν_0 with intensity B_0. Denoting e_1 and e_2 as the received voltages at the reference and remote stations, respectively, we have, using complex phasor notation,

$$e_1(t) = \sqrt{B_0}\ e^{i2\pi\nu_0 t}$$

$$e_2(t) = \sqrt{B_0}\ e^{i2\pi\nu_0(t-\tau_g)}$$

The interferometer correlates these two received voltages. [See Rogers (1976) and Kraus (1966) for discussions of various techniques of detection and concomitant correlation method. We will assume a simple phase-switched, or multiplying, interferometer.]

The cross correlation of two real complex functions in the interval $[0,t_0]$ is defined by [Bracewell (1978)]:

$$R(x) \equiv \int_0^{t_0} du\, g(u-x)\, h(u)$$

For our interferometer, then, the cross-correlation function for the signals received in the time period $[0,t_0]$ is

$$R(\tau_g) = \frac{1}{t_0}\int_0^{t_0} e_1(t)\, e_2^*(t-\tau_g)\, dt = B_0\, e^{i2\pi\nu_0\tau_g}$$

where superscript "*" denotes complex conjugation. The time period t_0 is referred to as the integration time period. $R(\tau_g)$ is the response of the interferometer for the point source. Now,

$$\tau_g = \frac{1}{c}\vec{b}\cdot\hat{s}_0 = \frac{1}{\lambda\nu_0}\, b\cos\varphi(t)$$

where we have made the angle ϕ between $\vec{b}$ and $\hat{s}_0$ a time dependent parameter because the relative orientations of $\vec{b}$ and $\hat{s}_0$ are changing as a result of the earth's rotation (and satellite motion for a satellite element in the two element interferometer). We can then write

$$R(\varphi) = B_0\; e^{i2\pi\frac{b}{\lambda}\cos\varphi(t)}$$

We see that $R(\phi)$ is an oscillatory quantity with a mean of zero, amplitude of B_0, and time-varying phase factor of $2\pi\frac{b}{\lambda}\cos\phi(t)$. An alternative description for the slow oscillations in $R(\phi)$ derives the cross-correlation function in terms of beating between the two signal frequencies from the two elements, whose difference (in general from ν_0 and from each other) arises from the differential Doppler shift in the received frequencies due to the relative motion of the elements with respect to the source. [See Rogers (1976) for this approach.]

In terms of ϕ, we may think of $R(\phi)$ as a spatial correlation function. The spatial correlation of the incident radiation field is determined by the correlation of the signals from the two elements located at different points in space, and we see from Figure 2.3 and from the expression for $R(\phi)$ that the two signal phases will be mutually reinforcing (or partially reinforcing) or cancelling depending upon the magnitude of $\tau_g = \frac{b}{c}\cos\phi$, i.e., depending upon the difference in phase path length for each wavefront reaching the two elements. (We have tacitly assumed the limit $T \to 0$ here so that the spatial correlation is performed point-wise in space as opposed to averaging over segments of space for non-zero integration time periods.) This phenomenon is directly analogous to the fringe patterns of optical interferometry, and $R(\phi)$ is known as the fringe pattern.

The phase factor $2\frac{b}{\lambda}\cos\phi$ in $R(\phi)$ is known as the fringe phase $\phi(t)$. $R(\phi)$ assumes its maximum value B_o when $\frac{b}{\lambda}\cos\phi$ is equal to an integer. The interval between successive maxima in $R(\phi)$ denoted $\Delta\phi$, is known as the fringe spacing. Let ϕ_1 and ϕ_2 be two values of $\phi(t)$ which produce adjacent maxima in $R(\phi)$. Then

$$2\pi\frac{b}{\lambda}\cos\phi_2 - 2\pi\frac{b}{\lambda}\cos\phi_1 = 2\pi(n+1) - 2\pi n = 2\pi$$

$$\frac{b}{\lambda}\left(\cos\phi_2 - \cos\phi_1\right) = \frac{b}{\lambda}\left(-2\sin\frac{\phi_2+\phi_1}{2}\sin\frac{\phi_2-\phi_1}{2}\right) = 1$$

Assuming that $\phi_2 \approx \phi_1$, we write $\frac{\phi_2+\phi_1}{2} \equiv \phi \approx \phi_1 \approx \phi_2$ and $\sin\frac{\phi_2-\phi_1}{2} \approx \frac{\phi_2-\phi_1}{2} \equiv \frac{\Delta\phi}{2}$. Then, $-2\frac{b}{\lambda}\frac{\Delta\phi}{2}\sin\phi = 1$, which gives the magnitude of the fringe spacing as $\Delta\phi = \frac{\lambda}{b\sin\phi}$ But, $b_{\sin\phi} = |\vec{b}\times\hat{s}_o|$

which is the component of $\vec{b}$ normal to the souce vector $\hat{s}_0$. We therefore see that the fringephase provides information about the source location $\hat{s}_0$.

Having obtained some understanding of an idealistic interferometer response for an infinitely distance point source emitting monochromatic radiation, we now want to look at the more realistic case where an extended source with centroid approximately at $\hat{s}_0$ is observed in the bandwidth $\Delta\nu$ centered on ν_0 by an interferometer with frequency characteristic $F(\nu)$ and primary power pattern $G(\hat{s}-\hat{s}_0)$ (defined as the product of the two elements' voltage patterns). Heretofore, we had assumed $G(\hat{s}-\hat{s}_0)=\delta(\hat{s}-\hat{s}_0)$ and $F(\nu)=\delta(\nu-\nu_0)$.

First, we note that if Θ_s is the maximum angular source extent, then we must have

$$\Delta\Phi \equiv \frac{\lambda}{b \sin\phi} > \Theta_s$$

since a source larger than the fringe spaceing will have simultaneous reinforcements and cancellations from its various parts and therefore the meaningful fringe pattern is lost. The amplitude of the fringes for an extended source will, in general, be different from the amplitude for a point source of the same strength, and the ratio of these amplitudes is known as the fringeamplitude.

The reason for a specified reference direction $\hat{s}_0$ for an extended source is seen in the following analysis. For observation

of a point source over bandwidth $\Delta\nu$ [but assuming an infinitely narrow beam for the primary power pattern, $G(\hat{s}-\hat{s}_0) = \delta(\hat{s}-\hat{s}_0)$] we have

$$R(\varphi) = \frac{1}{\Delta\nu}\int_{\nu_0-\frac{\Delta\nu}{2}}^{\nu_0+\frac{\Delta\nu}{2}} d\nu\, R(\varphi,\nu) = \frac{B_0}{\Delta\nu}\int_{\nu_0-\frac{\Delta\nu}{2}}^{\nu_0+\frac{\Delta\nu}{2}} d\nu\, e^{i2\pi\frac{b\nu}{c}\cos\varphi}$$

$$= B_0\,\frac{\sin\left(\pi\frac{b}{c}\Delta\nu\cos\varphi\right)}{\pi\frac{b}{c}\Delta\nu\cos\varphi}\, e^{i2\pi\frac{b}{c}\nu_0\cos\varphi}$$

where we have assumed a flat frequency response

$$F(\nu) = \begin{cases} 1 & \nu \in [(\nu_0-\Delta\nu)/2,\ (\nu_0+\Delta\nu)/2] \\ 0 & \text{OTHERWISE} \end{cases}$$

and included $\frac{1}{\Delta\nu}$ as a normalization factor to compare this result with the monochromatic result above. We see that this result is identical with the monochromatic result except for the factor

$$\frac{\sin\xi}{\xi}\ ,\quad \xi \equiv \pi\frac{b}{c}\Delta\nu\cos\varphi = \pi\Delta\nu\tau_g$$

which is a tapering factor which reduces the fringe pattern amplitude. This presents the conflicting goals of using $\tau_g \ll \frac{1}{\Delta\nu}$ (i.e., the signal correlation time $\frac{1}{\Delta\nu}$ must be much greater than the group delay time) in order that the fringe amplitude be sufficiently large, and the other goal of using as large a bandwidth as possible to be able to detect weak sources or source components without excessively long integration times (since sensitivity α $\frac{1}{\sqrt{\Delta\nu\ t_0}}$). We can achieve both of these goals if we can keep τ_g very small. To do this, we define a reference direction $\hat{s}_0$ to be roughly in the

direction of the point source or the direction of the centroid of an extended source. A delay factor is then incorporated into the reference station arm of the interferometer by using, say an extra length of cable, such that $\tau_g=0$ when the interferometer elements are pointed in the direction $\hat{s}_o$. Then, τ_g will be small for all $\hat{s}$ near $\hat{s}_o$, which is usually the case for observed celestial sources. In VLBI, this delay factor can be introduced by an appropriate delay synchronization between the magnetic tapes from the two elements when they are brought together and played back for correlation, or equivalently by introducing a relative shift in the bit strings of data during cross correlation for digital systems. With the delay factor, the fringe phase is set to zero at $\hat{s}_o$, so the fringe amplitude is maximum there and falls off very slowly due to the $\frac{\sin\xi}{\xi}$ factor for $\hat{s}$ slightly offset from $\hat{s}_o$. We note that the delay factor can also be tracked to compensate for changing τ_g and thereby allow $\Delta\nu$ to be even larger than for fixed delay.

The appropriate generalization for the correlation function giving the interferometer response for a point source observed in bandwidth $\Delta\nu$ with accurate delay tracking is

$$R(\nu,\hat{s}) = B_o\, e^{i2\pi\frac{\nu_o}{c}\vec{b}\cdot\hat{s}_o}\; e^{i2\pi\frac{\nu}{c}\vec{b}\cdot(\hat{s}-\hat{s}_o)}$$

Generalizaing this to the case of an extended source with brightness distribution function $B(\hat{s}-\hat{s}_o)$, we have

$$R = e^{i2\pi \frac{\nu_0}{c} \vec{b}\cdot\hat{s}_0} \int_{\nu_0 - \frac{\Delta\nu}{2}}^{\nu_0 + \frac{\Delta\nu}{2}} d\nu \int d\hat{s}\, F(\nu)\, G(\hat{s}-\hat{s}_0)\, B(\hat{s}-\hat{s}_0)\, e^{i2\pi \frac{\nu}{c} \vec{b}\cdot(\hat{s}-\hat{s}_0)}$$

$$= e^{i2\pi \frac{\nu_0}{c} \vec{b}\cdot\hat{s}_0} V(\vec{b})$$

where the function $V(\vec{b})$ is defined to be

$$V(\vec{b}) \equiv \int_{\nu_0 - \frac{\Delta\nu}{2}}^{\nu_0 + \frac{\Delta\nu}{2}} d\nu \int d\hat{s}\, F(\nu)\, G(\hat{s}-\hat{s}_0)\, B(\hat{s}-\hat{s}_0)\, e^{i2\pi \frac{\nu}{c} \vec{b}\cdot(\hat{s}-\hat{s}_0)}$$

We can interpret this result as follows. The factor $e^{i2\pi \frac{\nu_0}{c} \vec{b}\cdot\hat{s}_0}$ is just the interferometer response to a monochromatic point source with unity intensity. This factor has a relatively fast oscillation rate corresponding to closely spaced fringes. The complex function $V(\vec{b})$ gives the amplitude and phase offset needed to properly characterize the extended, non-monochromatic source which is actually observed. Oscillations in $V(\vec{b})$ are large compared to the fringe spacing (or, equivalently in terms of a temporal parameter, $V(\vec{b})$ oscillates slower than do the fringes as the baseline rotates relative to $\hat{s}_0$).

We can express the result in a more convenient form in terms of a suitable astrometric coordinate system. First, we note that the vector $\hat{s}$ can be expressed by an angle x in right ascension and y in declination relative to the reference direction $\hat{s}_0$. Alternatively, but equivalently, we can think in terms of a rectangular coordinate system on the plane of the sky, with origin

at the point where $\hat{s}_0$ intersects the plane of the sky, and with unit vectors x and y with ground projections in the east and north directions, respectively. We will adopt the latter terminology here. The appropriate units for x and y are radians, since the angular description is the operationally correct one, although the planar description makes it easier to conceptualize brightness distribution functions on the sky. (We will not be concerned with the longitudinal component here, which is in the direction $\hat{s}_0 = \hat{x} \times \hat{y}$.) With this notation, $G(\hat{s}-\hat{s}_0)$ can be written $G(x,y)$, $B(\hat{s}-\hat{s}_0)$ as $B(x,y)$, $d\hat{s}$ as $(dx \cdot dy)$, and $(\hat{s}-\hat{s}_0)$ as $x\hat{x} + y\hat{y}$. For monochromatic radiation, we may now write

$$V(\vec{b}) = \int dx \int dy \; G(x,y)\, B(x,y)\, e^{i2\pi \frac{\vec{b}}{\lambda_0} \cdot (x\hat{x} + y\hat{y})}$$

Considerations of diffraction limiting effects in one dimension show that the maximum resolution of a two-element interferometer is $\frac{|\vec{b}|}{\lambda}$ (to within a factor of order unity), which occurs when the baseline is normal to $\hat{s}_0$. Clearly, infinite resolution is possible only for an infinitely long baseline. Infinite resolution corresponds to zero fringe spacing, and the resolution decreases as the spacing between fringes increases. In the two-dimensional problem wich we are considering here, we must deal with two orthogonal components of resolution. We use the $\hat{x}$ and $\hat{y}$ directions, and we define unit vectors $\hat{u} \equiv \hat{x}$ and $\hat{v} \equiv \hat{y}$ in a u-v plane which is parallel to the x-y plane. The u and v axes then give the orthogonal

resolution components in the east-west and north-south directions, respectively. The units of u and v are the same and are reciprocals of the units of x and y; for x and y in radians, u and v are in fringes per radian.

We can express $\frac{\vec{b}}{\lambda_o}$ in terms of the resolution components:

$$\frac{\vec{b}}{\lambda_o} \equiv u\hat{x} + v\hat{y} + (\vec{b}\cdot\hat{s}_o)$$

We will neglect the last term which gives the longitudinal component, and consider only the transverse component $\vec{b}_p \equiv u\hat{x} + v\hat{y}$. In terms of the standard earth-based coordinates of right ascension α and declination δ, we write (α_o, δ_o) for the angular coordinates of $\hat{s}_o$ and (α_b, δ_b) for b. The transverse component of b, which is normal to the source direction $\hat{s}_o$, can then be written as

$$\vec{b}_p = (\hat{s}_o \times \vec{b}) \times \hat{s}_o = \hat{x}\, b \cos\delta_b \sin(\alpha_b - \alpha_s)$$
$$+ \hat{y}\, b\left[\sin\delta_b \cos\delta_s - \sin\delta_s \cos\delta_b \cos(\alpha_b - \alpha_s)\right]$$

We identify

$$u \equiv \frac{b}{\lambda_o} \cos\delta_b \sin(\alpha_b - \alpha_s)$$

and

$$v \equiv \frac{b}{\lambda_o}\left[\sin\delta_b \cos\delta_s - \sin\delta_s \cos\delta_b \cos(\alpha_b - \alpha_s)\right]$$

Now, expressing $V(\vec{b})$ in terms of u and v, and noting that $(\hat{s}-\hat{s}_o)_p = x\hat{x} + y\hat{y}$, we can write

$$V(u,v) = \int dx \int dy \; G(x,y)\, B(x,y)\, e^{i2\pi(ux+vy)}$$

The function V(u,v) is know as the visibility function, and for an isotropic primary power pattern, we have

$$V(u,v) = \int dx \int dy \; B(x,y)\, e^{i2\pi(ux+vy)}$$

Thus, the visibility function and the source brightness distribution function are a Fourier transform pair. Fomalont (1973) discusses the major assumptions and simplifications which are incorporated into this result and its inherent limitations, as well as the effect of a large bandwidth $\Delta\nu$.

We note that u and v are time-varying parameters due to the relative motion between $\vec{b}$ and $\hat{s}_o$. For an interferometer with two earth-based elements, the locus of points in the u-v plane transversed by u and v will lie on an elliptical tract, since

$$\frac{u^2}{a^2} + \frac{(v-v_o)^2}{d^2} = 1$$

where

$$a \equiv \frac{b}{\lambda_o}\cos\delta_b \qquad d \equiv \frac{b}{\lambda_o}\cos\delta_b \sin\delta_s$$

and $v_o \equiv \frac{b}{\lambda_o}\sin\delta_b\cos\delta_s$

However, when one or both elements of an interferometer are on satellites, the periods of the individual elements (which for two earth-based elements are both 24 hours) are no longer necessarily commensurate, and it can be shown that the track in the u-v plane is not a closed figure, but rather is "open-ended" and undergoes a precessional-type advance through the u-v plane. Thus, a two element interferometer whose elements have non-commensurate periodic motions can (in principle, with infinite observation time) provide observational coverage over the entire u-v plane inside the truncation limits (which are the maximun resolution limits along the u and v axes).

Figure 2.4 illustrates a portion of the track which is traced out in the u-v plane for the case of an earth station located at 43° latitude and 70° longitude and a satellite element in a circular orbit over the poles at distance $8 \cdot 10^9$ cm from the center of the earth ($1.62 \cdot 10^4$km altitude). The source coordinates used were those for 3C273, right ascension 12H 26m 33s and declination 2°20' [Kraus (1966)], and the observation wavelength was taken as 3cm. The only portions of the u-v plane which may actually be observed are those portions where the source is visible to both elements. From the figure, we can get an appreciation for the role of the integration time period in terms of the extent to which the visibility function is averaged as opposed to being sampled (i.e., measured point-wise). The integration time t_o was taken as 1000 seconds for the example case here. As discussed previously, the

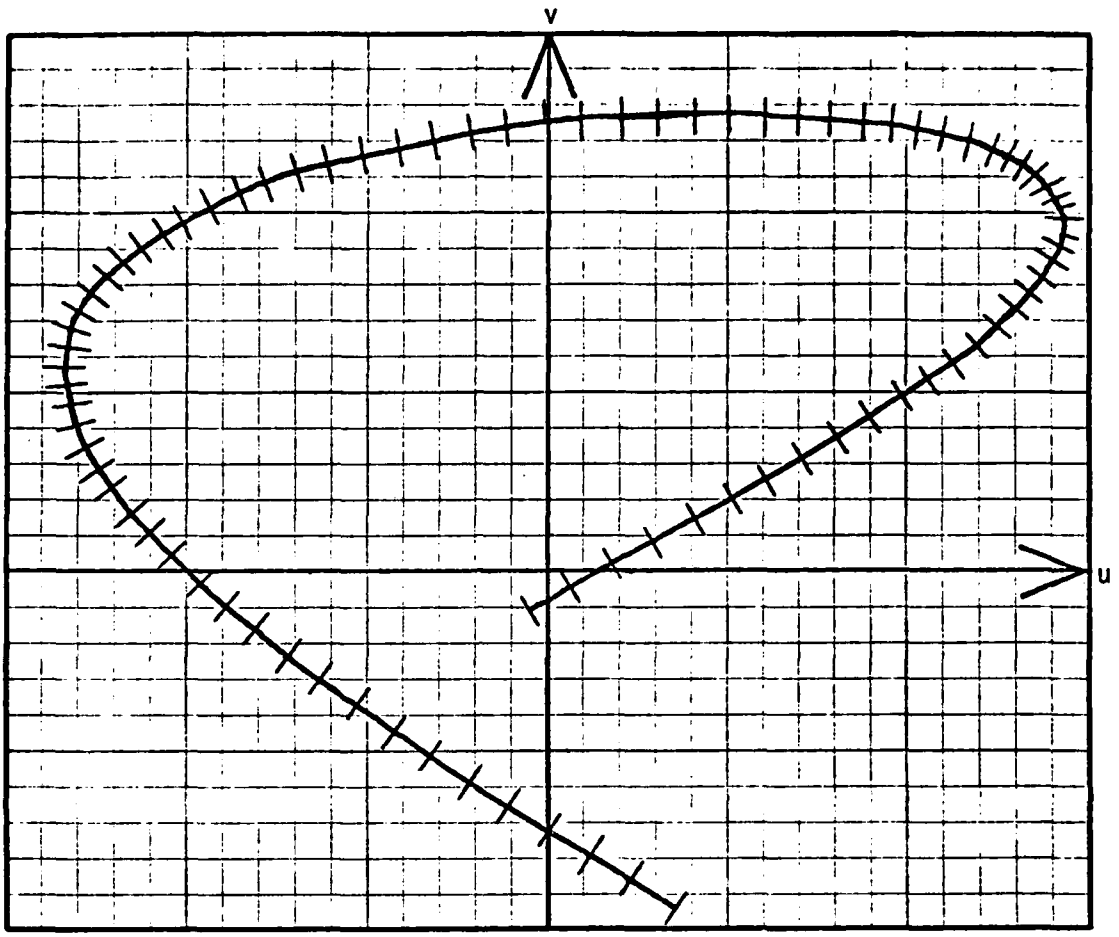

FIGURE 2.4 -- Track in the u-v plane.

Note: The inteval between markers corresponds to a 1000 second integration time. The start of this portion of the track is the end near the origin.

integration time period is of the order of 100 times greater for an earth-satellite interferometer as compared to an earth-based system. The effects of averaging must therefore be accounted for when a satellite is used as an interferometer element. A useful simplification arises if we shift axes so that $v_0=0$ or if the data are "gridded" (see discussion below) onto a aregular lattice. In this case, then, the arc or cell midpoint at (u_n,v_m) has the same projection magnitudes on the u and v axes as does the arc or cell with midpoint at (u_{-n},v_{-m}), where $u_{-n}=-u_n$, $v_{-m}=-v_m$. If we can call these projections $T_{u,n}$ and $T_{v,m}$, respectively, then we can write $T_{u,n}=T_{u,-n}$ and $T_{v,m}=T_{v,-m}$. This simplification will be used later in our discussion of averaging effects.

Essentially, we have found that the interferometer measures the Fourier components of the source brightness distribution. As we will prove later, the Sampling Theorem states that knowing the Fourier components of a function at discrete, properly spaced lattice points in the u-v plane enables one to completely specify the brightness function. This concept is the basis for aperture synethesis techniques, in which B(x,y) is determined from incomplete sampling of the visibility function in the u-v plane. Since the coverage of the u-v plane is confined to the tracks made as the relative orientation of $\vec{b}$ and $\hat{s}_0$ changes, it is desirable to use many-element arrays with various baseline vectors so that ample coverage of the u-v plane results from an observation. Each pair of elements in this array produces a track in the u-v plane. If the signal from the source is not a rapidly time-varying phenomenon

(such as the solar brightness function), or is approximately a steady-state phenomenon over the period of all observations, then the various observations to be incorporated into the aperture synthesis map need not be made simultaneously. This fact presents the added advantage of allowing one to use a certain number of elements for a series of observations, where the baseline vectors are changed (say by moving elements on railroad platforms) from one observation period to the next. In this manner, it has been possible to obtain aperture synthesis maps which result from excellent coverage of the u-v plane. Although the density of observation points may be reasonably high, there still remains the problem that the tracks in the u-v plane do not (in general) pass through the properly spaced lattice points required by the Sampling Theorem to yield the brightness function exactly and uniquely. Various methods are in use for extrapolating (or "gridding") the known data to the lattice points, including convolution and cell averaging techniques [see Thompson and Bracewell (1974) for a discussion of these methods]. An additional problem concerns the fact that, although good coverage of the u-v plane may be obtained, full coverage (i.e., infinite resolution from infinite baselines) is not possible and effectively we are dealing with a truncated version of the true visibility function.

Aperture synthesis theory applies to VLBI. In a particular case, if it is not possible to obtain sufficient coverage of the u-v plane to enable a high resolution brightness distribution map

to be constructed, then a simple model source, commensurate with the known data, may be constructed to represent the true source [see, for example, Knight, et al (1971)]. With a sufficient number of ground based stations, and by using satellites as interferometer elements, it should be possible to obtain good coverage of the u-v plane to enable very high resolution aperture synthesis maps to be produced.

Having demonstrated that the relationship between the visibility function and the source brightness function is a Fourier transformation, we now review the basics of Fourier transform theory, and subsequently, we will study the effect on the brightness function due to truncating and averaging the visibility function.

2.3 The Two-Dimensional Fourier Transform

2.3.1 Usefulness of the Fourier Transform as an Integral Transform

Of the different possible integral transforms, the Fourier transform, because of its basic properties, is one of the most useful and widely employed. These basic properties are linearity, shift invariance, and orthogonality of the integral transform's kernel.

If we denote the Fourier transform operation by the operator symbol $\mathcal{F}$, then

$$\mathcal{F}\{B(x)\} = V(u)$$

means that the Fourier transform of a function B of variable x gives a function V of the conjugate variable u. In terms of units, u and x are reciprocals; for example, if x is in centimeters, then u is in inverse centimeters.

The property of linearity means that

$$\mathcal{F}\{\alpha B_1(x) + \beta B_2(x)\} = \alpha V_1(u) + \beta V_2(u)$$

where

$$\mathcal{F}\{B_1(x)\} = V_1(u), \qquad \mathcal{F}\{B_2(x)\} = V_2(u).$$

Shift invariance implies, for a constant c,

$$\mathcal{F}\{B(x+c)\} = f(c)\,V(u)$$

where $\mathcal{F}\{B(x)\} = V(u)$

and f(c) is a phase factor, depending upon constant c and u, but independent of x. The orthogonality property enables the inverse Fourier transform, denoted by the operator $\mathcal{F}^{-1}$, to be defined. Thus if, $\mathcal{F}\{B(x)\} = V(u)$

then $\mathcal{F}^{-1}\{V(u)\} = B(x)$

In one dimension, the Fourier kernel is written as $e^{i2\pi ux}$, so that the integral transform appears explicitly as

$$V(u) = \mathcal{F}\{B(x)\} = \int_{-\infty}^{\infty} e^{i2\pi ux} B(x)\, dx$$

The orthogonality of the Fourier kernel then lets us write

$$\int_{-\infty}^{\infty} du\, e^{-i2\pi ux'} V(u) = \int_{-\infty}^{\infty} du\, e^{-i2\pi ux'} \left[\int_{-\infty}^{\infty} e^{i2\pi ux} B(x)\, dx\right]$$

$$= \int_{-\infty}^{\infty} dx\, B(x) \int_{-\infty}^{\infty} du\, e^{i2\pi u(x-x')}$$

$$= \int_{-\infty}^{\infty} dx\, B(x)\, \delta(x-x') = B(x')$$

We, therefore, see that the orthogonality property let's define the inverse transform kernel as $e^{-i2\pi ux}$, and the inverse transformation appears explicity as

$$B(x) = \mathcal{F}^{-1}\{V(u)\} = \int_{-\infty}^{\infty} du\, e^{-i2\pi ux} V(u)$$

It is the importance of linearity, shift invariance, and inverse transformation operations in practical applications which accounts for the diverse and widespread use of Fourier transforms.

2.3.2 The 2-D Fourier Transform

Multi-dimensional Fourier transforms are defined analogously to the one-dimensional form, with the number of conjugate variable pairs being equal to the dimension. In particular, the 2-D Fourier transforms are given by

$$B(x,y) = \mathcal{F}^{-1}\{V(u,v)\} = \int_{-\infty}^{\infty} du \int_{-\infty}^{\infty} dv\, e^{-i2\pi(ux+vy)} V(u,v)$$

$$= \int_{-\infty}^{\infty} du\, e^{-i2\pi ux} \int_{-\infty}^{\infty} dv\, e^{-i2\pi vy} V(u,v)$$

and $$V(u,v) = \mathcal{F}\{B(x,y)\} = \int_{-\infty}^{\infty} dx \int_{-\infty}^{\infty} dy\, e^{i2\pi(ux+vy)} B(x,y)$$
$$= \int_{-\infty}^{\infty} dx\, e^{i2\pi ux} \int_{-\infty}^{\infty} dy\, e^{i2\pi vy} B(x,y).$$

We will now consider a few examples of the 2-D Fourier transform which will prove relevant in our discussion below.

A point source at the origin is represented by $B(x,y)=\delta(x,y)$, where the 2-D Dirac delta function is defined by $\delta(x,y)\equiv\delta(x)\delta(y)$. The corresponding visibility function would be

$$V(u,v) = \int_{-\infty}^{\infty} dx \int_{-\infty}^{\infty} dy\, e^{i2\pi(ux+vy)} \delta(x,y) = 1$$

Thus, a point source has an associated visibility function of constant amplitude over the entire u-v plane. If the visibility function were of constant amplitude over only a finite rectangular area of the u-v plane

$$V(u,v) = \begin{cases} 1 & \text{FOR } u \in [-u_0, u_0],\ v \in [-v_0, v_0] \\ 0 & \text{ELSEWHERE} \end{cases}$$

the corresponding source brightness function would be

$$B(x,y) = \int_{-\infty}^{\infty} du \int_{-\infty}^{\infty} dv\, e^{-i2\pi(ux+vy)} V(u,v)$$
$$= \int_{-u_0}^{u_0} du \int_{-v_0}^{v_0} dv\, e^{-i2\pi(ux+vy)}$$
$$= \left[\frac{e^{i2\pi u_0 x} - e^{-i2\pi u_0 x}}{i2\pi x}\right]\left[\frac{e^{i2\pi v_0 y} - e^{-i2\pi v_0 y}}{i2\pi y}\right]$$
$$= \frac{\sin 2\pi u_0 x}{\pi x} \cdot \frac{\sin 2\pi v_0 y}{\pi y}$$

The sine function divided by its argument will appear frequently in our work, and will be called a sinc function following Bracewell's convention: $\text{sinc } x \equiv \frac{\sin \pi x}{\pi x}$. Thus, the previous brightness function may be written as

$$B(x,y) = 2U_0 \,\text{sinc}\, 2U_0 x \cdot 2V_0 \,\text{sinc}\, 2V_0 y .$$

As a final example, we will consider a Gaussian visibility function,

$$V(u,v) = e^{-\pi(u^2+v^2)}$$

Then $$B(x,y) = \int_{-\infty}^{\infty} du \int_{-\infty}^{\infty} dv \; e^{-i2\pi(ux+vy)} \; e^{-\pi(u^2+v^2)}$$

$$= \left[\int_{-\infty}^{\infty} du \; e^{-[\pi u^2 + (i2\pi x)u]}\right] \left[\int_{-\infty}^{\infty} dv \; e^{-[\pi v^2 + (i2\pi y)v]}\right].$$

Consider the u integral. Completing the square of the exponent,

$$\pi u^2 + (i2\pi x)u = (\sqrt{\pi}\, u + i\sqrt{\pi}\, x)^2 + \pi x^2$$

let us write $$I \equiv \int_{-\infty}^{\infty} du \; e^{-[\pi u^2 + i2\pi ux]}$$

$$= e^{-\pi x^2} \int_{-\infty}^{\infty} du \; e^{-[\sqrt{\pi}\, u + i\sqrt{\pi}\, x]^2} .$$

Define $\xi \equiv \sqrt{\pi}\, u + i\sqrt{\pi}\, x$, so

$$d\xi = \sqrt{\pi}\, du .$$

Then, $$I = e^{-\pi x^2} \int_{-\infty}^{\infty} \frac{d\xi}{\sqrt{\pi}} \; e^{-\xi^2} = \frac{e^{-\pi x^2}}{\sqrt{\pi}} (\sqrt{\pi})$$

$$= e^{-\pi x^2}$$

So we can see that the corresponding brightness function to a Gaussian visibility function is

$$B(x,y) = e^{-\pi(x^2+y^2)}$$

It should be noted that the Gaussian is the only non-generalized function which preserves its function form under Fourier transformation. (The generalized function III, discussed later, will also be seen to have this property.)

2.3.3 Fundamental Theorems

We have seen that even a simple Gaussian requires some effort to perform the Fourier transformation by direct evaluation of the integral. Fortunately, there are a number of fundamental theorems which not only ease the calculation of transforms, but also provide further insight into properties of Fourier transforms. Since we will extensively rely on these theorems in what follows, we will prove a number of them here. [Most of these theorems are stated without proof for the 2-D Fourier transform by Bracewell (1978).] The symbol "$\supset$" will be used to denote a Fourier transform pair, so that

$$V(u,v) \supset B(x,y) \quad \text{AND} \quad B(x,y) \supset V(u,v)$$

Note that one dimensional versions of these theorems are easily realized by setting y and v to constants in the equations. (Of course, these arbitrary constants do not affect the results.)

Separable Product Theorem: If $B_1(x) \supset V_1(u)$ and $B_2(y) \supset V_2(v)$, then $B_1(x)B_2(y) \supset V_1(u)V_2(v)$.

Proof: Let $V(u,v) \equiv V_1(u)V_2(v)$ and $B(x,y) \equiv B_1(x)B_2(y)$.

Then $$\mathcal{F}^{-1}\{V(u,v)\} = \int_{-\infty}^{\infty} du \int_{-\infty}^{\infty} dv\, e^{-i2\pi(ux+vy)} V_1(u) V_2(v)$$

$$= \left[\int_{-\infty}^{\infty} du\, e^{-i2\pi ux} V_1(u)\right]\left[\int_{-\infty}^{\infty} dv\, e^{-i2\pi vy} V_2(v)\right]$$

$$= B_1(x)\, B_2(y)$$ ∎

2-D Addition Theorem: If $B_1(x,y) \supset V_1(u,v)$ and $B_2(x,y) \supset V_2(u,v)$, then

$$B_1(x,y) + B_2(x,y) \supset V_1(u,v) + V_2(u,v)$$

Proof:
$$\mathcal{F}^{-1}\{V_1 + V_2\} = \int_{-\infty}^{\infty} du \int_{-\infty}^{\infty} dv\, e^{-i2\pi(ux+vy)}\left[V_1(u,v) + V_2(u,v)\right]$$

$$= \int_{-\infty}^{\infty} du \int_{-\infty}^{\infty} dv\, e^{-i2\pi(ux+vy)} V_1(u,v) + \int_{-\infty}^{\infty} du \int_{-\infty}^{\infty} dv\, e^{-i2\pi(ux+vy)} V_2(u,v)$$

$$= B_1(x,y) + B_2(x,y)$$

It is readily apparent that

$$\mathcal{F}\{B_1(x,y) + B_2(x,y)\} = V_1(u,v) + V_2(u,v)$$ ∎

2-D Shift Theorem: If $B(x,y) \supset V(u,v)$, then

$$B(x-a, y-b) \supset e^{i2\pi(au+bv)} V(u,v)$$

and $V(u-a, v-b) \supset e^{-i2\pi(ax+by)} B(x,y)$

Proof:

$$\mathcal{F}^{-1}\{V(u-a,v-b)\} = \int_{-\infty}^{\infty} du \int_{-\infty}^{\infty} dv \; e^{-i2\pi(ux+vy)} V(u-a,v-b)$$

$$= \int_{-\infty}^{\infty} d(u-a) \int_{-\infty}^{\infty} d(v-b) \; e^{-i2\pi(ax+by)} e^{-i2\pi[(u-a)x+(v-b)y]} V(u-a,v-b)$$

$$= e^{-i2\pi(ax+by)} B(x,y)$$

Similarly, we have

$$\mathcal{F}\{B(x-a,y-b)\} = \int_{-\infty}^{\infty} dx \int_{-\infty}^{\infty} dy \; e^{i2\pi(ux+vy)} B(x-a,y-b)$$

$$= \int_{-\infty}^{\infty} d(x-a) \int_{-\infty}^{\infty} d(y-b) \; e^{i2\pi(au+bv)} e^{i2\pi[(x-a)u+(y-b)v]} B(x-a,y-b)$$

$$= e^{i2\pi(au+bv)} V(u,v)$$

■

2-D Similarity Theorem: If $B(x,y) \supset V(u,v)$, then

$$V(au, bv) \supset \frac{1}{|ab|} B\left(\frac{x}{a}, \frac{y}{b}\right)$$

and

$$B(ax, by) \supset \frac{1}{|ab|} V\left(\frac{u}{a}, \frac{v}{b}\right)$$

Proof:

$$\mathcal{F}^{-1}\{V(au,bv)\} = \int_{-\infty}^{\infty} du \int_{-\infty}^{\infty} dv \; e^{-i2\pi(ux+vy)} V(au,bv)$$

$$= \frac{1}{|a|} \frac{1}{|b|} \int_{-\infty}^{\infty} d(au) \int_{-\infty}^{\infty} d(bv) \; e^{-i2\pi\left(au\frac{x}{a} + bv\frac{y}{b}\right)} V(au,bv)$$

$$= \frac{1}{|ab|} B\left(\frac{x}{a}, \frac{y}{b}\right)$$

Similarly, we have

$$\mathcal{F}\{B(ax,by)\} = \int_{-\infty}^{\infty} dx \int_{-\infty}^{\infty} dy\, e^{i2\pi(ux+vy)} B(ax,by)$$

$$= \frac{1}{|a|}\frac{1}{|b|}\int_{-\infty}^{\infty} d(ax)\int_{-\infty}^{\infty} d(by)\, e^{i2\pi(ax\frac{u}{a}+by\frac{v}{b})} B(ax,by)$$

$$= \frac{1}{|ab|} V\left(\frac{u}{a},\frac{v}{b}\right) \quad \blacksquare$$

2-D Definite Integral Theorem:

$$\int_{-\infty}^{\infty} dx \int_{-\infty}^{\infty} dy\, B(x,y) = V(0,0)$$

Proof:

$$\int_{-\infty}^{\infty} dx \int_{-\infty}^{\infty} dy\, B(x,y) = \left[\int_{-\infty}^{\infty} dx \int_{-\infty}^{\infty} dy\, e^{i2\pi(ux+vy)} B(x,y)\right]_{\substack{u=0\\v=0}}$$

$$\left[V(u,v)\right]_{\substack{u=0\\v=0}} = V(0,0)$$

Similarly,

$$\int_{-\infty}^{\infty} du \int_{-\infty}^{\infty} dv\, V(u,v) = B(0,0) \quad \blacksquare$$

2-D Differentiation Theorem:

$$\left(\frac{\partial}{\partial x}\right)^n \left(\frac{\partial}{\partial y}\right)^m B(x,y) = (-i2\pi u)^n (-i2\pi v)^m V(u,v)$$

Proof:

$$\mathcal{F}\left\{\left(\frac{\partial}{\partial x}\right)^n \left(\frac{\partial}{\partial y}\right)^m B(x,y)\right\} = \int_{-\infty}^{\infty} dx\, e^{i2\pi ux}\left(\frac{\partial}{\partial x}\right)^n$$

$$\cdot \int_{-\infty}^{\infty} dy\, e^{i2\pi vy}\left(\frac{\partial}{\partial y}\right)^m B(x,y)$$

Integrate by parts once for the y integral:

$$\mathcal{F}\left\{\left(\frac{\partial}{\partial x}\right)^n\left(\frac{\partial}{\partial y}\right)^m B(x,y)\right\} =$$

$$\int_{-\infty}^{\infty} dx\, e^{i2\pi ux}\left(\frac{\partial}{\partial x}\right)^n\left[e^{i2\pi vy}\left(\frac{\partial}{\partial y}\right)^{m-1} B(x,y)\Big|_{y=-\infty}^{\infty} - \int_{-\infty}^{\infty} dy\,(i2\pi v)\, e^{i2\pi vy} \cdot\left(\frac{\partial}{\partial y}\right)^{m-1} B(x,y)\right]$$

The integrated part vanishes if

$$\lim_{y\to\infty} B(x,y) = 0$$

(as we will be concerned with). Perform (m-1) further intergrations by parts for the y integral, and then n integrations by parts for the x integral; the result is

$$\mathcal{F}\left\{\left(\frac{\partial}{\partial x}\right)^n\left(\frac{\partial}{\partial y}\right)^m B(x,y)\right\} = \int_{-\infty}^{\infty} dx \int_{-\infty}^{\infty} dy\,(-i2\pi u)^n (-i2\pi v)^m e^{i2\pi(ux+vy)} B(x,y)$$

$$= (-i2\pi u)^n (-i2\pi v)^m V(u,v)$$

Similarly,

$$\mathcal{F}^{-1}\left\{\left(\frac{\partial}{\partial u}\right)^m\left(\frac{\partial}{\partial v}\right)^m V(u,v)\right\} = (i2\pi x)^m (i2\pi y)^m B(x,y) \quad \blacksquare$$

Hermiticity Theorem: If B(x,y) is a real function, then V(u,v) must be Hermitian, i.e.,

$$V(u,v) = V^*(-u,-v)$$

Proof:

$$V(u,v) = \mathcal{F}\{B(x,y)\} = \int_{-\infty}^{\infty} dx \int_{-\infty}^{\infty} dy\; e^{i2\pi(ux+vy)} B(x,y)$$

Since B is real, we have $V_r(u,v) = \int_{-\infty}^{\infty}\int_{-\infty}^{\infty} dx\,dy \cos[2\pi(ux+vy)]\, B(x,y)$

$V_i(u,v) = \int_{-\infty}^{\infty}\int_{-\infty}^{\infty} dx\,dy \sin[2\pi(ux+vy)]\, B(x,y)$

where $V(u,v) = V_r(u,v) + i V_i(u,v)$.

We clearly see that $V_r(u,v) = V_r(-u,-v)$, $V_i(u,v) = -V_i(-u,-v)$.

Hence $V(u,v) = V^*(-u,-v)$. ∎

Hermiticity Corollary 1 -- If B(x,y) is a real function and is even in its joint argument, B(x,y) = B(-x,-y), then V(u,v) is real and even in its joint argument, V(u,v) = V_r(u,v) = V_r(-u,-v).

Proof: From the equations for V_r(u,v) and V_i(u,v) in the proof of the Hermiticity Theorem, we need only note that if B is even in x and y, then the integrals in the V_i equation vanish, and the V_r equation yields V_r(u,v) = V_r(-u,-v).

Hermiticity Corollary 2 -- If B(x,y) is a real function and odd in its joint argument, B(x,y) = -B(-x,-y), then V(u,v) is imaginary and odd in its joint argument.

Proof: From the proof of the Hermiticity Theorem, this case causes the V_r equation integrals to vanish while yielding V_i(u,v) = -V_i(-u,-v).

From these theorems, we deduce the concepts that reality of one function in a fourier transform pair implies

Hermiticity of its conjugate function, and that a real even function has a real even conjugate while a real odd function has a pure imaginary odd conjugate.

The convolution of two functions, $B_1(x,y)$ and $B_2(x,y)$, is denoted by $B_1 * B_2$, and is defined by

$$B_1(x,y) * B_2(x,y) \equiv \int_{-\infty}^{\infty} dx' \int_{-\infty}^{\infty} dy'\, B_1(x',y')\, B_2(x-x', y-y')$$
$$= \int_{-\infty}^{\infty} dx' \int_{-\infty}^{\infty} dy'\, B_1(x-x', y-y')\, B_2(x',y') .$$

We now prove a very useful theorem relating the Fourier transform of the convolution of two functions to a product of their separate transforms.

2-D Convolution Theorem: If $B_1 \supset V_1$ and $B_2 \supset V_2$, then

$$B_1(x,y) * B_2(x,y) \supset V_1(u,v) \cdot V_2(u,v)$$

Proof:

$$B_1(x,y) * B_2(x,y) = \int_{-\infty}^{\infty} dx' \int_{-\infty}^{\infty} dy'\, B_1(x',y')\, B_2(x-x', y-y').$$

So,

$$\mathcal{F}\{B_1 * B_2\} = \int_{-\infty}^{\infty} dx \int_{-\infty}^{\infty} dy\, e^{i2\pi(ux+vy)} \left[\int_{-\infty}^{\infty} dx' \int_{-\infty}^{\infty} dy'\, B_1(x',y')\, B_2(x-x', y-y') \right]$$

$$= \int_{-\infty}^{\infty} dx' \int_{-\infty}^{\infty} dy'\, B_1(x',y') \left[\int_{-\infty}^{\infty} dx \int_{-\infty}^{\infty} dy\, e^{i2\pi(ux+vy)} B_2(x-x', y-y') \right]$$

$$= \int_{-\infty}^{\infty} dx' \int_{-\infty}^{\infty} dy'\, B_1(x',y') \left[e^{i2\pi(ux'+vy')} V_2(u,v) \right] \quad \text{(SHIFT THM)}$$

$$= V_2(u,v) \int_{-\infty}^{\infty} dx' \int_{-\infty}^{\infty} dy'\, e^{i2\pi(ux'+vy')} B_1(x',y')$$

$$= V_1(u,v) \cdot V_2(u,v)$$

We similarly obtain the converse of this theorem as:

$$V_1(u,v) * V_2(u,v) \supset B_1(x,y) \cdot B_2(x,y) \quad \blacksquare$$

2.3.4 Truncation Effects

We define the 2-D box function in terms of 1-D rectangle functions, following Bracewell's notation (1978):

$$\Pi(u,v) \equiv \Pi(u) \cdot \Pi(v)$$

where

$$\Pi(u) \equiv \begin{cases} 1 & |u| < \frac{1}{2} \\ \frac{1}{2} & |u| = \frac{1}{2} \\ 0 & |u| > \frac{1}{2} \end{cases}$$

Rectangular truncation of a visibility function in the u-v plane is equivalent to multiplying that visibility function by a 2-D box function which has zero amplitude outside the specified rectangular region. Since truncation can be expressed as a product of functions in u-v space, then the corresponding brightness function can be determined by the Convolution Theorem. To consider the general case of rectangular truncation, we must know the transform of $\Pi\left(\frac{u-c_u}{b_u}, \frac{v-c_v}{b_v}\right)$

which specifies a box function with unit height inside the rectangular

region with edge lengths b_u and b_v, centered on c_u along the u axis and c_v along the v axis, respectively. Since this transform will be important later, we now prove a theorem for the general case.

Box Function Transform Theorem:

$$\mathcal{F}^{-1}\left\{\Pi\left(\frac{u-c_u}{b_u}, \frac{v-c_v}{b_v}\right)\right\} = e^{-i2\pi(c_u x + c_v y)} \frac{\sin \pi b_u x}{\pi x} \frac{\sin \pi b_v y}{\pi y}.$$

Proof:

$$\mathcal{F}^{-1}\left\{\Pi\left(\frac{u-c_u}{b_u}, \frac{v-c_v}{b_v}\right)\right\} = \int_{-\infty}^{\infty} du \int_{-\infty}^{\infty} dv \; e^{-i2\pi(ux+vy)} \Pi\left(\frac{u-c_u}{b_u}, \frac{v-c_v}{b_v}\right)$$

$$= \int_{c_u - \frac{b_u}{2}}^{c_u + \frac{b_u}{2}} du \int_{c_v - \frac{b_v}{2}}^{c_v + \frac{b_v}{2}} dv \; e^{-i2\pi(ux+vy)}$$

$$= \frac{e^{-i2\pi x(c_u + \frac{b_u}{2})} - e^{-i2\pi x(c_u - \frac{b_u}{2})}}{-i2\pi x} \cdot \frac{e^{-i2\pi y(c_v + \frac{b_v}{2})} - e^{-i2\pi y(c_v - \frac{b_v}{2})}}{-i2\pi y}$$

$$= e^{-i2\pi(c_u x + c_v y)} \frac{\sin \pi b_u x}{\pi x} \frac{\sin \pi b_v y}{\pi y} \quad \blacksquare$$

The effect on the brightness function resulting from the truncation of the visibility function is expressed by the following theorem.

Truncation Effect Theorem: If $V \supset B$, then if $\tilde{V}$ represents the truncated visibility function,

$$\tilde{B}(x,y) = \mathcal{F}^{-1}\{\tilde{V}(u,v)\}$$

$$= \int_{-\infty}^{\infty} dx' \int_{-\infty}^{\infty} dy' \; e^{-i2\pi(c_u x' + c_v y')} \frac{\sin \pi b_u x'}{\pi x'} \frac{\sin \pi b_v y'}{\pi y'} \cdot B(x-x', y-y')$$

Proof: For 2-D rectangular truncation of V(u,v), we can write $\tilde{V}(u,v) = V(u,v) \cdot \Pi\left(\frac{u-c_u}{b_u}, \frac{v-c_v}{b_v}\right)$

We will use the curly overbar "$\sim$" to denote a truncated visibility function and its associated transform. Then, by the Convolution Theorem

$$\tilde{B}(x,y) = \mathcal{F}^{-1}\{\tilde{V}(u,v)\}$$

$$= B(x,y) * e^{-i2\pi(c_u x + c_v y)} \frac{\sin \pi b_u x}{\pi x} \frac{\sin \pi b_v y}{\pi y}$$

$$= \int_{-\infty}^{\infty} dx' \int_{-\infty}^{\infty} dy' \, e^{-i2\pi(c_u x' + c_v y')} \frac{\sin \pi b_u x'}{\pi x'} \frac{\sin \pi b_v y'}{\pi y'} \cdot B(x-x', y-y') \blacksquare$$

Qualitatively, truncation of V(u,v) gives rise to oscillations, or ringing, in the function $\tilde{B}(x,y)$ as compared to B(x,y). The origin of the ringing is seen in the convolution of B(x,y) with an oscillatory factor $e^{-i2\pi(c_u x + c_v y)}$ and with the sinc functions, which have decaying oscillations. The effect of truncation can also be qualitatively described in terms of a loss of resolution in the sharp features of the conjugate function. This is especially clear for the conjugate functions of interferometry, since truncating V(u,v) means that we are not using the high resolution information for large u and v outside of the truncation limits, and therefore B(x,y) is "blurred" or "smoothed" by being convoluted with the sinc factors to produce $\tilde{B}(x,y)$.

2.3.5 Representation of an Averaged Function

Consider a visibility function which is averaged in rectangular cells over the u-v plane. Let one cell be centered on

the point (0,0). Then we can specify any cell by double integer indices (n,m), where the "n" specifies the n^{th} cell along the u axis and "m" the m^{th} cell along the v axis. We let n and m range from $-\infty$ to $+\infty$, where the +/- sign will denote the relevant half-axis which the cell is referenced to. The $(n,m)^{th}$ average value of V(u,v) is then given by

$$[\bar{V}_{n,m}] \equiv \frac{1}{T_{u,n} T_{v,m}} \int_{u_n - \frac{T_{u,n}}{2}}^{u_n + \frac{T_{u,n}}{2}} du \int_{v_m - \frac{T_{v,m}}{2}}^{v_m + \frac{T_{v,m}}{2}} dv \; V(u,v)$$

where $T_{u,n}$ and $T_{v,m}$ denote the lengths of the $(n,m)^{th}$ averaging cell along the u and v axes, respectively, and u_n and v_m are the midpoint coordinates for the $(n,m)^{th}$ cell. The overbar and brackets will be used to denote an average value of the visibility function.

To represent the average value of V(u,v) in the $(n,m)^{th}$ cell as a function of u and v, we will use a 2-D delta function at the cell's midpoint whose strength is given by the average value over that cell. We therefore write

$$\bar{V}_{n,m}(u,v) \equiv T_{u,n} T_{v,m} [\bar{V}_{n,m}] \, \delta(u - u_n, v - v_m).$$

Note that the area of the $(n,m)^{th}$ cell, $(T_{u,n} \cdot T_{v,m})$, has been included as a factor multiplying the delta function in order that the delta function properly represent the average value over the entire cell. The V(u,v) function averaged over its entire domain can now be written as a sum over these average value terms, and will be

designated by $\bar{\gamma}(u,v)$:

$$\bar{\gamma}(u,v) \equiv \sum_{n=-\infty}^{\infty} T_{u,n} \sum_{m=-\infty}^{\infty} T_{v,m} [\bar{V}_{n,m}] \, \delta(u-u_n, v-v_m).$$

A few comments are in order regarding the specification of the (n=0,m=0) cell as being centered at the origin (u=0,v=0), and the particular choice of representation for the average value in a cell as a function of u and v. Specifying that the (n=0,m=0) cell be centered on the origin is based upon a natural generalization of the 2-D Sampling Theorem to the case of averaging. The Sampling Theorem specifies that sampling be performed in a regular fashion with one sampling point located at the origin. The effect of the epoch of sampling will be further discussed below in our considerations of the Sampling Theorem. The use of delta functions to represent the average values is also a natural generalization from the Sampling Theorem. The other reasonable way to represent the average values would be by rectangular boxes whose height is the relevant average value in the particular cell. Now, a box representation for a particular cell can be expressed as the convolution of a delta function, which is located at the cell midpoint and whose amplitude is the average value of V(u,v) over that cell, with a box of unit height and identical cross section to the relevant averaging cell:

$$V^{\square}_{n,m}(u,v) \equiv \left\{ [\bar{V}_{n,m}] \, \delta(u-u_n, v-v_m) \right\} * \Pi\left(\frac{u}{T_{u,n}}, \frac{v}{T_{v,m}}\right)$$

where $V^{\square}_{n,m}$ denotes the box representation function. Consider the case of constant cell sizes, so $T_{u,n}$ and $T_{v,m}$ are constants for all n and m. From the convolution theorem, we immediately see that, if $\hat{B}_{\delta}(x,y)$ represents the transform of the delta function representation for the averaged visibility function:

$$\hat{B}_{\delta}(x,y) \equiv \mathcal{F}^{-1}\left\{\sum_{n}\sum_{m} T_{u,n} T_{v,m} \left[\bar{V}_{n,m}\right] \delta(u-u_n, v-v_m)\right\},$$

then $\hat{B}_{\square}(x,y)$, which represents the transform of the box representation for the averaged function, can be written as

$$\hat{B}_{\square}(x,y) = \frac{\hat{B}_{\delta}(x,y)}{T_u T_v} \cdot \left(\frac{\sin \pi T_u x}{\pi x} \frac{\sin \pi T_v y}{\pi y}\right)$$

Since

$$\lim_{\substack{T_u \to 0 \\ T_v \to 0}} \left[(T_u \operatorname{sinc} T_u x)(T_v \operatorname{sinc} T_v y)\right] = T_u T_v$$

we see that, as the averaging cell sizes go to zero, $\hat{B}_{\square}$ and $\hat{B}_{\delta}$ become identical. However for large T_u and T_v, as we will be concerned with, the box representation results in preferentially decreasing the amplitude of $\hat{B}_{\delta}$ as we move away from the origin, by the factor

$$(T_u \operatorname{sinc} T_u x)(T_v \operatorname{sinc} T_v y) < 1 \quad \text{FOR } x,y \neq 0$$

In fact, the box representation produces zero brightness at all zeros of $\sin(\pi T_u x)$ and $\sin(\pi T_v y)$. We would like $\hat{B}_{\delta}$ and $\hat{B}_{\square}$ to match the true brightness function B(x,y) as closely as possible. However, $\hat{B}_{\square}(x,y)$ incorporates a sinc modulation factor which must have zeros

at definite points in the x-y plane, regardless of the amplitude of B(x,y) at those points. This consideration, as well as that of the natural generalization of the Sampling Theorem, makes the delta function representation the preferrable method to use to represent the averaged visibility function. A comparison of these two representations for a number of one-dimensional test functions was conducted, and those results support the choice in favor of the delta function representation.

2.3.6 The Standard Fourier Transform for an Averaged Function

The averaged visibility function is specified by

$$\bar{\mathcal{V}}(u,v) = \sum_{n=-\infty}^{\infty} \sum_{m=-\infty}^{\infty} T_{u,n}\, T_{v,m} \left[\bar{V}_{n,m}\right] \delta(u-u_n, v-v_m) \; .$$

The Fourier transform of this function, designated $\hat{B}_\delta(x,y)$ will be an approximation to the true brightness function $B(x,y)$. Taking the Fourier transform of $\bar{\mathcal{V}}$ gives

$$\hat{B}_\delta(x,y) = \sum_{n=-\infty}^{\infty} \sum_{m=-\infty}^{\infty} T_{u,n}\, T_{v,m} \left[\bar{V}_{n,m}\right] \int_{-\infty}^{\infty} du \int_{-\infty}^{\infty} dv\; e^{-i2\pi(ux+vy)}\, \delta(u-u_n, v-v_m)$$

$$= \sum_{n=-\infty}^{\infty} \sum_{m=-\infty}^{\infty} T_{u,n}\, T_{v,m} \left[\bar{V}_{n,m}\right] e^{-i2\pi(u_n x + v_m y)} \; .$$

If V(u,v) has been truncated, then we will have only a finite number of terms in the sum, which can then be written as

$$\hat{B}_\delta(x,y) = \sum_{n=-N}^{N} \sum_{m=-M}^{M} T_{u,n}\, T_{v,m} \left[\bar{V}_{n,m}\right] e^{-i2\pi(u_n x + v_m y)} \; .$$

where we have assumed symmetric truncation about the origin along the u and v axes.

Now, B(x,y) must be a real, non-negative function since it represents the radiation intensity from a physical body. The visibility is, in general, a complex function. We can therefore write $[\bar{V}_{n,m}] = [\bar{V}_{n,m}]_r + i[\bar{V}_{n,m}]_i$, where the subscripts refer to real and imaginary parts. It appears at first sight that $\hat{B}_\delta$ may be a complex function, and would therefore not be a good approximation to B(x,y). However, we have shown that the Fourier transform of a real function must satisfy the Hermiticity property, and this property is invariant under averaging operations. We will see that, for an untruncated or symmetrically truncated visibility function, B_δ will always be real, although it may possibly assume negative values contrary to the nature of the true brightness function.

Clearly, since

$$[\bar{V}_{n,m}] = \frac{1}{T_{u,n}\,T_{v,m}} \int_{u_n - \frac{T_{u,n}}{2}}^{u_n + \frac{T_{u,n}}{2}} du \int_{v_m - \frac{T_{v,m}}{2}}^{v_m + \frac{T_{v,m}}{2}} dv \; V(u,v)$$

the average values $[\bar{V}_{n,m}]$ will satisfy a "discrete Hermiticity relation" if V is Hermitian:

$$V(u,v) = V^*(-u,-v) \Longrightarrow [\bar{V}_{n,m}] = [\bar{V}_{-n,-m}]^*$$

This statement assumes that the epoch of averaging is at the origin [(n=0,m=0)→(u=0,v=0)]. If we write

$$[\bar{V}_{n,m}] = [\bar{V}_{n,m}]_r + i[\bar{V}_{n,m}]_i$$

then for symmetric truncation (or no truncation if N→∞, M→∞) we have

$$\hat{B}_\delta(x,y) = \sum_{n=-N}^{N}\sum_{m=-M}^{M} T_{u,n}T_{v,m}\left\{\left[[\bar{V}_{n,m}]_r \cos 2\pi(u_n x+v_m y) + [\bar{V}_{n,m}]_i \cdot \sin 2\pi(u_n x+v_m y)\right] + i\left[[\bar{V}_{n,m}]_r \sin 2\pi(u_n x+v_m y) - [\bar{V}_{n,m}]_i \cos 2\pi(u_n x+v_m y)\right]\right\}$$

Since $[\bar{V}_{n,m}]_r$ is even in n and m while $\sin 2\pi(u_n x+v_m y)$ is odd in (u_n, v_m), then their product is odd and vanishes in the double summation process. Similarly, the second imaginary term vanishes in the double summation. Both of the real terms are even in (n,m) and (u_n, v_m), so we can write

$$\hat{B}_\delta(x,y) = \sum_{n=-N}^{N} T_{u,n}T_{v,0}\left\{[\bar{V}_{n,0}]_r \cos 2\pi u_n x + [\bar{V}_{n,0}]_i \sin 2\pi u_n x\right\} + 2\sum_{n=-N}^{N}\sum_{m=1}^{M} T_{u,n}T_{v,m}\left\{[\bar{V}_{n,m}]_r \cos 2\pi(u_n x+v_m y) + [\bar{V}_{n,m}]_i \sin 2\pi(u_n x+v_m y)\right\}$$

We have shown that $\hat{B}_\delta$ is indeed real for symmetric truncation of V(u,v) (and for no truncation at all). Furthermore, the last equation implies that a knowledge of the average values of V(u,v) over only half the u-v plane is required to specify $\hat{B}_\delta$. The two quadrants in the chosen half plane must be adjacent, not diagonal to one another, in order that the Hermiticity property be used to deduce the average values in the other half of the u-v plane.

If the visibility function is truncated asymmetrically, then $\hat{B}_\delta$ may be complex valued. The Hermiticity property satisfied by V(u,v) for real B(x,y) enables us to relate the values of the visibility function in two adjacent quadrants of the u-v plane to

its values in the other two quadrants. Therefore, in cases of asymmetric truncation, it may be possible to ascertain the average values of V(u,v) needed to symmetrize the truncation. If this is not possible, then the set of average values of V(u,v) should be decreased to result in a data set reflecting symmetric truncation in order to produce a real-valued $\hat{B}_\delta(x,y)$. One dimensional test functions were examined for the case of asymmetric truncation, and the results corroborate the assertion that asymmetric trunction produces a complex $\hat{B}_\delta(x,y)$ with the imaginary portion contributing no information useful in discerning B(x,y) or a best approximation to it.

2.4 The Sampling Theorem for Fourier Transforms

2.4.1 Statement of the Sampling Theorem in 1-D

The Sampling, or Nyquist, theorem for Fourier transforms in 1-D may be stated as follows. Consider a function B(x) which is non-zero only in a finite portion of the x-axis, from $-L_x$ to L_x. Such a function is usually referred to as being "band-limited". Let V(u) be the Fourier transform of B(x), and let V(u) be periodically sampled with the epoch of sampling at the origin (i.e., a sample is taken at u=0 and periodically thereafter in both directions). If the sampling interval is less than or equal to $\frac{1}{2L_x}$, then it is possible to reconstruct the function B(x) exactly [and hence of course also V(u)]. The largest sampling interval which can be used and still reproduce B(x) undistorted is known as

the Nyquist interval, which we will denote by T_{NI}.

In its one-dimensional form, the Sampling Theorem is of use in signal processing applications. A suitable generalization to 2-D makes this theorem of use in VLBI data analysis. Since the proof of the Sampling Theorem in 2-D is entirely analogous to the one-dimensional proof, we will prove this theorem below only for the 2-D case of interest.

2.4.2 Relevance to VLBI Data Analysis

Since all celestial emitters of radio waves have a finite physical size, their brightness distribution functions have non-zero amplitude only over a finite, bounded region on the plane of the sky. In two dimensions, we will refer to such a function which is non-zero only in a certain portion of the plane of definition as being "region-limited".

As discussed above, an interferometer measures the visibility function which is the Fourier transform of the brightness function. But since all brightness functions are region-limited, then a generalization of the Sampling Theorem to 2-D would imply that sampling V(u,v) in some periodic lattice fashion over the u-v plane would provide sufficient information to reconstruct B(x,y) exactly, provided that the sampling cells were acceptably small. The ramification of this theorem for radio interferometric observations using aperture synthesis is obvious, and with this motivation we now consider the 2-D Sampling Theorem in detail.

2.4.3 Derivation and Discussion of 2-D Sampling Theorem

Consider a region-limited brightness function:

$$B(x,y) = \begin{cases} B(x,y) & |x| \leq L_x,\ |y| \leq L_y \\ 0 & \text{otherwise} \end{cases}$$

Let $\beta(x,y)$ be the periodic extension of $B(x,y)$, such that $\beta(x+pL_x,\ y+qL_y) = B(x,y)$, if p,q are integers.. We can expand $\beta(x,y)$ in a 2-D Fourier series:

$$\beta(x,y) = \sum_{n=-\infty}^{\infty} \sum_{m=-\infty}^{\infty} C_{n,m}\, e^{-i\left(\frac{2\pi nx}{2L_x} + \frac{2\pi my}{2L_y}\right)}$$

Notethat $2L_x$ and $2L_y$ give the full source extent along the x and y axes, respectively. The Fourier coefficients are given by

$$C_{n,m} = \frac{1}{2L_x}\int_{-L_x}^{L_x} dx\, e^{i\frac{2\pi nx}{2L_x}} \left\{ \frac{1}{2L_y}\int_{-L_y}^{L_y} \frac{dy}{} e^{i\frac{2\pi my}{2L_y}}\, \beta(x,y) \right\}$$

$$= \frac{1}{4L_xL_y}\int_{-L_x}^{L_x} dx \int_{-L_y}^{L_y} dy\, \beta(x,y)\, e^{i\left(\frac{2\pi nx}{2L_x} + \frac{2\pi my}{2L_y}\right)}$$

In the region of interest, $\beta(x,y)$ $B(x,y)$, so we may write

$$B(x,y) = \begin{cases} \sum_{n=-\infty}^{\infty} \sum_{m=-\infty}^{\infty} C_{n,m}\, e^{-i\left(\frac{2\pi nx}{2L_x} + \frac{2\pi my}{2L_y}\right)} & \text{FOR } |x| \leq L_x,\ |y| \leq L_y \\ 0 & \text{OTHERWISE} \end{cases}$$

Let V(u,v) be the visibility function which is the Fourier transform of the brightness function B(x,y):

$$B(x,y) = \int_{-\infty}^{\infty} du \int_{-\infty}^{\infty} dv\, e^{-i2\pi(ux+vy)}\, V(u,v)$$

Since B(x,y)=0 outside the region $|x| \leq L_x$, $|y| \leq L_y$, we have for the inverse transformation:

$$V(u,v) = \int_{-L_x}^{L_x} dx \int_{-L_y}^{L_y} dy \; e^{i2\pi(ux+vy)} B(x,y).$$

Consider the particular values of V(u,v) at the regularly spaced lattice points

$$\left(u = \frac{n}{2L_x}, \; v = \frac{m}{2L_y}\right).$$

Note that the point (0,0) is included in this set. At these points, we have

$$V\left(\frac{n}{2L_x}, \frac{m}{2L_y}\right) = \int_{-L_x}^{L_x} dx \int_{-L_y}^{L_y} dy \; B(x,y) \, e^{i\left(\frac{2\pi nx}{2L_x} + \frac{2\pi my}{2L_y}\right)}.$$

Comparing this equation with the previous one for $C_{n,m}$ shows that

$$C_{n,m} = \frac{1}{4L_xL_y} V\left(\frac{n}{2L_x}, \frac{m}{2L_y}\right)$$

Thus, we see that a knowledge of periodically sampled values of the visibility function in the u-v plane provides all necessary Fourier series coefficients $C_{n,m}$ to completely determine the function B(x,y) exactly. Hence we can write

$$B(x,y) = \sum_{n=-\infty}^{\infty} \sum_{m=-\infty}^{\infty} C_{n,m} \, e^{-i\left(\frac{2\pi nx}{2L_x} + \frac{2\pi my}{2L_y}\right)}$$

$$= \frac{1}{4L_xL_y} \sum_{n=-\infty}^{\infty} \sum_{m=-\infty}^{\infty} V\left(\frac{n}{2L_x}, \frac{m}{2L_y}\right) e^{-i\left(\frac{2\pi nx}{2L_x} + \frac{2\pi my}{2L_y}\right)}.$$

Of course, exact knowledge of B(x,y) implies that V(u,v) is also completely specified from the Fourier transform relations.

We therefore conclude that for a region-limited brightness function, knowledge of periodically sampled values of the associated

visibility function completely specifies B(x,y) and V(u,v). The proper lattice constants for the periodic sampling lattice are

$$\Delta u = \frac{1}{2L_x} \equiv T_{u,NI} \quad , \quad \Delta v = \frac{1}{2L_y} \equiv T_{v,NI}$$

where $T_{u,NI}$ and $T_{v,NI}$ refer to the "Nyquist interval" lengths along the u and v axes, repectively.

Because B is a real function and V is therefore Hermitian, we can further reduce the sampling requirement. Only two adjacent quadrants need be periodically sampled in order to reproduce B(x,y) and V(u,v) exactly, since samples of V(u,v) in these two quadrants are related to the sample values (on a regular lattice) in the other two quadrants by the Hermiticity property. If we write

$$V\left(\frac{n}{2L_x}, \frac{m}{2L_y}\right) = V_r\left(\frac{n}{2L_x}, \frac{m}{2L_y}\right) + i\, V_i\left(\frac{n}{2L_x}, \frac{m}{2L_y}\right)$$

and expand the complex exponential in terms of sines and cosines, we can simplify to get

$$B(x,y) = \sum_{n=-\infty}^{\infty} \frac{1}{4L_xL_y} \left\{ V_r\left(\frac{n}{2L_x}, 0\right) \cos 2\pi \frac{nx}{2L_x} + V_i\left(\frac{n}{2L_x}, 0\right) \sin 2\pi \frac{nx}{2L_x} \right\}$$

$$+ \frac{1}{2L_xL_y} \sum_{n=-\infty}^{\infty} \sum_{m=1}^{\infty} \left\{ V_r\left(\frac{n}{2L_x}, \frac{m}{2L_y}\right) \cos 2\pi \left(\frac{nx}{2L_x} + \frac{my}{2L_y}\right) + V_i\left(\frac{n}{2L_x}, \frac{m}{2L_y}\right) \cdot \sin 2\pi \left(\frac{nx}{2L_x} + \frac{my}{2L_y}\right) \right\}$$

Note the similarity of this result to that obtained for $B_\delta(x,y)$; if the averaging intervals $T_{u,n}$ and $T_{v,m}$ were fixed at the Nyquist intervals, and we replaced the average values by sample values, then the results would be identical (since $u_n = \frac{n}{2L_x}$ and $v_m = \frac{m}{2L_y}$ now).

2.4.4 Aliasing

Conceptually, the aliasing effect in 1-D is identical to the effect in 2-D. Therefore, we will base our discussion and work in one dimension, and state the very obvious generalizations to two dimensions.

In one dimension, the Sampling Theorem may be written for a real function B(x) which is band-limited in $|x| \leq L_x$, as:

$$B(x) = T_{NI} V_r(0) + 2T_{NI} \sum_{n=1}^{\infty} \left\{ V_r(nT_{NI}) \cos 2\pi n T_{NI} x + V_i(nT_{NI}) \sin 2\pi n T_{NI} x \right\}$$

where $T_{NI} \equiv \frac{1}{2L_x}$, and $2L_x$ is the full 1-D source extent. The expression written for B(x) is recognized as just a standard Fourier series expansion for that function in its domain of definition $[-L_x, L_x]$. Note that the periods, $X_{p,NI}$, of both trig functions are defined by

$$X_{p,NI} = \frac{1}{nT_{NI}} = \frac{2L_x}{n}$$

The fundamental period occurs for n=1, with all other values of n producing shorter harmonic periods. Since all terms in the sum have the common beat period $2L_x$, we see that the superposition of the various harmonic terms produces a function $\beta(x)$ which is identical to B(x) in the interval $[-L_x, L_x]$ and reproduces B(x) periodically along the entire x axis with period $X_{p=1,NI}=2L_x$ in the bands $[rL_x, (r+2)L_x]$, r=odd integer. This is, of course, the standard periodic extension of a function when represented by its Fourier series. What is important to recognize for our considera-

tions is that the particular choice of T_{NI} for the sampling interval produces a Fourier expansion which properly "fits" into the true domain of definition for B(x), $[-L_x, L_x]$. $\beta(x)$ reproduces B(x) in each band without interference between bands if we sample at intervals T_{NI} because all terms in $\beta(x)$ have the common beat period $2L_x$. Figure 2.5a illustrates this case.

Suppose now that we consider sampling V(u) at intervals $T_< < T_{NI}$. The Sampling Theorem result then is

$$B_<(x) = T_< V_r(0) + 2T_< \sum_{n=1}^{\infty} \left\{ V_r(nT_<) \cos 2\pi n T_< x + V_i(nT_<) \sin 2\pi n T_< x \right\}.$$

The period is, now

$$X_{p,<} = \frac{1}{nT_<} > \frac{1}{nT_{NI}}$$

and the common beat period is

$$\frac{1}{T_>} > \frac{1}{T_{NI}}.$$

$\beta_<(x)$ is the periodic extension for this Fourier series which matches B(x) in the interval

$$\left[-\frac{1}{2T_<}, \frac{1}{2T_<}\right]$$

and reproduces B(x) an all intervals

$$\left[-\frac{r}{2T_<}, \frac{r+2}{2T_<}\right]$$

with r an odd integer. We immediately see that, since the period here is greater than $X_{p=1,NI}$ we still prevent interference between bands. Note that we may define a band-limited function $B_<(x)$ which is identical with B(x) in $[-L_x, L_x]$ and zero outside this interval, but whose basic domain of definition is chosen as

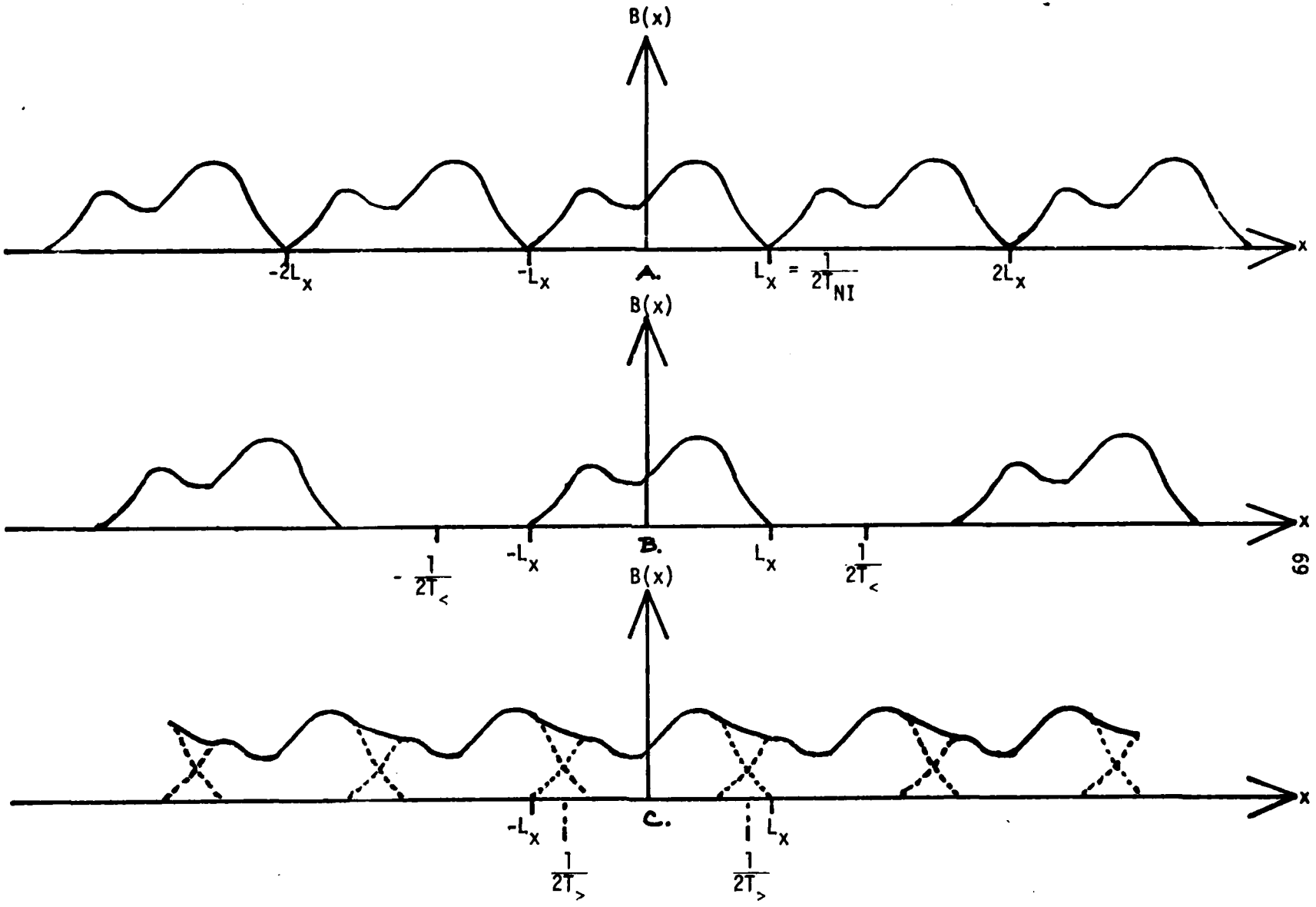

FIGURE 2.5 -- Aliasing Effects

$[-L_x-\delta_x, L_x+\delta_x], \delta_x>0$. If $V_<(u)$ $B_<(x)$ then the sampling theorem properly applies here with $T_{<,Ni} \equiv \frac{1}{2(L_x+\delta_x)}$. But clearly $V(u) \equiv V_<(u)$ since the Fourier transform integral is performed over the entire one-dimensional space. As illustrated in Figure 2.5b, $B_<(x)$ is identical with $B(x)$ in $[-L_x, L_x]$ but its periodic bands are now spaced a distance apart instead of being juxtaposed. Since we are really interested only in the function $B(x)$, we conclude that sampling at $T \leq T_{NI}$ is capable of reproducing $B(x)$ exactly in the region of interest.

Now consider $T_>>T_{NI}$ as the sampling interval. The component periods in $\beta_>(x)$ now are

$$X_{p,>} = \frac{1}{nT_>} < \frac{1}{nT_{NI}}$$

and the common beat period for all terms is

$$\frac{1}{T_>} < \frac{1}{T_{NI}} = 2L_x$$

We have a situation where other bands have a non-harmonic overlap into the interval $[-L_x, L_x]$, and $B(x)$ is not exactly reproduced in its basic domain of definition. Thus, sampling at $T>T_{NI}$ causes distortion of $B(x)$. We will presently show by an argument using the Convolution Theorem [based on a similar discussion by Bracewell (1978)] that the effect of using $T_>$ is to simply cause $\beta_>(x)$ to be a superposition of overlapping bands wherein $\beta_>(x)$ would match $B(x)$ except for the overlap effects. It is not possible to deduce the true form of $B(x)$ by compensating for the overlap in some way, and thus sampling $V(u)$ at $T>T_{NI}$ results in an unrecoverable loss of information on $B(x)$.

We can concisely prove these observations by using the Convolution Theorem. We define the Sampling Function by

$$\text{III}\left(\frac{u}{T}\right) \equiv T \sum_{n=-\infty}^{\infty} \delta(u - nT)$$

where T is the sampling interval. Sampling V(u) at intervals T is equivalent to multiplying V(u) by $\text{III}(\frac{u}{T})$. Denoting the sampled visibility function by $V_s(u)$, we write $V_s(u) = V(u) \cdot \text{III}(\frac{u}{T})$. Let $B(x)$ be the Fourier transform of $V_s(u)$. Then the Convolution Theorem gives us

$$B(x) = \mathcal{F}^{-1}\{V_s(u)\} = \mathcal{F}^{-1}\{V(u)\} * \mathcal{F}^{-1}\left\{\text{III}\left(\frac{u}{T}\right)\right\}$$
$$= B(x) * \mathcal{F}^{-1}\left\{\text{III}\left(\frac{u}{T}\right)\right\}.$$

The Fourier transform of a sampling function is another sampling function, $\text{III}(u) \supset \text{III}(x)$ [see Bracewell (1978) for a discussion of the proof of this transform pair]. By the Similarity Theorem, we then have

$$\mathcal{F}^{-1}\left\{\text{III}\left(\frac{u}{T}\right)\right\} = \sum_{n=-\infty}^{\infty} \delta\left(x - \frac{n}{T}\right) \equiv T\,\text{III}(Tx).$$

So,

$$B(x) = B(x) * T\,\text{III}(Tx)$$
$$= \int_{-\infty}^{\infty} dx'\, B(x') \left[\sum_{n=-\infty}^{\infty} \delta\left(x - x' - \frac{n}{T}\right)\right]$$
$$= \sum_{n=-\infty}^{\infty} \int_{-\infty}^{\infty} dx'\, B(x')\, \delta\left(x - x' - \frac{n}{T}\right)$$
$$= \sum_{n=-\infty}^{\infty} B\left(x - \frac{n}{T}\right).$$

This result clearly reveals the effect of the size of the sampling inteval. For B(x) band-limited in $[-L_x,L_x]$, then clearly $T_{NI}=\frac{1}{2L_x}$ causes $\beta(x)$ to be a non-overlapping periodic extension of B(x). Similarly, for $T<T_{NI}$, we simply widen the bands, as was illustrated in Figure 2.5b. For $T>T_{NI}$, then $\frac{1}{T}<2L_x$ and we see that the bands now overlap, producing a distored version of B(x) in the interval of interest $[-L_x,L_x]$. The present statement of this result lucidly shows that the distortion results from superposition of different bands, each of which may be conceived as containing one undistorted period of B(x). (See Figure 2.5c)

The term "aliasing" has been used to describe this effect because sampling at intervals greater than the Nyquist causes spatial frequencies in different bands to mix due to the overlapping of the bands. It is therefore said that higher spatial frequencies are posing as lower frequencies, and hence the higher frequencies have lower frequency aliases because of the overlapping.

The generalization to two dimensions is quite straightforward. Sampling in 2-D is performed on a rectangular lattice in the u-v plane, and sampling along any line of lattice points in the u or v directions is independent of behavior in the other direction and hence exactly equivalent to the 1-D case. We can therefore think of the 2-D lattice as being a direct product of two 1-D lattices. We then have

$$\beta(x,y) = B(x,y) * T_u T_v \text{III}(T_u x, T_v y)$$

where

$$\text{III}(T_u x, T_v y) \equiv \text{III}(T_u x)\,\text{III}(T_v y)$$

$$= \left[\sum_{m=-\infty}^{\infty} \frac{1}{T_u}\,\delta\left(x - \frac{m}{T_u}\right)\right] \cdot \left[\sum_{m=-\infty}^{\infty} \frac{1}{T_v}\,\delta\left(y - \frac{m}{T_v}\right)\right]$$

The result is:

$$\beta(x,y) = \sum_{n=-\infty}^{\infty} \sum_{m=-\infty}^{\infty} B\left(x - \frac{n}{T_u}, y - \frac{m}{T_v}\right).$$

We immediately see that all of the previously discussed cases for one-dimension apply to <u>each</u> argument of B independently. In other words, for true recovery of B(x,y) in the region of interest $\{[-L_x, L_x], [-L_y, L_y]\}$, we must have $T_u \leq T_{u,NI} \equiv \frac{1}{2L_x}$ <u>and</u> $T_v \leq T_{v,NI} \equiv \frac{1}{2L_y}$. If the sampling interval along u or v exceeds its relevant Nyquist length, then aliasing effects occur and B(x,y) will be distorted along the respective direction (i.e., if $T_u \leq T_{u,NI}$ but $T_v > T_{v,NI}$, distortion of B(x,y) occurs only parallel to the y axis).

We will call a rectangular cell with edge lengths $T_{u,NI}$ and $T_{v,NI}$ a Nyquist cell. When we say that a given cell is smaller than the Nyquist cell size, we mean that $T_u \leq T_{u,NI}$ and $T_v \leq T_{v,NI}$ for the given cell. A cell which is referred to as being larger than a Nyquist cell will have $T_u > T_{u,NI}$ or $T_v > T_{v,NI}$, or both.

2.4.5 <u>Effect of the Epoch of Sampling</u>

Heretofore, we have used the Sampling Theorem with the epoch of sampling at the origin, which is the conventional statement of the theorem. We now investigate the effect of an epoch of sampling

not based on the origin. Again, we will work in 1-D and state the generalization to 2-D.

Suppose that we sample V(u) at regular intervals T, but we do not center the samples on u=0; this is equivalent to shifting the Sampling Function by some increment a, with 0<a<T. Then

$$\text{Ш}\left(\frac{u}{T}\right) \rightarrow \text{Ш}\left(\frac{u}{T}-a\right).$$

The sampled visibility function $V_s(u)$ is now

$$V_s(u) = V(u)\cdot \text{Ш}\left(\frac{u}{T}-a\right).$$

From the Shift Theorem, we have

$$\mathcal{F}^{-1}\left\{\text{Ш}\left(\frac{u}{T}-a\right)\right\} = e^{-i2\pi a x}\, T\,\text{Ш}(Tx).$$

The Convolution Theorem then requires that the Fourier transform of $V_s(u)$ be:

$$\beta_a(x) = \mathcal{F}^{-1}\{V_s(u)\} = B(x) * e^{-i2\pi a x}\, T\,\text{Ш}(Tx)$$
$$= T\int_{-\infty}^{\infty} dx'\, B(x-x')\, e^{-i2\pi a x'}\left[\frac{1}{T}\sum_{n=-\infty}^{\infty}\delta\left(x'-\frac{n}{T}\right)\right]$$
$$= \sum_{n=-\infty}^{\infty} e^{-i2\pi a\frac{n}{T}}\, B\left(x-\frac{n}{T}\right)$$

As before, $B(x-\frac{n}{T})$ is a periodic extension of the band-limited function B(x). Now, however, $\beta_a(x)$ has a complex factor in its terms. Note that $\frac{a}{T}<1$, and if $\frac{a}{T}$ is irrational, then $e^{-i2\pi n\frac{a}{T}}$ is non-periodic. If $\frac{a}{T}$ is rational, then $e^{-i2\pi n\frac{a}{T}}$ is periodic in n. Suppose that $\bar{n}$ is the integer period such that $\bar{n}a=T$ and

$$e^{-i2\pi\frac{a}{T}(n+r\bar{n})} = e^{-i2\pi\frac{a}{T}n}$$

for any integer r. Then the complex function $\beta_a(x)$ will have a period $\frac{\bar{n}}{T} = \frac{1}{a}$. In particular, for $T=T_{NI}$, $\beta_a(x)$ has a period $\bar{n}2L_x = \frac{2TL_x}{a} > 2L_x$. Hence, if $T \leq T_{Ni}$, no overlapping occurs, and we see that for n=0, we do in fact recover B(x) in the interval of interest $[-L_x, L_x]$.

Consider the case $T>T_{NI}$ now. Clearly, we will have overlapping as discussed previously, but the distortion now will be far worse than when the epoch of sampling was at the origin, because the adjacent bands which mix into the region of interest have complex weighting factors in them.

The generalization to 2-D incorporates a translational displacement of the epoch of sampling for the lattice from (u=0,v=0) to (a,b). The result is

$$\beta_{a,b}(x,y) = \sum_{n=-\infty}^{\infty} \sum_{m=-\infty}^{\infty} B\left(x - \frac{n}{T_u}, y - \frac{m}{T_v}\right) e^{-i2\pi \frac{a}{T_u} n} e^{-i2\pi \frac{b}{T_v} m}.$$

The cases discussed above for 1-D apply separately now to each coordinate.

As a simple illustration of the effect of the epoch of sampling in one-dimension, let us consider a case where $a=\frac{T}{2}$ for the conjugate pair V(u) = sinc u $1-|x| = B(x)$ for $|x| \leq 1$. We have $T_{NI} = \frac{1}{2L_x} = .5$. The complex modulating factor is now $e^{-i\pi n}$, with period $\bar{n}=2$. But

$$e^{-in\pi} = \begin{cases} +1 & n \text{ even} \\ -1 & n \text{ odd} \end{cases}$$

The resulting function $\beta_a(x)$ for $T=T_{NI}$ is pictured as:

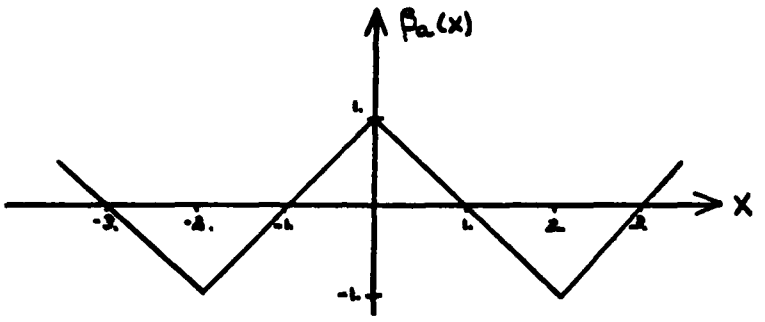

as compared with the standard Sampling Theorem result for sampling epoch at the origin:

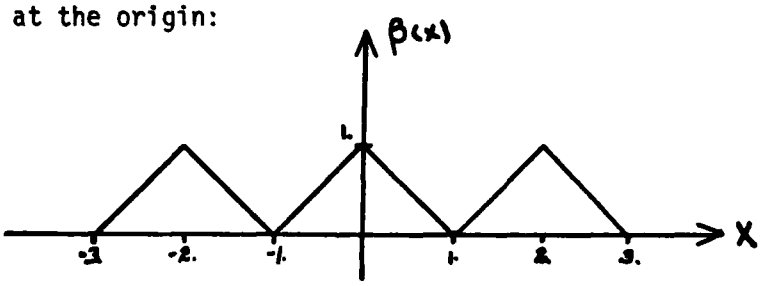

Based on the considerations of this section, it is considered preferable to use an epoch of sampling at the origin. In our discussions, we will want to consider averaging cells with dimensions both smaller and larger than the Nyquist cell. When we represent the average value of V(u,v) over a cell by a delta function at the cell midpoint, we are imitating the sampling process, and hence the observations on the effects of cell size versus Nyquist cell size are applicable. If we average over the entire visibility

function with cell sizes equal to or smaller than the Nyquist cell size, then aliasing effects will not be present and the transform of the averaged function will represent B(x,y) except for possible distortion due to the fact that average values were used instead of true sample values. Averaging with cell sizes greater than the Nyquist cell size produces greater distortion due to aliasing effects. As we have seen, an epoch at the origin produces less distortion than a shifted epoch in cases where the Nyquist size is exceeded, and we would therefore prefer to use an averaging epoch at the origin (u=0,v=0) for these cases. Since we will be considering various averaging cell sizes, and since the epoch does not affect the result in the region of interest for cells smaller than the Nyquist cell whereas it may adversely affect the result for cell sizes greater than the Nyquist cell size, we see that fixing the epoch of averaging at the origin for all cases of cell size (including mixed cell sizes) is the best prescription. It should be noted that in an actual experiment, it may not be possible to choose an epoch of sampling at the origin. However, although the elliptical tracks may not conform with a sampling or averaging epoch at the origin, if the data are gridded onto a rectangular lattice, then it would be preferable to use a lattice with epoch at the origin if such an extrapolation is feasible.

CHAPTER 3

THE STANDARD FOURIER TRANSFORM METHOD

3.1 Statement of the Method

In an actual experiment, $V(u,v)$ can be examined over only a finite portion of the u-v plane, and hence the visibility function is effectively truncated. We will assume that the truncation is symmetric in u and v (or has been made symmetric as previously discussed). We have shown above that the Fourier transform of the truncated and averaged visibility function is

$$\hat{B}_\delta(x,y) = \sum_{n=-N}^{N} T_{u,n} T_{v,0} \left\{ [\bar{V}_{n,0}]_r \cos 2\pi u_n x + [\bar{V}_{n,0}]_i \sin 2\pi u_n x \right\}$$
$$+ 2 \sum_{n=-N}^{N} \sum_{m=1}^{M} T_{u,n} T_{v,m} \left\{ [\bar{V}_{n,m}]_r \cos 2\pi (u_n x + v_m y) \right.$$
$$\left. + [\bar{V}_{n,m}]_i \sin 2\pi (u_n x + v_m y) \right\}$$

where $T_{u,n}, T_{v,m}$ are the averaging cell lengths in the u and v directions, respectively; (u_n, v_m) is the midpoint of the $(n,m)^{th}$ cell in which the average value is

$$[\bar{V}_{n,m}] = [\bar{V}_{n,m}]_r + i\,[\bar{V}_{n,m}]_i \,.$$

For completeness, we state the result for asymmetrical truncation:

$$\hat{B}_\delta(x,y) = \sum_{n=-N_1}^{N_2} \sum_{m=-M_1}^{M_2} T_{u,n} T_{v,m} [\bar{V}_{n,m}] e^{-i2\pi(u_n x + v_m y)} .$$

For asymmetrical truncation, $\hat{B}_\delta(x,y)$ will be complex.

We can easily show that, for a given truncation of the

visibility function, the value of $\hat{B}_\delta(0,0)$ is independent of the particular averaging lattice which is used, and is in fact equal to $\tilde{B}(0,0)$, the origin value of the function resulting from truncation of V(u,v) alone, without averaging. We have shown that the effect of truncating V(u,v) produces

$$\tilde{B}(x,y) = B(x,y) * \left[e^{-i2\pi(c_u x + c_v y)} \frac{\sin \pi b_u x}{\pi x} \quad \frac{\sin \pi b_v y}{\pi y} \right]$$

where: c_i = i coordinate value of the midpoint of the non-truncated portion of V(u,v)

b_i = length along the i axis of the non-truncated part of V(u,v).

By the Convolution Theorem,

$$\tilde{B}(x,y) = \int_{-\infty}^{\infty} du \int_{-\infty}^{\infty} dv \; e^{-i2\pi(ux+vy)} \left[V(u,v) \cdot \Pi\left(\frac{u - c_u}{b_u}, \frac{v - c_v}{b_v} \right) \right]$$

Since the integrations are independent of x and y, we have, using the definition of $\Pi\left(\frac{u - c_u}{b_u}, \frac{v - c_v}{b_v} \right)$,

$$\tilde{B}(x=0, y=0) = \int_{c_u - \frac{b_u}{2}}^{c_u + \frac{b_u}{2}} du \int_{c_v - \frac{b_v}{2}}^{c_v + \frac{b_v}{2}} dv \; V(u,v).$$

We can write $\hat{B}_\delta(x,y)$ in a form which applies to either symmetric or asymmetric truncation,

$$\hat{B}_\delta(x,y) = \sum_{n=-N_1}^{N_2} \sum_{m=-M_1}^{M_2} T_{u,n} T_{v,m} \left[\bar{V}_{n,m} \right] e^{-i2\pi(u_n x + v_m y)}$$

where $\sum_{m=-M_1}^{M_2} T_{u,m} = b_u$, $\sum_{m=-M_1}^{M_2} T_{v,m} = b_v$,

$$\left(\frac{T_{u,0}}{2} + \sum_{m=1}^{M_2} T_{u,m}\right) - \left(\frac{T_{u,0}}{2} + \sum_{m=-M_1}^{-1} T_{u,m}\right) = C_u \quad , \quad \left(\frac{T_{v,0}}{2} + \sum_{m=1}^{M_2} T_{v,m}\right) - \left(\frac{T_{v,0}}{2} + \sum_{m=-M_1}^{-1} T_{v,m}\right) = C_v .$$

For x=y=0, $\hat{B}_\delta(0,0) = \sum_{n=-N_1}^{N_2} \sum_{m=-M_1}^{M_2} T_{u,n}\, T_{v,m} \left[\bar{V}_{n,m}\right]$

$$= \sum_{n=-N_1, m=-M_1}^{N_2, M_2} T_{u,n}\, T_{v,m} \left\{ \frac{1}{T_{u,n}\, T_{v,m}} \int_{u_n - \frac{T_{u,n}}{2}}^{u_n + \frac{T_{u,n}}{2}} du \int_{v_m - \frac{T_{v,m}}{2}}^{v_m + \frac{T_{v,m}}{2}} dv\, V(u,v) \right\}$$

$$= \int_{C_u - \frac{b_u}{2}}^{C_u + \frac{b_u}{2}} du \int_{C_v - \frac{b_v}{2}}^{C_v + \frac{b_v}{2}} dv\, V(u,v)$$

Thus, $\hat{B}_\delta(0,0) = \tilde{B}(0,0)$ = Volume under the visibility function inside the truncation limits.

3.2 Illustrative Case: The Two Component Gaussian Source

We now want to consider a practical example to examine the effects on resolution due to truncating and averaging the visibility function. As our model source, we chose a two component Gaussian brightness distribution function. This model source has been chosen not only because of its relevance to actual observed sources which have two or more peak components in the brightness function which we wish to resolve, but also because it provides an excellent case to study changes in symmetries, the vector between the peak brightness points, and the width of the components as functions of truncation limits and averaging cell sizes.

The basic form of the brightness function for this model

source is

$$B(x,y) = e^{-\pi w[(x-1)^2+y^2]} + e^{-\pi w[(x+1)^2+y^2]}$$

where w is a parameter characterizing the width of each component. The Gaussian components have peak brightness of unity at the points (-1,0) and (1,0). Figure 3.1 illustrates the cross-section of the model source for four different values of w. Figure 3.2, a-d, presents three dimensional views of the model source for the four values of w, as well as their associated visibility functions. (Note that these source and visibility functions are smooth functions; any sharp edges in the 3-D plots are due to the mesh size used in the plotting algorithm.)

3.2.1 Exact Brightness Distribution function and Its Transform

The Fourier transform of the brightness function

$$B(x,y) = e^{-\pi w[(x-1)^2+y^2]} + e^{-\pi w[(x+1)^2+y^2]}$$

is derived as follows. Let

$$V(u,v) = \mathcal{F}\{B(x,y)\}$$

Note that

$$B(x,y) = e^{-\pi w[x^2+y^2]} * [\delta(x-1) + \delta(x+1)]$$

By the Similarity Theorem and the Separable Product Theorem, we

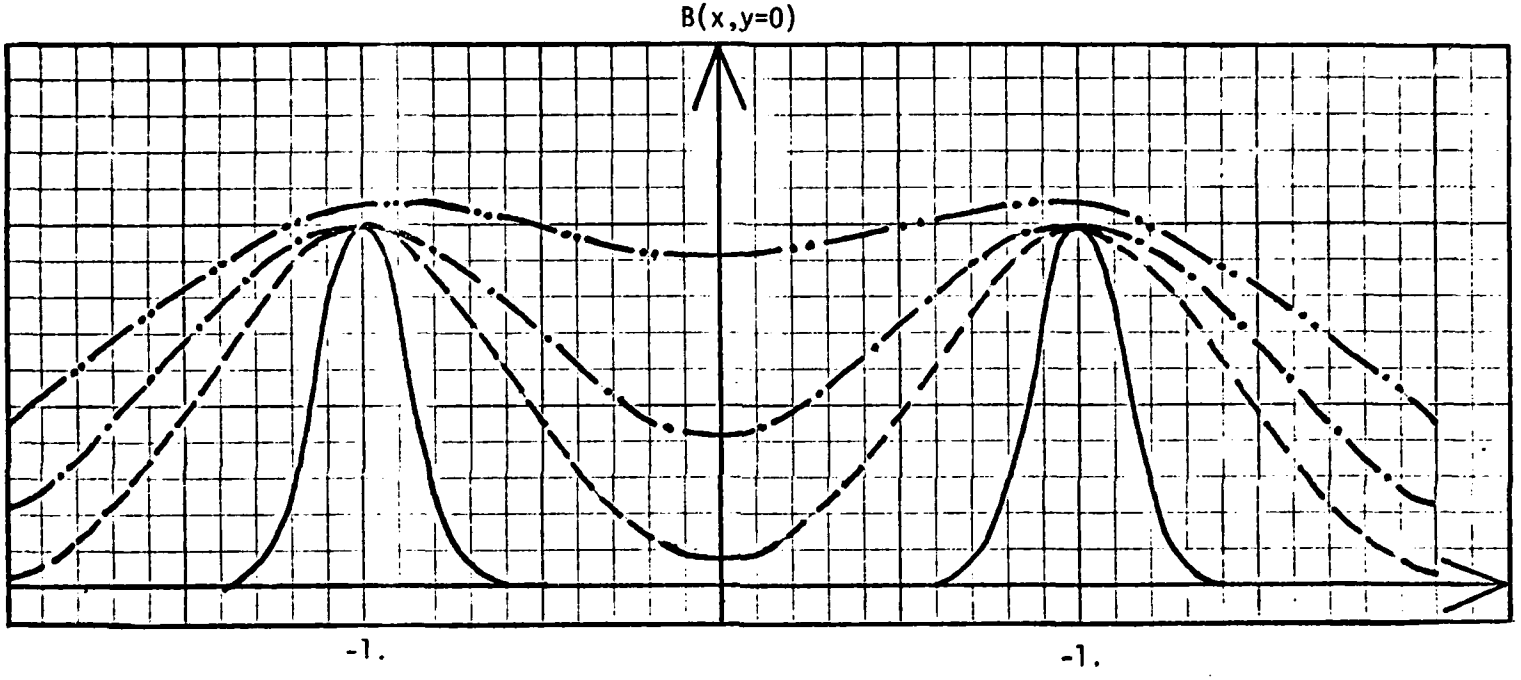

$$B_w(x,y) = e^{-\pi w[(x-1)^2+y^2]} + e^{-\pi w[(x+1)^2+y^2]}$$

——— w=10

- - - w= 1

- . - w=.5

- ·· - w=.25

FIGURE 3.1

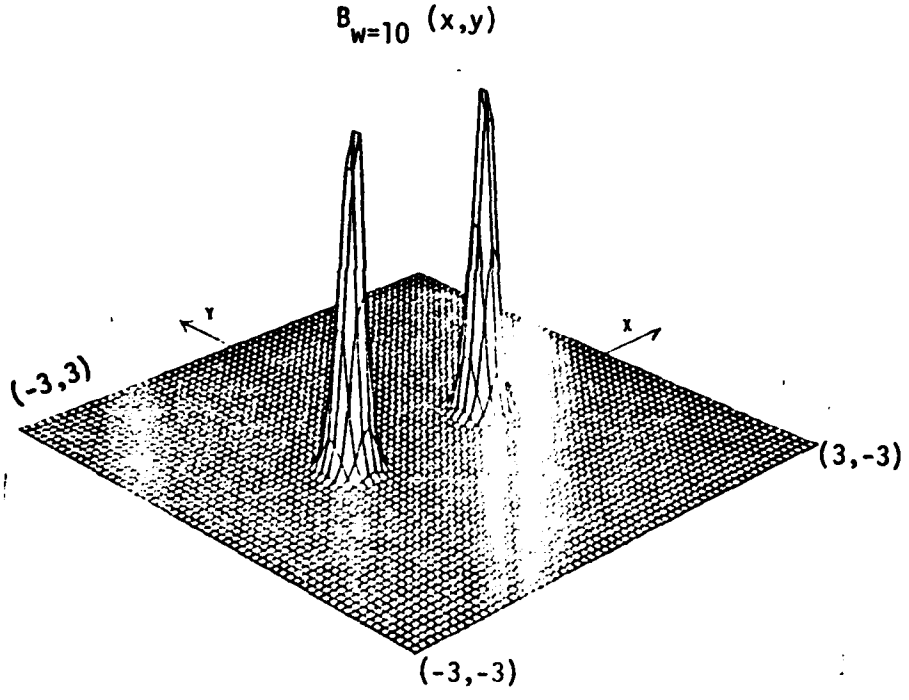
$B_{w=10}$ (x,y)
Y
X
(-3,3)
(3,-3)
(-3,-3)
$B(x,y) = e^{-\pi w[(x-1)^2+y^2]} + e^{-\pi w[(x+1)^2+y^2]}$

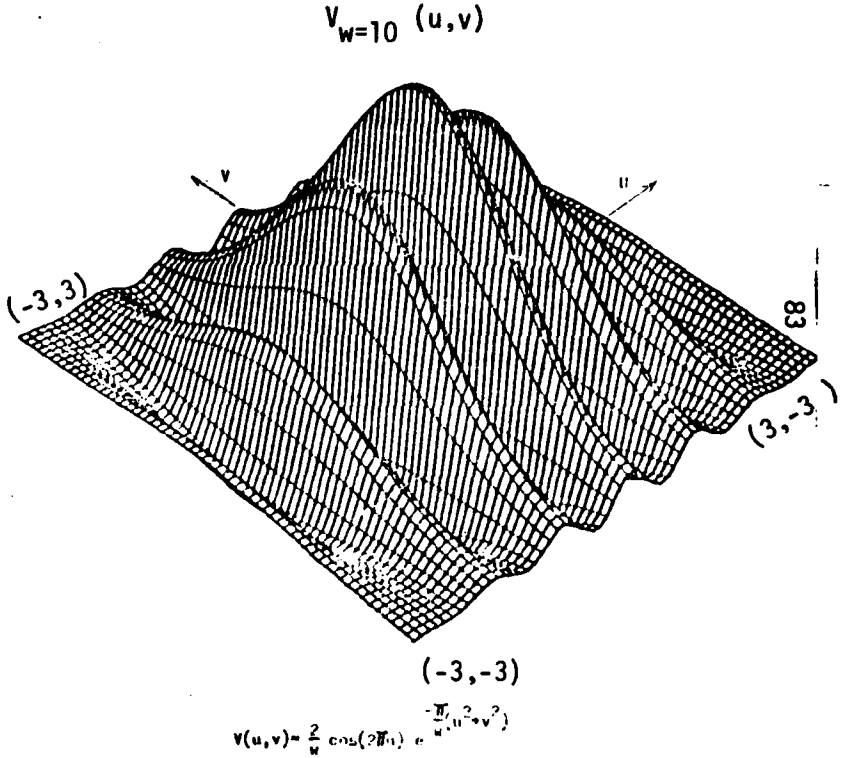
$V_{w=10}$ (u,v)
V
U
(-3,3)
(3,-3)
(-3,-3)
83
$V(u,v) = \frac{2}{w}\cos(2\pi u)\, e^{-\frac{\pi}{w}(u^2+v^2)}$

FIGURE 3.2a

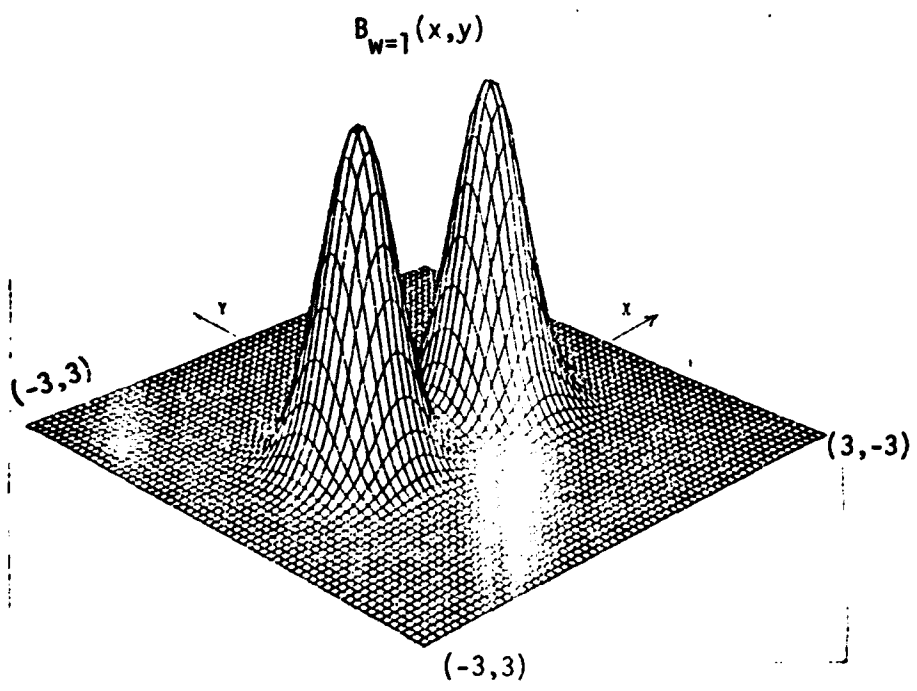

$$B(x,y) = e^{-\frac{\pi}{W}[(x-1)^2+y^2]} + e^{-\frac{\pi}{W}[(x+1)^2+y^2]}$$

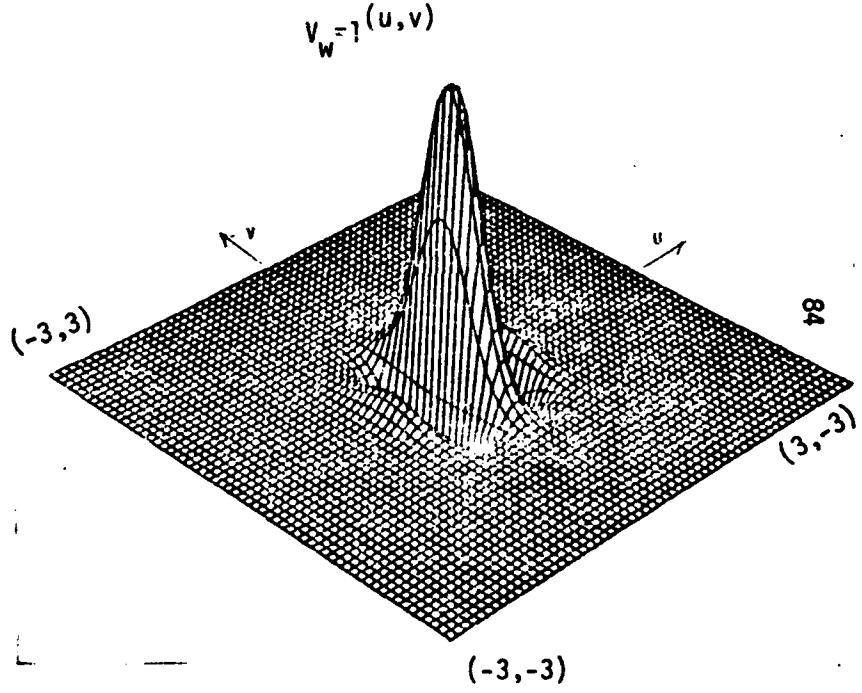

$$V(u,v) = \frac{2}{W}\cos(2\pi u)\, e^{-\frac{\pi}{W}(u^2+v^2)}$$

FIGURE 3.2b

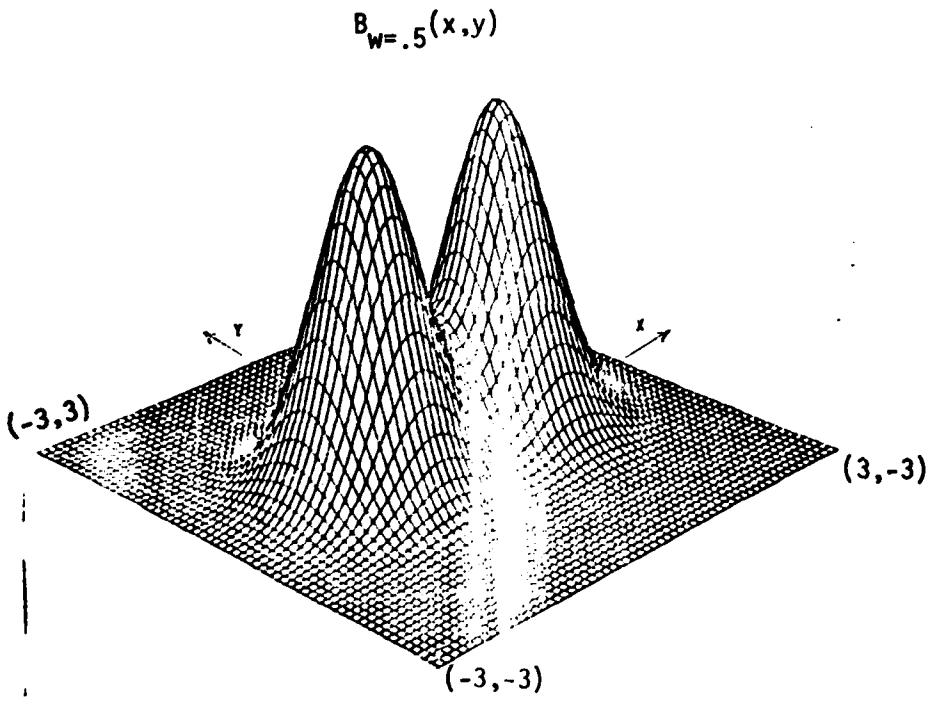
$B_{W=.5}(x,y)$
Y
X
(-3,3)
(3,-3)
(-3,-3)
$B(x,y) = e^{-\pi w[(x-1)^2+y^2]} + e^{-\pi w[(x+1)^2+y^2]}$

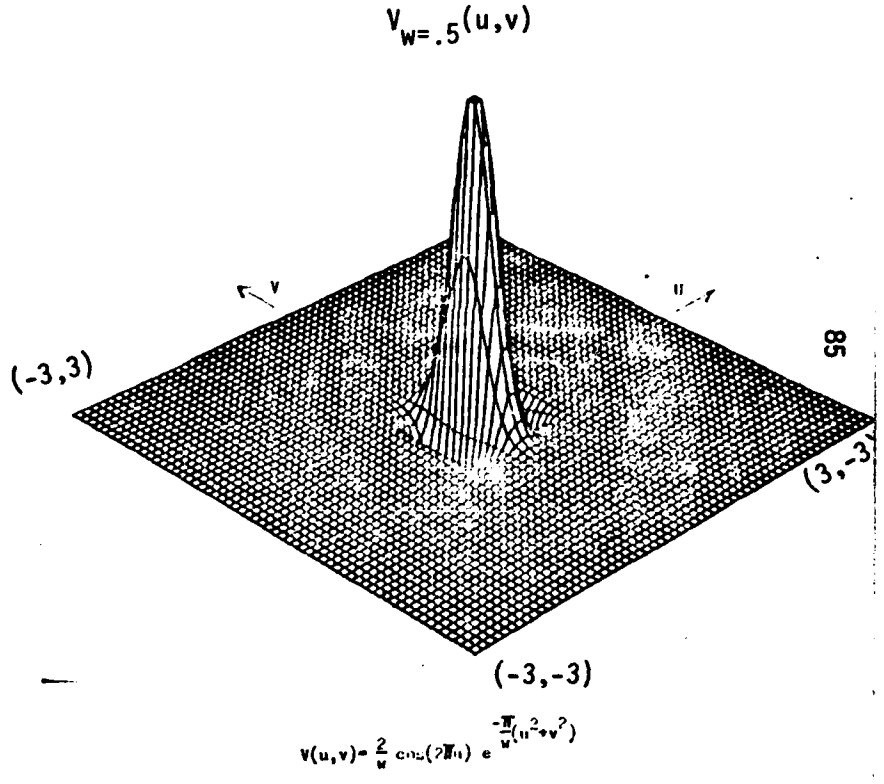
$V_{W=.5}(u,v)$
V
U
(-3,3)
(3,-3)
(-3,-3)
$V(u,v) = \frac{2}{w}\cos(2\pi u)\, e^{-\frac{\pi}{w}(u^2+v^2)}$

FIGURE 3.2c

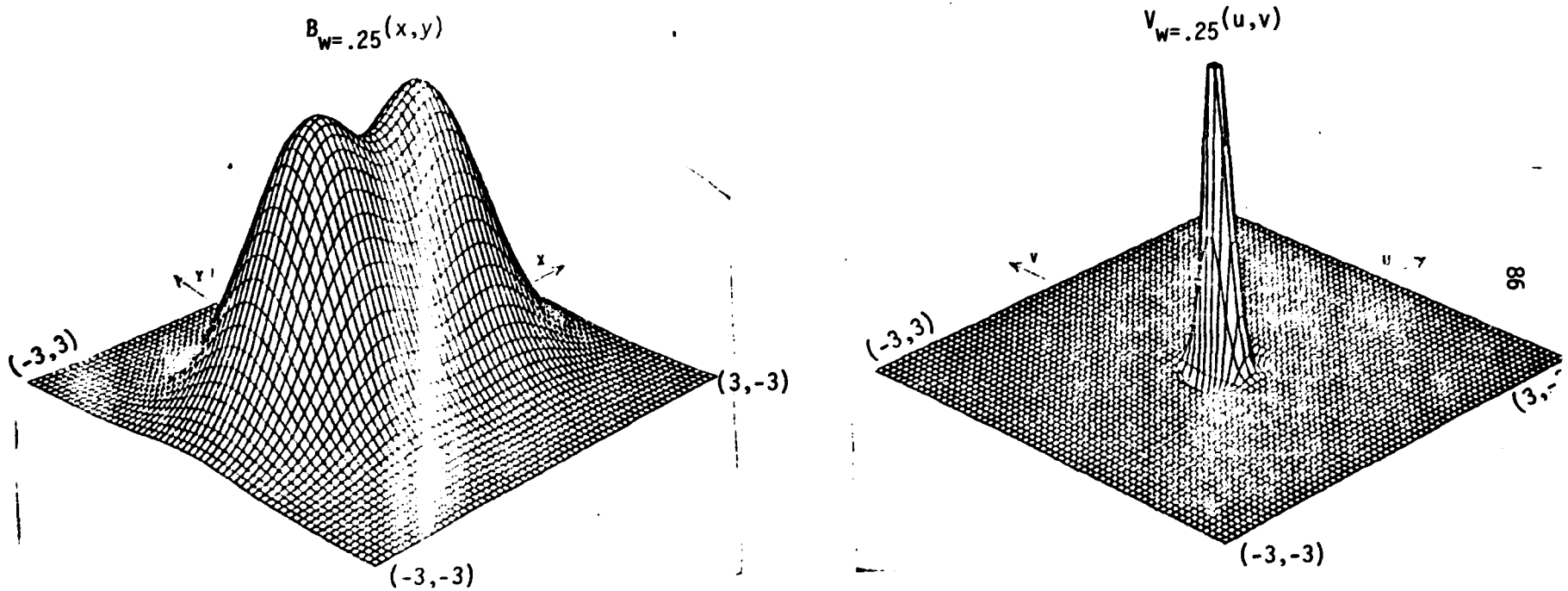

$$B(x,y) = e^{-\pi w[(x-1)^2+y^2]} + e^{-\pi w[(x+1)^2+y^2]}$$

$$V(u,v) = \frac{2}{w}\cos(2\pi u)\, e^{-\frac{\pi}{w^2}(u^2+v^2)}$$

FIGURE 3.2d

immediately have

$$\mathcal{F}\left\{e^{-\pi w[x^2+y^2]}\right\} = \frac{1}{w} e^{-\frac{\pi}{w}[u^2+v^2]}$$

and by the Shift and Addition Theorems we have

$$\mathcal{F}\left\{\delta(x-1) + \delta(x+1)\right\} = 2\cos 2\pi u.$$

Hence, by the Convolution Theorem, we get

$$V(u,v) = \frac{2}{w}\cos 2\pi u \; e^{-\frac{\pi}{w}[u^2+v^2]}.$$

Note the ease with which this transform is obtained using the theorems as opposed to a direct calculation.

Since the double-Gaussian model that we are using is not a truly region-limited function, one cannot properly define a Nyquist cell size. However, the Gaussians fall-off sufficiently fast so that we may define effective limits for the extent of B(x,y) in the x and y directions. This effective length will be specified as twice the value x_c for which B(x,y) has an amplitude less than or of the order of .001 of its peak amplitude for all $x \geq x_c$, and similarly for y_c. The effective Nyquist interval lengths are then

$$T_{u,NI} = \frac{1}{2X_c} \quad \text{and} \quad T_{v,NI} = \frac{1}{2Y_c}.$$

Table 3.1 shows the effective cut-off lengths and corresponding Nyquist intervals, as well as the peak values of B(x,y), the

TABLE 3.1

MODEL SOURCE CHARACTERISTICS

w	$B(\lvert x\rvert \geq x_c, y) \leq .001$ x_c	$T_{u,NI}$	$B(x, \lvert y\rvert \geq y_c) \leq .001$ y_c	$T_{v,NI}$	Peak Locations	Peak Magnitudes	Halfwidths
10.	1.47	.340	.47	1.064	(-1,0) (1,0)	1. 1.	.1485 .1485
1.	2.48	.2016	1.48	.3378	(-1,0) (1,0)	1. 1.	.4697 .4697
.5	3.1	.1613	2.1	.2381	(-.996,0) (.996,0)	1.0019 1.0019	.6642 .6642
.25	3.96	.1263	2.97	.1694	(-.882,0) (.882,0)	1.051 1.051	.9344 .9344

location of these peaks in the brightness function and the half-widths [defined as half the peak value in B(x,y)] for the four width values w used in this study.

It was desired to examine cases of both severe and negligible truncation of the visibility function. Since V(u,v) is sharply peaked and falls-off very fast for w=.25, whereas it decays quite slowly for w=10, it was decided that a common truncation limit of $|u|=1$ and $|v|=1$ for all cases studied would achieve the goal of examing both radical and minimal truncations.

Three different sets of averaging intervals commensurate with these truncation limits were used. One set, designated A, used averaging cells which were all smaller than the effective Nyquist cells for the w=10 and w=1 cases (but were larger than the Nyquist cells for the other two w cases). Set B used cell sizes which were all greater than the effective Nyquist cell sizes for all four w cases. Set C used cell sizes which were a mixture of cells both smaller than the smallest effective Nyquist cell and larger than the largest effective Nyquest cell in the four w cases. All cells were taken to be squares, i.e., the u and v edge lengths of any given cell were the same. The three different averaging schemes are summarized below, where it is understood that the intervals along the v axis are the same as the intervals along the u axis which are illustrated.

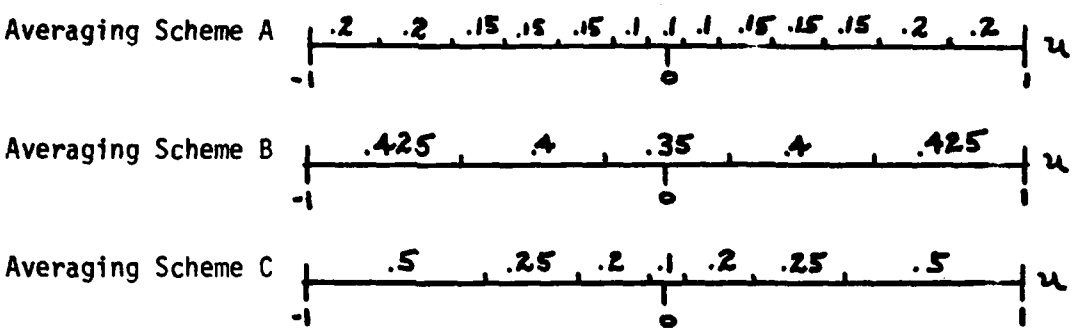

3.2.2 Method of Analysis

All of the program references in this section refer to Program A of the Appendix.

The function B(x,y) was obtained by performing the relevant convolution integral numerically. Since the magnitude of B(x,y) is less than .001 for all x and/or y values greater than 3.5 for the three cases w=10, 1, .5 (the corresponding value along the x axis for the case w=.25 is 3.96), the highest x and y values for which B(x,y) can be caluclated must be 3.5 less than the magnitude of the x' and y' limits on the respective integrals. In other words, since we must put a practical bound on how far out we go to integrate over x' and y' in the convolution integral, we must insure that the chosen limits are sufficiently far out so that effectively all of the volume under the shifted function B(x-x', y-y') in the intergrand is included in the numerical integration. The falling sinc factors, which are less than unity except at the origin, actually help to taper the integrand,

$\mathrm{sinc}(t_{u,n}x)\ \mathrm{sinc}(T_{v,m}y)\ B(x-x',y-y;)$, so that the cut-offs at 3.5 are somewhat conservative.

The expense and CPU time involved in performing the convolution integrals to a reasonable level of accuracy (about .05 of true values) limited the range of x and y values from 0 to 2.5 in increments of .25. Furthermore, $\tilde{B}(x,y)$ was actually evaluated only at lattice points in one quadrant. This was considered acceptable because the integrand arguments are even in x and y, and truncation of V(u,v) was also performed symmetrically, so that the values of $\tilde{B}(x,y)$ in one quadrant should be symmetrically related to its values in the other three quadrants.

The effective limits used for both the x' and y' integrations were -6 to 6, in accordance with the comments above. A mesh with step size .1 in both x' and y' was used to numerically evaluate the integrals. The simplest integration technique of summing over cell volumes (value of integrand at cell midpoint times the cell's base area) was used for speed; improved accuracy would involve at least a fourfold increase in computer time. To generate one value of $\tilde{B}(x,y)$ required 14,400 iterations of the summation loop to evaluate the integrals numerically,, so that even the very sparce x-y lattice containing 100 points required considerable computer time. Attempts to increase the density or extent of the lattice points examined were considered cost-ineffective for our purposes here.

Figure 3-3, a-d, illustrates the visibility function after truncation. Truncation is negligible for the cases w=.5, .25, and therefore the long convolution integral calculations were omitted for those cases.

To obtain an overall comparison of $\tilde{B}(x,y)$ with $B(x,y)$, the following parameters were defined:

$$\text{Normalized Deviation} \equiv \frac{\int dx \int dy \ [B(x,y) - \tilde{B}(x,y)]}{A}$$

$$\text{Normalized Root Deviation Squared} \equiv \frac{\sqrt{\int dx \int dy \ [B(x,y) - \tilde{B}(x,y)]^2}}{A}$$

where the integrals are performed over a square region of the x-y plane whose area is A. The division by area was included to normalize the result so that comparisons could be made with other cases where the section of the x-y plane which was examined had a different area. Since we evaluated B(x,y) only over the region 0 to 2.5 along the x and y axes, the integrals above had to be numerically performed over this single quadrant. The mesh step size was .25 along the x and y axes (the available data values for B(x,y) have this increment step), which is quite large. Therefore, the calculated parameters should not be viewed as very accurate quantities here, but rather as quantities which are only sufficiently accurate for comparitive purposes with other similarly calculated parameters.

AD-A093 792 ARMY MILITARY PERSONNEL CENTER ALEXANDRIA VA F/G 17/9
FOURIER TRANSFORMATION THEORY FOR AVERAGED FUNCTIONS, WITH APPL--ETC(U)
FEB 81 R J BONOMETTI

UNCLASSIFIED NL

2 OF 3
AD
A093792

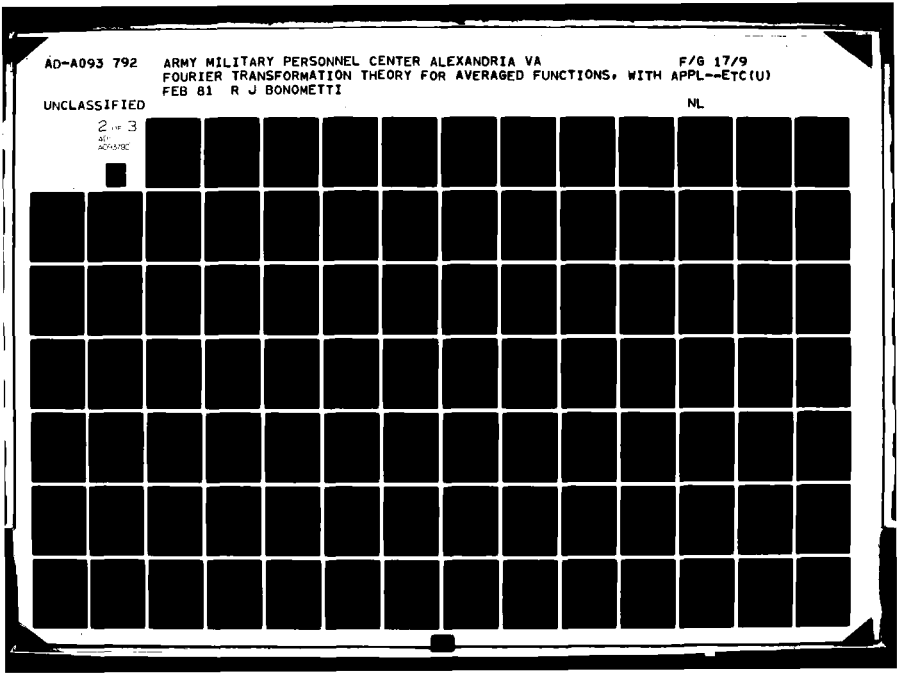

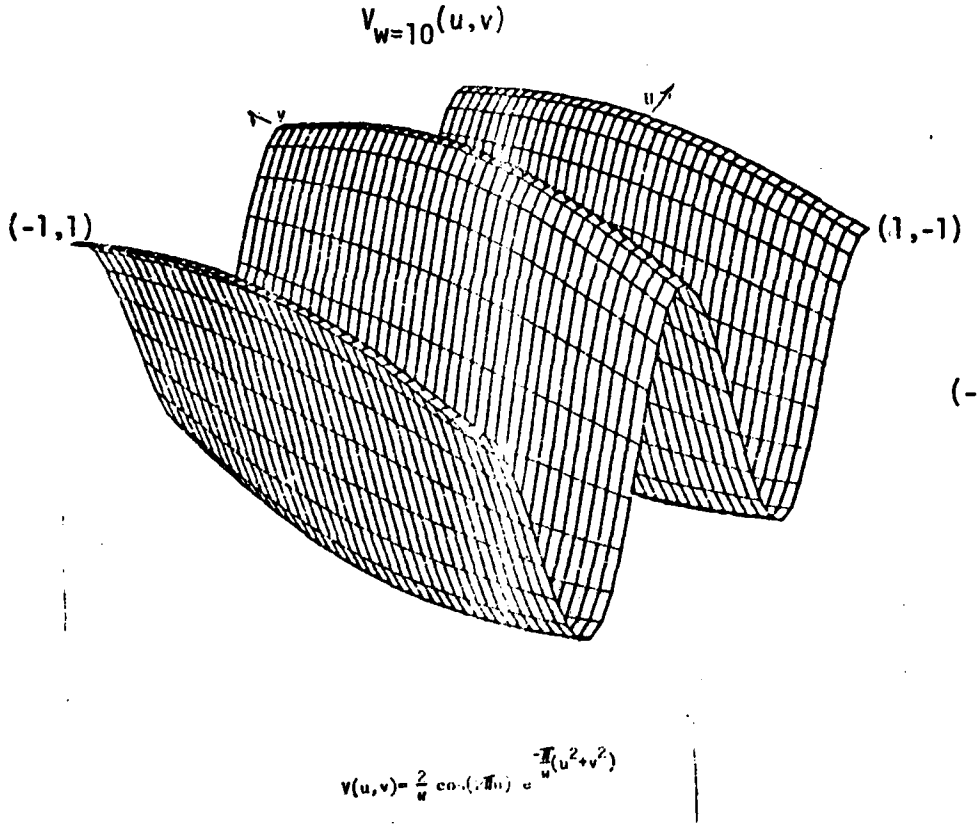

A

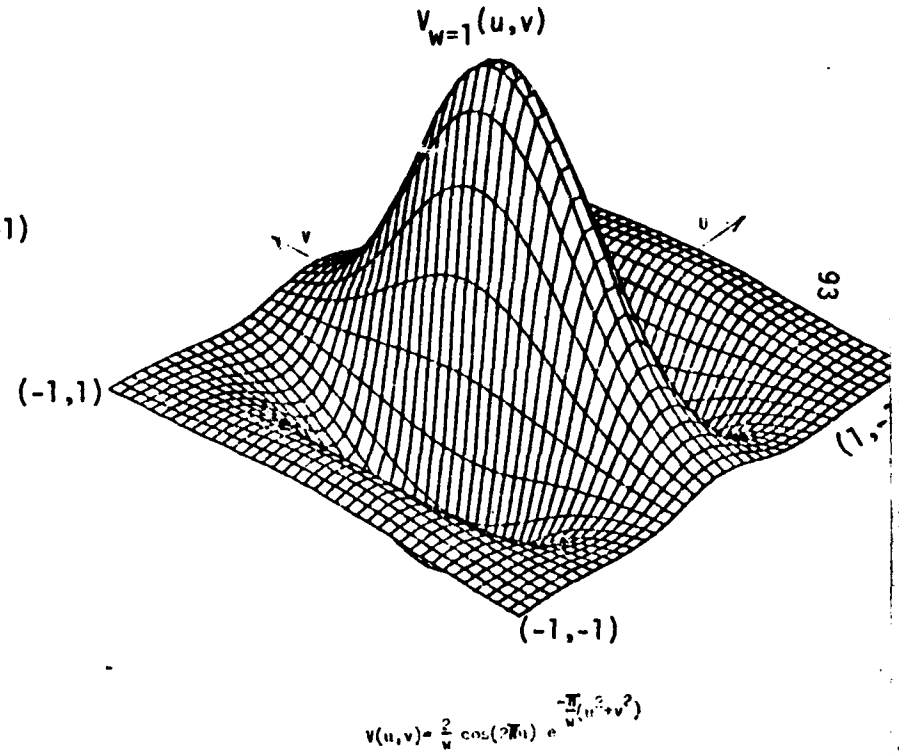

B

Truncated Visibility Functions

FIGURE 3-3

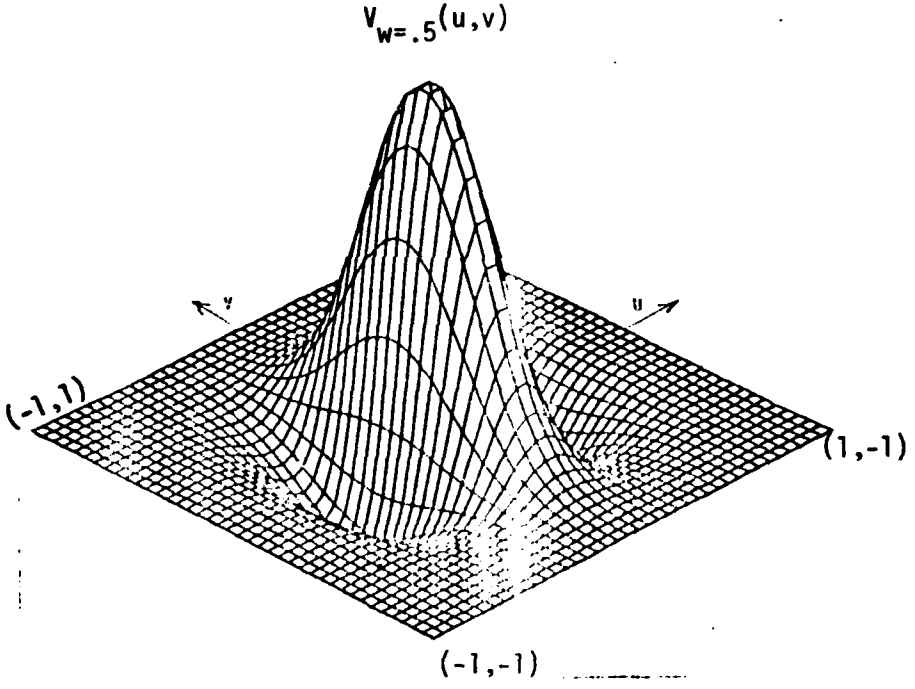

$$V(u,v) = \frac{2}{W}\cos(\pi W u)\, e^{\frac{-\pi}{W}(u^2+v^2)}$$

C

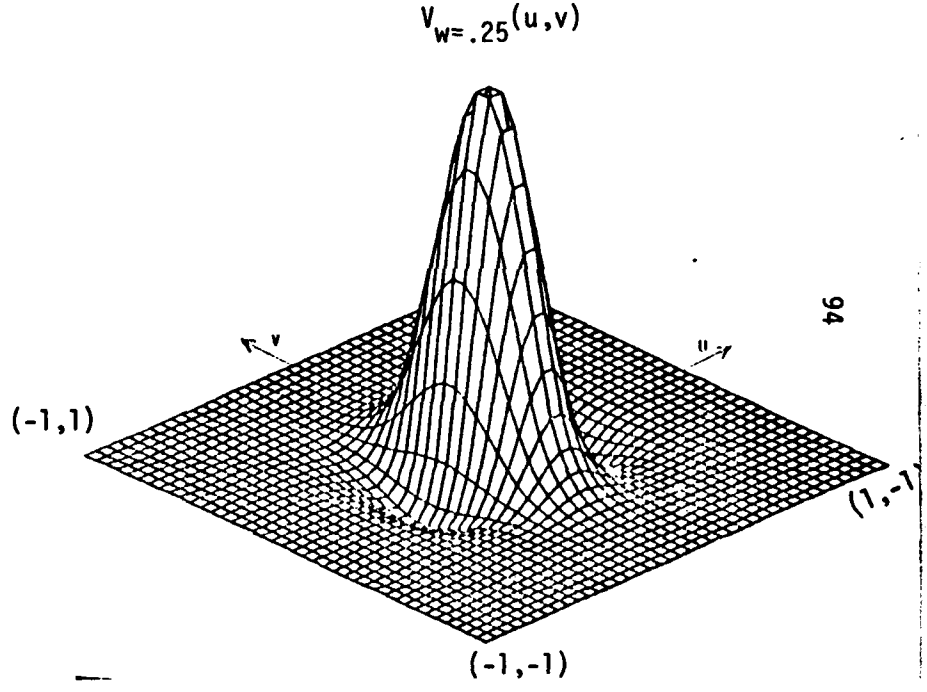

$$V(u,v) = \frac{2}{W}\cos(\pi W u)\, e^{\frac{-\pi}{W}(u^2+v^2)}$$

D

Truncated Visibility Functions

FIGURE 3-3

Other tests (such as peak locations and halfwidths) were not performed for $\tilde{B}(x,y)$ due to the prohibitively long calculations needed at each step of the iterative procedures required for such tests.

Numerically performing the averaging process for the visibility function was considerably faster and more accurate, using a mesh with step .025 along both the u and v axes. The visibility function was numerically integrated over an averaging cell and the average value calculated by dividing by the averaging cell's area. Only the upper half-plane was used (by virtue of the Hermiticity relation) and the values of $\hat{B}_\delta(x,y)$ were calculated using the standard discrete Fourier inversion method discussed in Chapter 2.

Several tests were then performed to study the function $\hat{B}_\delta(x,y)$ and its relation to $\tilde{B}(x,y)$ and $\hat{B}^-_\delta(x,y)$. The two main peaks in $\hat{B}_\delta(x,y)$ were located using an iterative search procedure incorporating the subrotine VA06A of the Harwel Library.[6] The accuracy control for this calculation was specified by the condition

$$|\nabla \hat{B}|^2 = \left[\frac{\partial \hat{B}_\delta(x,y)}{\partial x}\right]^2 + \left[\frac{\partial \hat{B}_\delta(x,y)}{\partial y}\right]^2 < .01$$

for the iteration to terminate.

The magnitude and angle (with respect to the x axis) of the vector connecting the two peaks was then calculated. Since the half-widths of the separate Gaussian components are not well-defined in the x direction due to overlapping of the two components,

the determination of the half-width for each component in $\hat{B}_\delta(x,y)$ was performed in the y direction where half-width is well-defined (i.e., unaffected by overlap effects). The half-width was defined as the distance between the y value at a component peak and the y value where the brightness magnitude is half the peak magnitude. The half-widths were determined by iterative search, and the error bound criterion specified that the magnitude of $\hat{B}_\delta(x,y)$ be within .01 of the true half-width magnitude for the iterative search to terminate.

Overall comparative parameters were defined for $\hat{B}_\delta(x,y)$ in an analogous fashion to those used for $\tilde{B}(x,y)$. For comparison with the exact brightness function, the parameters were:

$$\text{Normalized Deviation} \equiv \frac{\int dx \int dy \left[B(x,y) - \hat{B}_\delta(x,y)\right]}{A}$$

$$\text{Normalized Root Deviation Squared} \equiv \frac{\sqrt{\int dx \int dy \left[B(x,y) - \hat{B}_\delta(x,y)\right]^2}}{A}$$

The square region (with area 64) from -4 to 4 along both the x and y axes was examined, and the mesh step size used to perform the integrations numerically was .2 along both the x and y axes. Again, the results here should be viewed as sufficiently accurate for comparative purposes but not highly accurate in themselves.

For overall comparisons with $\tilde{B}(x,y)$, the following parameters were used:

$$\text{Normalized Deviation} \equiv \frac{\int dx \int dy \left[\tilde{B}(x,y) - \hat{B}_\delta(x,y)\right]}{A}$$

$$\text{Normalized Root Deviation Squared} \equiv \frac{\sqrt{\int dx \int dy \left[\tilde{B}(x,y) - \hat{B}_\delta(x,y)\right]^2}}{A}$$

the same first quadrant region and mesh size as used for the comparison of $\tilde{B}(x,y)$ with $B(x,y)$ was used here.

$\hat{B}_\delta(x,y)$ was also examined to see if the reflection symmetries through the x and y axes which are present in $B(x,y)$ are preserved in $\hat{B}_\delta(x,y)$. The region from -6 to 6 along both the x and y axes was examined using a mesh with step size .1 along each direction. The criterion for symmetry between two reflection symmetric points was that the two values of $\hat{B}_\delta(x,y)$ agree with each other to within .001, and the condition for an overall judgement that $B(x,y)$ was symmetric under reflection through the x and y axis was that no more than 10 pair of points, of the 7200 pairs examined for each reflection symmetry case, be unsymmetric. This tolerance of about .1% was incorporated to allow for any possible rounding errors or other inaccuracies in the computer's calculations which may have been present and incorrectly imply an asymmetry.

3.2.3 Results

Table 3.2 summarizes the results of the model study. Every case was found to preserve the reflection symmetries through x and y axes, and therefore these results were not included in Table 3.2 Similarly, the component peaks were symmetric about the origin in all cases studied, so that only the second component peak (at positive x value) was included in the Table.

TABLE 3.2 Results of Standard Fourier Inversion Method

	Function	Averaging Scheme	Component Location	2 Peak Magnitude	Vector Magnitude	SEP'N. Of Peaks Angle	Halfwidth	Norm Dev $(B-\hat{B}_\delta)$	Norm RDS $(B-\hat{B})^2$	Norm Dev $(\tilde{B}-\hat{B})$	Norm RDS $(\tilde{B}-\hat{B})^2$	Norm Dev $(B-\tilde{B})$	Norm RDS $(B-\tilde{B})^2$
w = 10	B	N/A	(1,0)	1.	2	0°	.1485	N/A	N/A	N/A	N/A	N/A	N/A
	$\tilde{B}$	N/A	N/C	N/C	N/C	N/C	N/C	N/A	N/A	N/A	N/A	.002548	.029025
	$\hat{B}$	A	(1.05,0)	.3105	2.1	0°	.324	.000798	.000999	.000706	.000019	N/A	N/A
	$\hat{B}$	B	(1.34,0)	.2784	2.684	0°	.324	-.019745	.005096	-.016617	.004808	N/A	N/A
	$\hat{B}$	C	(1,0)	.1595	2	0°	.299	.002554	.002554	.002888	.002444	N/A	N/A
w = 1	B	N/A	(1,0)	1	2	0°	.4697	N/A	N/A	N/A	N/A	N/A	N/A
	$\tilde{B}$	N/A	N/C	N/C	N/C	N/C	N/C	N/A	N/A	N/A	N/A	.000129	.002438
	$\hat{B}$	A	(1,0)	.9255	2	0°	.470	.000913	.000253	.000879	.000231	N/A	N/A
	$\hat{B}$	B	(1.35,0)	.9298	2.7	0°	.457	-.165536	.089349	-.136123	.078620	N/A	N/A
	$\hat{B}$	C	(.75,0)	.7435	1.7	0°	.445	.026679	.019359	.021103	.016106	N/A	N/A
w = .5	B	N/A	(.996,0)	1.0019	1.998	0°	.6642	N/A	N/A	N/A	N/A	N/A	N/A
	$\hat{B}$	A	(1,0)	.9570	2	0°	.652	-.000606	.000516	N/C	N/C	N/A	N/A
	$\hat{B}$	B	(1.35,0)	1.064	2.7	0°	.602	-.305176	.183310	N/C	N/C	N/A	N/A
	$\hat{B}$	C	(.85,0)	.8688	1.7	0°	.614	.052251	.024016	N/C	N/C	N/A	N/A
w = .25	B	N/A	(.882,0)	1.051	1.76	0°	.9344	N/A	N/A	N/A	N/A	N/A	N/A
	$\hat{B}$	A	(.85,0)	1.02	1.7	0°	.914	-.002233	.001327	N/C	N/C	N/A	N/A
	$\hat{B}$	B	(1.15,0)	1.125	2.3	0°	.802	-.536396	.399241	N/C	N/C	N/A	N/A
	$\hat{B}$	C	(.692,0)	.9948	1.38	0°	.864	.098851	.034594	N/C	N/C	N/A	N/A

N/A - Not Applicable Norm Dev - Normalized Deviation
N/C - Not Calculated Norm RDS - Normalized Root Deviation Squared

3.2.4 Observations and Discussion

Preservation of the reflection symmetries of B(x,y) in $\hat{B}_\delta(x,y)$ is an expected result, since V(u,v) was symmetrically truncated and the averaging cells were symmetric in the sense that $T_{u,n}=T_{u,-n}$ and $T_{v,m}=T_{v,-m}$.

The component peaks in $\hat{B}_\delta(x,y)$ are generally not coincident with the peaks in B(x,y). In some cases, the peaks are seen to shift inward along the x axis toward the origin, in other cases the shift is outward; however, in all cases, there is no shift in peak location along the y direction. Peak shift is most severe for averaging scheme B, where the cells are all larger than the relevant Nyquist cell size (for all four w cases). In an extensive study of about 300 one-dimensional sample cases, it was found that peak shifts result from truncation effects alone as well as from the combined effects of truncation and averaging. Qualitatively, we can account for peak shifting by realizing that a peak in B(x,y) results from the overall cumulative reinforcement of the component sinusoids of which B(x,y) is composed in its Fourier expansion, and therefore omitting some of these sinusoids [due to truncating V(u,v)], altering their relative amplitudes [due to averaging V(u,v)], and using a limited set of "non-Nyquist" expansion "frequencies" (specified by the aveaging cell midpoints) can give rise to a reinforcement peak at a point which is displaced from the peak in B(x,y). Three cases in the model survey show a peak in $\hat{B}_\delta(x,y)$ coincident with the peak in B(x,y), to within the accuracy limits

of the calculation as discussed above. Two of these cases are for averaging scheme A, where the cells are smaller than the respective Nyquist cell size. The truncation of V(u,v) was not severe for these cases. A very small shift (i.e., undetectable to our accuracy limit) is therefore not surprising for these cases. The third case involved radical truncation of the visibility function and used averaging scheme C which incorporates mixed cell sizes; apparently, the peak shifting influences of truncating and averaging V(u,v) tended to cancel in this case producing a very small (i.e., undetectable) net peak shift.

The peak magnitudes of $\hat{B}_\delta(x,y)$ are seen to differ from the peak magnitudes of B(x,y). In most cases, the peak magnitude of $\hat{B}_\delta(x,y)$ was less than the peak magnitude of the corresponding B(x,y); however, in two cases the converse is seen to hold. For w=10, all three averaging schemes show peaks in B (x,y) which are significantly less than the peak in B(x,y). The visibility function was severely truncated in this case, and therefore we would expect that the omitted Fourier components had significant amplitudes, so that a peak in B(x,y) results from a greater number of reinforcing Fourier components with significant amplitude than are available to form a peak in $\hat{B}_\delta(x,y)$. (The relation $\hat{B}_\delta(0,0)=\tilde{B}(0,0)$ for any averaging scheme holds here. Note, however, that different averaging schemes with the same truncation limits can lead to different peak brightness magnitudes here because the peaks are not at the origin.) The effect of truncation is only one factor accounting for the differ-

ence in peak magnitudes between $\hat{B}_\delta(x,y)$ and $B(x,y)$. The relative amplitudes and "frequencies" of the component sinusoids in $\hat{B}_\delta(x,y)$ are determined by the particular averaging scheme which is used, and these factors also influence the peak brightness. For w=10, the effect of truncation is dominant, whereas for the other three cases, the peak magnitudes are determined by a more balanced contribution of the above cited factors. In particular, the two cases where the peak magnitude of $\hat{B}_\delta(x,y)$ exceeds the peak magnitude of $B(x,y)$ can be qualitatively viewed as cases in which the combined factors result in greater reinforcement magnitude for $\hat{B}_\delta$ than for B.

The halfwidth of $\hat{B}_\delta(x,y)$ is similarly influenced by truncation and averaging effects. From the previously discussed theorem for the effect of truncation, we know that truncating $V(u,v)$ leads to a broader and less sharply resolved function $B(x,y)$ as compared with the true source brightness function $B(x,y)$. For the case w=10 where truncation was severe, we clearly see that the truncation effect is dominant and the halfwidths are all larger (by about a factor of 2) than the halfwidth of $B(x,y)$. In the other cases where the truncation and averaging influences are more balanced, the differences between the halfwidths of $\hat{B}_\delta(x,y)$ and $B(x,y)$ is less severe than the case w=10. (These differences are about 10% as compared with the factor of 2 difference for w=10.)

The parameters defined to enable overall comparisons to be made between the various cases confirm the expected results that, generally, truncation without averaging yields a better approximation

to the brightness function than does truncation with averaging, and the smaller the averaging cells the better the overall approximation of $\hat{B}_\delta(x,y)$ to $B(x,y)$. Again, these are general trends and it is possible (as occurred in several cases) for $\hat{B}_\delta(x,y)$ to give a better approximation to $B(x,y)$ than does $\tilde{B}(x,y)$ for some particular choices of truncation limits and averaging scheme. This observation is supported by sample cases among about 300 one-dimensional test cases where $\tilde{B}(x)$ and $\hat{B}_\delta(x)$ were plotted and visually inspected for goodness of fit to $B(x)$. The entries in Table 3.2 clearly show that averaging scheme B (cell sizes all greater than the Nyquist cell size) was always significantly worse in fitting $B(x,y)$ than were the other two averaging schemes where some or all of the cells were smaller than the Nyquist cell size.

Having obtained a qualitative understanding from the model study of the effects on the brightness function resulting from truncating and averaging the visibility function, we now analyze these effects quantitatively in Chapter 4 to further elucidate the nature of these effects.

CHAPTER 4

THEORY OF TRUNCATION AND AVERAGING EFFECTS

Having seen the effects of truncation and averaging illustrated in Chapter III, we now take an analytical look at the causes of these effects.

4.1 Periodicity Considerations

Our discussion on the periodic nature of the brightness function resulting from sampling or averaging the visibility function has thus far been concerned with a fixed sampling or averaging interval. We now discuss the periodicity phenomenon for irregular intervals, i.e., intervals of varying sizes. We will work in one dimension and then generalize to 2-D.

Theorem 4.1: Consider a visibility function V(u) and let it be averaged, with averaging intervals in the set $\{T_n\}$. Then $\hat{B}_\delta(x)$ is a periodic function in x, with period

$$X_p = \text{LCM}\left[\left|\frac{1}{u_n}\right|\right]_{n\neq 0}$$

where LCM ≡ Least Common Multiple.

Proof: For the general case of truncation and averaging (including asymmetric truncation) we have

$$\hat{B}_s(x) = \sum_{n=-N_1}^{N_2} T_n [\bar{V}_n]\, e^{-i2\pi u_n x}$$

$$= \sum_{n=-N_1}^{N_2} T_n \left\{ \left[[\bar{V}_n]_r \cos 2\pi u_n x + [\bar{V}_n]_i \sin 2\pi u_n x \right] \right.$$

$$\left. -i \left[[\bar{V}_n]_r \sin 2\pi u_n x - [\bar{V}_n]_i \cos 2\pi u_n x \right] \right\}.$$

For a given n, all trig functions have the common period $X_{p,n} = |\frac{1}{u_n}|$. The number of distinct periods is just (N_2+N_1+1). The period of B will therefore be the lowest beat period of these "component" periods:

$$X_p = LCM[X_{p,n}] = LCM\left[\left|\frac{1}{u_n}\right|\right]_{\substack{n\neq 0 \\ n\in[-N_1,N_2]}}.$$

We specify $n\neq 0$ because $u_0=0$, for which the trig functions reduce to constants. Therefore, the n=0 term is automatically commensurate with the common period of all the other components. Now, u_n is the midpoint of the n^{th} averaging interval, and if u_{min} is the lower truncation limit, we can write

$$u_n = u_{min} + \sum_{\sigma=-N_1}^{n-1} T_\sigma + \frac{T_n}{2}.$$

If we use a constant averaging interval T and truncate symmetrically, then

$$n \in [-N, N]$$

and

$$u_n = u_{min} + \sum_{n=-N}^{n-1} T_\sigma + \frac{T_n}{2}$$

$$= u_{min} + (n-1+N+1)T + \frac{T}{2}$$

$$= u_{min} + (N+n+\tfrac{1}{2})T.$$

Then,

$$X_p = LCM\left[\left|\frac{1}{u_{min} + (N+n+\frac{1}{2})T}\right|\right]_{n\neq 0}$$

$$= LCM\left[\left|\frac{2}{2u_{min} + (2N+2n+1)T}\right|\right]_{n\neq 0}.$$

But,

$$2u_{min} = -(u_{max} - u_{min}) = -(2N+1)T, \text{ so}$$

$$X_p = LCM\left[\left|\frac{1}{T}\cdot\frac{2}{-2N-1+2N+2n+1}\right|\right]_{n\neq 0} = LCM\left[\left|\frac{1}{T}\cdot\frac{1}{n}\right|\right]_{n\neq 0}$$

$$= \frac{1}{T}.$$

This agrees with our previous results for fixed T, including the limiting case where V is not truncated so that $N\to\infty$ (provided that $N\neq\infty$ for then $\frac{1}{N}=0$).

In two dimensions, we have

$$\hat{B}_\delta(x,y) = \sum_{n=-N}^{N}\sum_{m=-M}^{M} T_{u,n}\, T_{v,m}\, [\bar{V}_{n,m}]\, e^{-i2\pi(u_n x + v_m y)}.$$

Clearly, if we fix one variable, say y, then $\hat{B}_\delta(x,y_0)$ is a periodic function in x with a period

$$X_p = LCM\left[\left|\frac{1}{u_n}\right|\right]_{n\in[-N,N],\, n\neq 0}$$

exactly analogous to the 1-D case considered above. Thus, both orthogonal components of the two dimensional brightness function satisfy the 1-D periodicity relation independently.

In a real experiment many different cell sizes occur, and their midpoint coordinates generally do not form a set whose inverses have a low Least Common Multiple. For example, if two values of $|\frac{1}{u_n}|$ in the set are 1 and .617, then their LCM is 617, without even considering other midpoint values. This observation leads to

the conclusion that the x and y periods of B (x,y) will be very large for a realistic case, and hence aliasing effects should not be important (unless the data is gridded onto a regular lattice with cell sizes greater than the Nyquist cell size).

4.2 Effect of Truncation Alone

We have previously shown that truncation of the visibility function V(u,v) into a rectangular region with sides b_u and b_v, and center at (c_u,c_v), results in a brightness function $\tilde{B}(x,y)$ given by

$$\tilde{B}(x,y) = \int_{-\infty}^{\infty}dx' \int_{-\infty}^{\infty}dy' \; e^{-i2\pi(c_u x' + c_v y')} \frac{\sin \pi b_u x'}{\pi x'} \frac{\sin \pi b_v y'}{\pi y'} \cdot B(x-x', y-y'),$$

where $B(x,y) \supset V(u,v)$. $\tilde{B}(x,y)$ exhibits ringing, i.e., it resembles B(x,y) (to an extent depending upon the severity of truncation), but with truncation-induced oscillations as a modulating factor, and $\tilde{B}$ is smoother than B(x,Y).

4.3 Effect of Averaging Only

In the next several sections, we investigate the effects of averaging over the entire visibility function and averaging a truncated visibility function. Initially, we will work in one dimension with a fixed averaging interval size. We then generalize to the case of irregular averaging intervals, and finally we will generalize the results to two dimensions.

The following theorem will be considered our basic theorem relating an average value of the visibility function to the true source brightness function. We will later formulate an algorithm which uses the information on the effect of averaging conveyed by this theorem in an attempt to improve the brightness function resolution by accounting, to some extent, for the fact that V(u,v) has been averaged. The standard Fourier inversion method does not incorporate this information.

Theorem 4.2: For the case of averaging with the epoch of averaging at the origin, each average value of the function V(u) can be written in terms of a definite integral over x which includes B(x), the true conjugate function for V(u), in the integrand.

Proof: Let V(u) be averaged with integer index $n\epsilon[-\infty,\infty]$ denoting the n^{th} averaging interval with epoch (n=0) at the origin, such that the sign of n denotes the relevant half-axis on which a particular interval is located. The n^{th} average value of V(u) is given by

$$[\bar{V}_n] = \frac{1}{T}\int_{u_n-\frac{T_n}{2}}^{u_n+\frac{T_n}{2}} du\ V(u).$$

We can replace V(u) in this expression by its Fourier transform relation:

$$[\bar{V}_n] = \frac{1}{T}\int_{u_n-\frac{T_n}{2}}^{u_n+\frac{T_n}{2}} du\ \left[\int_{-\infty}^{\infty} dx\ e^{i2\pi ux}\ B(x)\right].$$

We assume that the order of integrations can be reversed (which is true for analytic functions, and we will justify this even for the case where B(x) is a generalized function, say representing a point source). Then,

$$[\bar{V}_n] = \frac{1}{T_n}\int_{-\infty}^{\infty} dx\, B(x)\left[\int_{u_n-\frac{T_n}{2}}^{u_n+\frac{T_n}{2}} du\, e^{i2\pi ux}\right] = \frac{1}{T_n}\int_{-\infty}^{\infty} dx\, B(x)\left[\frac{e^{i2\pi ux}}{i2\pi x}\right]_{u_n-\frac{T_n}{2}}^{u_n+\frac{T_n}{2}}$$

$$= \frac{1}{T_n}\int_{-\infty}^{\infty} dx\, B(x)\,\frac{e^{i2\pi u_n x}}{\pi x}\left(\frac{e^{i\pi T_n x} - e^{-i\pi T_n x}}{2i}\right)$$

$$= \frac{1}{T_n}\int_{-\infty}^{\infty} dx\, B(x)\, e^{i2\pi u_n x}\,\frac{\sin \pi T_n x}{\pi x}$$

$$= \int_{-\infty}^{\infty} dx\, B(x)\, \operatorname{sinc} T_n x\, e^{i2\pi u_n x}$$

$$= \left[\int_{-\infty}^{\infty} dx\, B(x)\operatorname{sinc} T_n x\, e^{i2\pi ux}\right]_{u=u_n} = \mathcal{F}\left\{B(x)\operatorname{sinc} T_n x\right\}_{u=u_n}$$

Note that if we average with a fixed interval T, then $u_n = nT$. We also note that if B(x) is a band-limited function in the interval $[-L_x, L_x]$, then the definite integral's limits need be only from $-L_x$ to L_x.

We must now prove several intermediate results which will be needed in our development.

Theorem 4.3:

$$\sum_{n=-\infty}^{\infty} e^{-i2\pi nTx} = \frac{1}{T}\sum_{n=-\infty}^{\infty} \delta\left(x-\frac{n}{T}\right)$$

Proof:

$$\frac{1}{T}\sum_{n=-\infty}^{\infty} \delta\left(x-\frac{n}{T}\right) \equiv \text{Ш}(Tx)$$

Now,

$$\mathcal{F}\left\{\text{Ш}(Tx)\right\} = \frac{1}{T}\,\text{Ш}\left(\frac{u}{T}\right) = \sum_{n=-\infty}^{\infty} \delta(u-nT)$$

But, $$\mathcal{F}^{-1}\left\{\frac{1}{T}\text{III}\left(\frac{u}{T}\right)\right\} = \int_{-\infty}^{\infty} du\, e^{-i2\pi ux} \sum_{n=-\infty}^{\infty} \delta(u-nT) = \sum_{n=-\infty}^{\infty} \int_{-\infty}^{\infty} du\, e^{-i2\pi ux}\, \delta(u-nT)$$

$$= \sum_{n=-\infty}^{\infty} e^{-i2\pi nTx}.$$

Hence,

$$\frac{1}{T}\sum_{n=-\infty}^{\infty} \delta\left(x-\frac{n}{T}\right) = \sum_{n=-\infty}^{\infty} e^{-i2\pi nTx}.$$

Qualitatively, we see that this result is reasonable because if $x=\frac{n}{T}$, then

$$e^{-i2\pi nT\left(\frac{n}{T}\right)} = 1$$

so the sum is infinite. However, for $x\neq\frac{n}{T}$, the infinite sum over sines and cosines with varying phases will vanish. ∎

Corollary 4.3A:

$$T\sum_{n=-N+\mathcal{N}}^{N+\mathcal{N}} e^{-i2\pi nTx} = \sum_{n=-\infty}^{\infty} e^{-i2\pi\mathcal{N}Tx}\, \frac{\sin 2\pi NT\left(x-\frac{n}{T}\right)}{\pi\left(x-\frac{n}{T}\right)}$$

where N and $\mathcal{N}$ are integers.

Proof:

$$\sum_{n=-N+\mathcal{N}}^{N+\mathcal{N}} \delta(u-nT) = \frac{1}{T}\text{III}\left(\frac{u}{T}\right) \cdot \pi\left(\frac{u-\mathcal{N}T}{2NT}\right).$$

Then analogous to the previous proof,

$$\mathcal{F}^{-1}\left\{\sum_{n=-N+\mathcal{N}}^{N+\mathcal{N}} \delta(u-nT)\right\} = \sum_{n=-N+\mathcal{N}}^{N+\mathcal{N}} e^{-i2\pi nTx}.$$

But, by the Convolution Theorem,

$$\mathcal{F}^{-1}\left\{\frac{1}{T}\amalg\left(\frac{u}{T}\right)\cdot\Pi\left(\frac{u-\eta}{2N}\right)\right\} = \amalg(Tx) * \left[e^{-i2\pi\eta Tx}\frac{\sin 2\pi NTx}{\pi x}\right]$$

$$= \int_{-\infty}^{\infty} dx' e^{-i2\pi\eta Tx'}\frac{\sin 2\pi NTx'}{\pi x'}\frac{1}{T}\sum_{n=-\infty}^{\infty}\delta\left(x-x'-\frac{n}{T}\right)$$

$$= \frac{1}{T}\sum_{n=-\infty}^{\infty} e^{-i2\pi\eta T\left(x-\frac{n}{T}\right)}\frac{\sin 2\pi NT\left(x-\frac{n}{T}\right)}{\pi\left(x-\frac{n}{T}\right)}$$

Comparing results, we find

$$T\sum_{n=-N+\eta}^{N+\eta} e^{-i2\pi nTx} = \sum_{n=-\infty}^{\infty} e^{-i2\pi\eta Tx}\frac{\sin 2\pi NT\left(x-\frac{n}{T}\right)}{\pi\left(x-\frac{n}{T}\right)}$$

■

Corollary 4.3B:

$$T\sum_{n=-N}^{N} e^{-i2\pi nTx} = \sum_{n=-\infty}^{\infty}\frac{\sin 2\pi NT\left(x-\frac{n}{T}\right)}{\pi\left(x-\frac{n}{T}\right)}.$$

Proof: Setting $\eta=0$ in Corollary A, this result is obvious.

We can now apply these intermediate results to prove several theorems on averaging effects.

Theorem 4.4: The effect of averaging V(u) over its entire domain with constant averaging interval T is to form the periodic extension of B(x) multiplied by sinc(Tx).

Proof: As previously defined,

$$\mathcal{V}(u) = \sum_{n=-\infty}^{\infty} T\left[\bar{V}_n\right]\delta(u-u_n)$$

Using Theorem 4.2 for $[\bar{V}n]$, we write

$$\bar{\mathcal{F}}(u) = T\sum_{n=-\infty}^{\infty}\left[\int_{-\infty}^{\infty} dx' B(x') \operatorname{sinc} Tx' e^{i2\pi nTx'}\right]\delta(u-u_n)$$

Now,

$$\hat{B}_\delta(x) = \mathcal{F}^{-1}\{\bar{\mathcal{F}}(u)\}$$

so

$$\hat{B}_\delta(x) = \int_{-\infty}^{\infty} du\, e^{-i2\pi ux}\left\{T\sum_{n=-\infty}^{\infty}\left[\int_{-\infty}^{\infty} dx' B(x') \operatorname{sinc} Tx' e^{i2\pi nTx'}\right]\delta(u-u_n)\right\}$$

$$= T\sum_{n=-\infty}^{\infty} e^{-i2\pi u_n x}\int_{-\infty}^{\infty} dx' B(x') \operatorname{sinc} Tx' e^{i2\pi nTx'}$$

For averaging with the epoch at the origin, $u_n = nT$, so we can write

$$\hat{B}_\delta(x) = T\sum_{n=-\infty}^{\infty}\int_{-\infty}^{\infty} dx' B(x') \operatorname{sinc} Tx' e^{-i2\pi nT(x-x')}$$

$$= T\int_{-\infty}^{\infty} dx' B(x') \operatorname{sinc} Tx' \sum_{n=-\infty}^{\infty} e^{-i2\pi nT(x-x')}$$

$$= \int_{-\infty}^{\infty} dx' B(x') \operatorname{sinc} Tx' \sum_{n=-\infty}^{\infty}\delta\left[(x-x') - \frac{n}{T}\right]$$

where we used Theorem 4.3. So,

$$\hat{B}_\delta(x) = \sum_{n=-\infty}^{\infty} B\left(x - \frac{n}{T}\right) \operatorname{sinc} T\left(x - \frac{n}{T}\right).$$

This is a periodic extension of the true brightness function modulated by the sinc factor. Note the implications for aliasing if B(x) is band-limited in $[-L_x, L_x]$ but $T > \frac{1}{2L_x}$, or if B were not band-limited at all.

We now consider the important case in which the visibility function has been symmetrically truncated and averaged with epoch at the origin.

Theorem 4.5: The effect of averaging a function V(u) which has been symmetrically truncated is expressed by a convolution integral which contains B(x), the true conjugate function to V(u), in its integrand.

Proof: If V(u) is symmetrically truncated and averaged, we have

$$\bar{\mathcal{V}}(u) = T \sum_{n=-N}^{N} [\bar{V}_n] \, \delta(u - nT)$$

where $u_n = nT$ for epoch at the origin. Proceeding exactly as we did in the previous theorem, we get

$$\hat{B}_\delta(x) = T \int_{-\infty}^{\infty} dx' \, B(x') \, \text{sinc}\, Tx' \sum_{n=-N}^{N} e^{-i2\pi nT(x-x')}$$

Since the summation is no longer from $-\infty, +\infty$, as it was in the previous theorem, we cannot simplify the convolution integral any further. Noting that

$$\sum_{n=-N}^{N} e^{-i2\pi nT(x-x')} = 1 + 2 \sum_{n=1}^{N} \cos[2\pi nT(x-x')],$$

we can give an alternate statement of the result:

$$\hat{B}_\delta(x) = T \int_{-\infty}^{\infty} dx' \, B(x') \, \text{sinc}\, Tx' \left[1 + 2 \sum_{n=1}^{N} \cos 2\pi nT(x-x')\right]$$

The presence of the cosine factor accounts for the ringing expected when the visibility function is truncated. A third alternate form

can be written using Corollary 4.3B:

$$\hat{B}_\delta(x) = \sum_{n=-\infty}^{\infty} \int_{-\infty}^{\infty} dx' \, B(x') \, \mathrm{sinc}\, Tx' \, \frac{\sin 2\pi NT(x - x' - \frac{n}{T})}{\pi(x - x' - \frac{n}{T})}.$$

4.4 Examination of the Theorems

We now examine the theorems in further detail. We will check for consistency with known results for the limiting case as T→0, and then discu s the case where V(u) is a linear function. This case is important because, if V(u) is linear, then averaging and sampling produce identical results, and thus the distortions predicted by our theorems should vanish for $T=T_{NI}$.

4.4.1 Limiting Cases

If V(u) is averaged over its entire domain, we found

$$\hat{B}_\delta(x) = \sum_{n=-\infty}^{\infty} B(x - \tfrac{n}{T}) \, \mathrm{sinc}\, T(x - \tfrac{n}{T}).$$

The limiting case is then

$$\lim_{T\to 0} \hat{B}_\delta(x) = \lim_{T\to 0} \sum_{n=-\infty}^{\infty} B(x - \tfrac{n}{T}) \, \frac{\sin \pi T(x - \frac{n}{T})}{\pi T(x - \frac{n}{T})}.$$

Using the theorem for the limit of a product (Kaplan, 1952), which states

$$\lim_{x\to x_1} [f(x) \cdot g(x)] = \left[\lim_{x\to x_1} f(x)\right] \cdot \left[\lim_{x\to x_1} g(x)\right],$$

we can write

$$\lim_{T\to 0} \hat{B}_\delta(x) = \sum_{n=-\infty}^{\infty} \left[\lim_{T\to 0} B(x - \tfrac{n}{T})\right] \cdot \left[\lim_{T\to 0} \frac{\sin \pi T(x - \frac{n}{T})}{\pi T(x - \frac{n}{T})}\right]$$

Now,

$$\lim_{T\to 0} B\left(X-\frac{n}{T}\right) = \begin{cases} B(X) & \text{IF } n=0 \\ B(X-\infty) & \text{IF } n\neq 0 \end{cases}$$

where we understand $B(x-\infty)$ to mean the function $B(x)$ displaced to ∞, and hence aliasing effects are no longer relevant (assuming

$$\lim_{X\to\infty} B(X) = 0$$

or that $B(x)$ is in fact a band-limited function). Also,

$$\lim_{T\to 0} \frac{\sin \pi T\left(X-\frac{n}{T}\right)}{\pi T\left(X-\frac{n}{T}\right)} = \lim_{T\to 0}\left\{\frac{\sin \pi TX \cos \pi n - \cos \pi TX \sin \pi n}{\pi T\left(X-\frac{n}{T}\right)}\right\}$$

$$= \lim_{T\to 0} \cos \pi n \frac{\sin \pi TX}{\pi TX - \pi n} = \begin{cases} 0 & \text{IF } n\neq 0 \\ 1 & \text{IF } n=0 \end{cases}.$$

Hence, we have

$$\lim_{T\to 0} \hat{B}_\delta(x) = \sum_{n=-\infty}^{\infty} [B]\, \delta_{1,n} = B(x)$$

where

$$[B] \equiv \begin{cases} B(X) & \text{IF } n=0 \\ B(X-\infty) & \text{IF } n\neq 0 \end{cases},$$

and the Knonecker delta is

$$\delta_{1,n} = \begin{cases} 1 & n=1 \\ 0 & n\neq 1 \end{cases}.$$

We have obtained $B(x)$ as expected for $T\to 0$, in which case we are effectively sampling every point in $V(u)$. Note that $B(x)$, not its periodic extension, is obtained.

If we symmetrically truncate $V(u)$ and average with intervals T with epoch at the origin, we found that

$$\hat{B}_\delta(x) = T\int_{-\infty}^{\infty} dx'\, B(x')\, \text{sinc}\, Tx' \sum_{n=-N}^{N} e^{-i2\pi nT(x-x')}.$$

Then, $$\lim_{T\to 0} \hat{B}_s(x) = \lim_{T\to 0} T\int_{-\infty}^{\infty} dx' B(x') \operatorname{sinc} Tx' \sum_{n=-N}^{N} e^{-i2\pi nT(x-x')}$$

$$= \int_{-\infty}^{\infty} dx' B(x') \lim_{T\to 0} \left[T \operatorname{sinc} Tx' \sum_{n=-N}^{N} e^{-i2\pi nT(x-x')} \right].$$

Note that, in this case, we require $N\to\infty$ as $T\to 0$, in order to keep the truncation limits $\pm(N+\frac{1}{2})T$ finite and fixed in value as we take the limit. Consider the limiting term:

$$L \equiv \lim_{T\to 0} T \operatorname{sinc} Tx' \sum_{n=-N}^{N} e^{-i2\pi nT(x-x')}$$

$$= \left[\lim_{T\to 0} \operatorname{sinc} Tx'\right] \cdot \left[\lim_{T\to 0} T \sum_{n=-N}^{N} e^{-i2\pi nT(x-x')}\right]$$

$$= [1] \cdot \left[\lim_{\substack{T\to 0 \\ N\to\infty}} T \sum_{n=-N}^{N} e^{-i2\pi nT(x-x')}\right]$$

$$= \lim_{\substack{T\to 0 \\ N\to\infty \\ NT \text{ FINITE}}} \sum_{n=-\infty}^{\infty} \frac{\sin 2\pi NT\left(x-x'-\frac{n}{T}\right)}{\pi\left(x-x'-\frac{n}{T}\right)}$$

where we have used Corollary 4.3B. So,

$$L = \sum_{n=-\infty}^{\infty} \lim_{\substack{T\to 0 \\ N\to\infty \\ NT \text{ FINITE}}} \frac{\sin 2\pi(NT)\left(x-x'-\frac{n}{T}\right)}{\pi\left(x-x'-\frac{n}{T}\right)} = \sum_{n=-\infty}^{\infty} \begin{cases} \dfrac{\sin 2\pi(NT)(x-x')}{\pi(x-x')} & \text{IF } n=0 \\ \dfrac{\sin 2\pi(NT)(x-x'-\infty)}{\pi(x-x'-\infty)} & \text{IF } n\neq 0 \end{cases}$$

For $n\neq 0$, the term is understood to represent the sinc function shifted to ∞, and since the magnitude of the sinc function goes to zero as $(x-x')\to\infty$, we see that in any region of interest for a band-limited brightness function, $(x-x')<\infty$, and then

$$\frac{\sin 2\pi(NT)(x-x'-\infty)}{\pi(x-x'-\infty)}$$

if effectively zero. Our result then is

$$\lim_{T\to 0} \hat{B}_\delta(x) = \int_{-\infty}^{\infty} dx'\, B(x')\, \frac{\sin \pi (2NT)(x-x')}{\pi(x-x')} .$$

But, for symmetric truncation,

$$\tilde{B}(x) \equiv \int_{-\infty}^{\infty} dx'\, B(x')\, \frac{\sin \pi b_u (x-x')}{\pi(x-x')}$$

where b_u is the length of the non-truncated portion of V(u), $b_u = u_{max} - u_{min} = (2N+1)T = 2NT$ for $T\to 0$, while NT remains finite. Hence,

$$\lim_{T\to 0} \hat{B}(x) = \tilde{B}(x),$$

as expected. It is straightforward to show that this result is also obtained if V(u) were asymmetrically truncated, but we will not go through the details here since the asymmetric truncation case is not of interest for our purposes.

4.42 Linear Visibility Function

If V(u) is a linear function with a real fourier transform, then V(u)=iau+b, and B(x) must then be a generalized function:

$$B(x) = \mathcal{F}^{-1}\{V(u)\} = -\frac{a}{2\pi}\frac{d}{dx}\delta(x) + b\delta(x)$$

where we have used the derivative theorem.

We first show that the previously discussed reversal of integration orders is valid if B(x) is a generalized function. Suppose $B(x)=\delta(x)$ and V(u)=1. Then

$$[\bar{V}_n] = \frac{1}{T_n}\int_{u_n - \frac{T_n}{2}}^{u_n + \frac{T_n}{2}} du\; V(u) = \frac{1}{T_n}\int_{u_n - \frac{T_n}{2}}^{u_n + \frac{T_n}{2}} du \left[\int_{-\infty}^{\infty} dx\, e^{i2\pi ux}\delta(x)\right]$$

$$= \frac{1}{T_n}\int_{u_n - \frac{T_n}{2}}^{u_n + \frac{T_n}{2}} du = 1 .$$

If we reverse integration orders, we get:

$$\frac{1}{T_n}\int_{-\infty}^{\infty} dx\ \delta(x)\left[\int_{u_n-\frac{T_n}{2}}^{u_n+\frac{T_n}{2}} du\ e^{i2\pi ux}\right] = \frac{1}{T_n}\int_{-\infty}^{\infty} dx\ \delta(x)\, e^{i2\pi u_n x}\ \frac{\sin \pi T_n x}{\pi x}$$

$$= \int_{-\infty}^{\infty} dx\ \delta(x)\ e^{i2\pi u_n x}\ \mathrm{sinc}\, T_n x = 1 .$$

Thus, reversing integration orders is acceptable if $B(x)=\delta(x)$.

Suppose now that $V(u)=i2\pi u$ and $B(x)=\frac{d}{dx}[\delta(x)]$. Then,

$$[\bar{V}_n] = \frac{1}{T_n}\int_{u_n-\frac{T_n}{2}}^{u_n+\frac{T_n}{2}} du\ V(u) = \frac{1}{T_n}\int_{u_n-\frac{T_n}{2}}^{u_n+\frac{T_n}{2}} du\left[\int_{-\infty}^{\infty} dx\ e^{i2\pi ux}\frac{d}{dx}\delta(x)\right]$$

$$= \frac{1}{T_n}\int_{u_n-\frac{T_n}{2}}^{u_n+\frac{T_n}{2}} du\left[(-i2\pi u)\, e^{i2\pi ux}\Big|_{x=0}\right]$$

$$= \frac{-i2\pi}{2T_n}\left[(u_n+\tfrac{T_n}{2})^2-(u_n-\tfrac{T_n}{2})^2\right] = \frac{-i2\pi}{2T_n}\left[2u_nT_n\right]$$

$$= -i2\pi u_n .$$

If we reverse integration orders, we get

$$\frac{1}{T_n}\int_{-\infty}^{\infty} dx\ \frac{d}{dx}[\delta(x)]\left[\int_{u_n-\frac{T_n}{2}}^{u_n+\frac{T_n}{2}} du\ e^{i2\pi ux}\right]$$

$$= \frac{1}{T_n}\int_{-\infty}^{\infty} dx\ \frac{d}{dx}[\delta(x)]\ e^{i2\pi u_n x}\ \frac{\sin \pi T_n x}{\pi x}$$

$$= -\frac{d}{dx}\left[e^{i2\pi u_n x}\ \mathrm{sinc}\, T_n x\right]_{x=0}$$

$$= -\left\{i2\pi u_n\, e^{i2\pi u_n x}\ \mathrm{sinc}\, T_n x\right\}_{x=0} - \left\{e^{i2\pi u_n x}\frac{d}{dx}\left[\mathrm{sinc}\, T_n x\right]\right\}_{x=0}$$

$$= -i2\pi u_n .$$

Thus, if V(u) is an arbitrary linear function such that B(x) is impulsive, then reversal of integration orders, which was essential in deriving the theorems, is valid.

Consider now the case where V(u)=1 so that B(x)=δ(x). The theorem for averaging over the entire visibility function with fixed interval T then says

$$\hat{B}_\delta(x) = \sum_{n=-\infty}^{\infty} B\left(x-\tfrac{n}{T}\right) \operatorname{sinc} T\left(x-\tfrac{n}{T}\right)$$

$$= \sum_{n=-\infty}^{\infty} \delta\left(x-\tfrac{n}{T}\right) \frac{\sin \pi T\left(x-\frac{n}{T}\right)}{\pi T\left(x-\frac{n}{T}\right)}$$

To analyze this result, consider the following integral. Let f(x) be some function of x.

$$\sum_{n=-\infty}^{\infty} \int_{-\infty}^{\infty} dx \left[\delta\left(x-\tfrac{n}{T}\right) \frac{\sin \pi T\left(x-\frac{n}{T}\right)}{\pi T\left(x-\frac{n}{T}\right)} \right] f(x) = \sum_{n=-\infty}^{\infty} \int_{-\infty}^{\infty} dx' \, \delta(x') \frac{\sin \pi T x'}{\pi T x'} f\left(x'+\tfrac{n}{T}\right) \Big|_{x'=x-\frac{n}{T}}$$

$$= \sum_{n=-\infty}^{\infty} f\left(\tfrac{n}{T}\right)$$

$$= \sum_{n=-\infty}^{\infty} \left[\int_{-\infty}^{\infty} dx' \, \delta(x') \, f\left(x'+\tfrac{n}{T}\right) \right] = \int_{-\infty}^{\infty} dx \left[\sum_{n=-\infty}^{\infty} \delta\left(x-\tfrac{n}{T}\right) \right] f(x) .$$

Therefore, the generalized function

$$\sum_{n=-\infty}^{\infty} \delta\left(x-\tfrac{n}{T}\right) \frac{\sin \pi T\left(x-\frac{n}{T}\right)}{\pi T\left(x-\frac{n}{T}\right)}$$

behaves as

$$\sum_{n=-\infty}^{\infty} \delta\left(x-\tfrac{n}{T}\right)$$

and so we may write

$$\hat{B}_\delta(x) = \sum_{n=-\infty}^{\infty} \delta\left(x-\tfrac{n}{T}\right)$$

which is the periodic extension of B(x).

Suppose now that $V(u)=i2\pi u$ so that $B(x)=\frac{d}{dx}[\delta(x)]$. Then we have

$$\hat{B}_\delta(x)=\sum_{n=-\infty}^{\infty}\left\{\frac{d}{dx}\left[\delta(x-\tfrac{n}{T})\right]\right\}\frac{\sin\pi T(x-\frac{n}{T})}{\pi T(x-\frac{n}{T})}$$

$$=\sum_{n=-\infty}^{\infty}\frac{d(x-\frac{n}{T})}{dx}\,\frac{d}{d(x-\frac{n}{T})}\left[\delta(x-\tfrac{n}{T})\right]\frac{\sin\pi T(x-\frac{n}{T})}{\pi T(x-\frac{n}{T})}.$$

To analyze this result, consider the following behavior, where $f(x)$ is some function of x:

$$\int_{-\infty}^{\infty}dx\sum_{n=-\infty}^{\infty}\frac{d}{dx}\left[\delta(x-\tfrac{n}{T})\right]\frac{\sin\pi T(x-\frac{n}{T})}{\pi T(x-\frac{n}{T})}f(x)$$

$$=\sum_{n=-\infty}^{\infty}\int_{-\infty}^{\infty}dx'\frac{d}{dx'}\left[\delta(x')\right]\frac{\sin\pi Tx'}{\pi Tx'}\,f(x'+\tfrac{n}{T})\Big|_{x'=x-\frac{n}{T}}$$

$$=\sum_{n=-\infty}^{\infty}\left\{-\frac{d}{dx'}\left[\frac{\sin\pi Tx'}{\pi Tx'}\,f(x'+\tfrac{n}{T})\right]_{x'=0}\right\}$$

$$=-\sum_{n=-\infty}^{\infty}\left[f(x'+\tfrac{n}{T})\frac{d}{dx'}\frac{\sin\pi Tx'}{\pi Tx'}+\frac{\sin\pi Tx'}{\pi Tx'}f'(x'+\tfrac{n}{T})\right]_{x'=0}$$

$$=-\sum_{n=-\infty}^{\infty}f'(\tfrac{n}{T})$$

$$=\int_{-\infty}^{\infty}dx\left[\sum_{n=-\infty}^{\infty}\frac{d}{dx}\left[\delta(x-\tfrac{n}{T})\right]f(x)\right].$$

We therefore see that the generalized function

$$\sum_{n=-\infty}^{\infty}\frac{d}{dx}\,\delta(x-\tfrac{n}{T})\,\frac{\sin\pi T(x-\frac{n}{T})}{\pi T(x-\frac{n}{T})}$$

behaves as

$$\sum_{n=-\infty}^{\infty}\frac{d}{dx}\,\delta(x-\tfrac{n}{T}).$$

Hence, we see that

$$\hat{B}_\delta=\sum_{n=-\infty}^{\infty}\frac{d}{dx}\,\delta(x-\tfrac{n}{T}),$$

the periodic extension of the brightness function $B(x)$.

We conclude that, if we average a visibility function $V(u)=iau+b$ with Fourier transform $B(x)$, then we get for the Fourier transform of the averaged function a periodic extension of $B(x)$ with period $\frac{1}{T}$. Note the similarity with the Sampling Theorem result for point-wise sampling at intervals T, which is the expected result here because, for a linear $V(u)$,

$$\text{Average Value} = [\bar{V}_n] = \frac{1}{T}\int_{(n-\frac{1}{2})T}^{(n+\frac{1}{2})T} V(u)du = V(nT)=V(u_n)=\text{Sample Value}$$

Note also that if $T>T_{NI}$ we will get aliasing in $\hat{B}_\delta$ since we have effectively point-wise sampled V at intervals $T>T_{NI}$.

We have tested the theorems on averaging for limiting cases as $T\to 0$ and for the case of a linear visibility function with constant-interval averaging over its entire domain. All tests have indicated that these theorems are consistent with the general properties of Fourier transforms. We will not examine the case of a symmetrically truncated and averaged visibility function here due to the algebraic complexity involved in that case. However, it is reasonable to expect that, based on the other successful consistency tests, this case also will yield the required result that averaging a linear visibility function is equivalent to sampling that function.

4.5 Peak Shift Effects

One of the most important pieces of information to be obtained from interferometric observations is the location of a point

source (or source below the resolution limits) or the peak brightness for an extended source. As we saw in Chapter 3, it is possible for truncation and averaging effects to distort the brightness function so as to cause shifts in the location of the peak brightness away from the true source peaks. This case can easily be demonstrated for the case of point sources.

Consider two point sources in one dimension with brightness function $B(x) = \frac{1}{2}\left[\delta(x-\frac{1}{2}) + \delta(x+\frac{1}{2})\right]$

The visibility function is then $V(u)=\cos\pi u$. Suppose we truncate $V(u)$ at $|u|=1$ and average with intervals of $T=.4$. Figure 4.1 illustrates the true source brightness function and compares it with $\tilde{B}(x)$ and $\hat{B}\delta(x)$. The peak shifts are quite evident.

In this section, we attempt to discern the origin of peak shifts and conditions for a peak in $\hat{B}_\delta(x)$ to be coincident with the corresponding peak in $B(x)$. We will discuss truncation and averaging effects separately, and then their combined effect will be examined. Although we are most interested in the peaks, the discussion will actually deal with relative extremum points. For the case of averaging over the entire visibility function, we can express $\hat{B}_\delta(x)$ directly in terms of $B(x)$: however, for $\tilde{B}(x)$ and for the case of averaging a truncated visibility function, the expressions involving $B(x)$ are convolution integrals and will be difficult to work with. For this reason, we will analyze the case of averaging over all of V in terms of $B(x)$, whereas we will analyze the other two

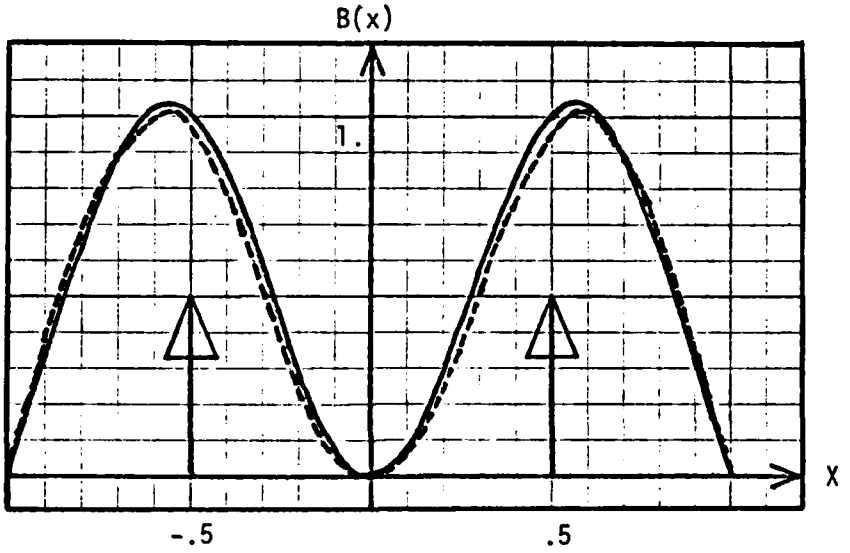

FIGURE 4.1 Peak Shift Effect in 1-D

cases in terms of the visibility function.

The Derivative and Convolution Theorems let us write $\frac{d}{dx}\tilde{B}(x)$ as

$$\frac{d}{dx}\tilde{B}(x)=\int_{-\infty}^{\infty}du\, e^{-i2\pi ux}\left\{-i2\pi u\, V(u)\, \Pi\left(\frac{u-C_u}{b_u}\right)\right\}$$
$$=-\int_{C_u-\frac{b_u}{2}}^{C_u+\frac{b_u}{2}}du\;\; i2\pi u\;\; e^{-i2\pi ux}\; V(u)$$

We will set $C_u=0$ so that the truncation is symmetric. Let $V(u)=V_r(u)+iV_i(u)$; we can then write

$$\frac{d}{dx}\tilde{B}(x)=2\pi\int_{-\frac{b_u}{2}}^{\frac{b_u}{2}}du\left[\left(uV_i\cos 2\pi ux-uV_r\sin 2\pi ux\right)\right.$$
$$\left.-i\left(uV_r\cos 2\pi ux+uV_i\sin 2\pi ux\right)\right]$$

The imaginary terms are odd functions of u, so they vanish in the symmetric integration. If $\frac{d}{dx}B(x_0)$ $\left[\frac{d}{dx}B(x)\right]_{x=x_0}=0$, then

$$\frac{d}{dx}\tilde{B}(x_0)=2\pi\int_{-\frac{b_u}{2}}^{\frac{b_u}{2}}du\left(uV_i\cos 2\pi ux_0-uV_r\sin 2\pi ux_0\right)$$

Similarly, we can obtain

$$\frac{d^2}{dx^2}\tilde{B}(x_0)=-4\pi^2\int_{-\frac{b_u}{2}}^{\frac{b_u}{2}}du\left(u^2V_r\cos 2\pi ux_0\right.$$
$$\left.+u^2V_i\sin 2\pi ux_0\right).$$

It is evident that, in general, $\frac{d}{dx}B(x_0)=0$ does not imply $\frac{d}{dx}\tilde{B}(x_0)=0$. Although $\frac{d}{dx}\tilde{B}(x_0)$ may be small, it will consistently vanish only for a peak at the origin for the case in which B(x) is an even function. In this case, $V_i(u)=0$, and $x_0=0$ causes the term in $V_r(u)$ in the expression for $\frac{d}{dx}\tilde{B}(x_0)$ to vanish, so $\frac{d}{dx}\tilde{B}(x_0)=0$ and $\frac{d^2}{dx^2}\tilde{B}(x_0)<0$. We are

usually assured that the second derivative is negative because V_r is symmetric with

$$V(0) = V_r(0) = \int_{-\infty}^{\infty} dx\ B(x) > 0$$

and

$$\int_{-\infty}^{\infty} du\ V_r(u) = B(0) \geq 0$$

although in some particular cases we may find a different result possible.

On the other hand, for a peak in B at $x_0 \neq 0$, or if B(x) is not an even function, then the general case will be that the peak in $\tilde{B}$ will occur at a different point than that in B(x), although again some particular cases should be possible where the peaks are coincident. One particular case, in which

$$V_i(u) \cos 2\pi u x_0 = V_r(u) \sin 2\pi u x_0$$

will cause the peaks to be coincident. Also, the more general case where

$$\int_{-\frac{b_u}{2}}^{\frac{b_u}{2}} du\ u\ V_i \cos 2\pi u x_0 = \int_{-\frac{b_u}{2}}^{\frac{b_u}{2}} du\ u\ V_r \sin 2\pi u x_0$$

can likewise lead to coincident peaks.

Unfortunately, it does not appear possible to write a concise expression, valid for a general visibility function with arbitrary symmetric truncation, which sets an upper bound for the peak shift in $\tilde{B}(x)$ resulting from truncation. However, if we assume that the peak shift is small, we can arrive at an approximation to

the peak shift, which we will designate by Δ_x.

Consider the case where $\frac{d}{dx}\tilde{B}(x_0+\Delta_x)=0$, if $\frac{d}{dx}B(x_0)=0$. Then

$$\frac{d}{dx}\tilde{B}(x_0+\Delta_x) = 0 = 2\pi\int_{-\frac{b_u}{2}}^{\frac{b_u}{2}} du\left[uV_i\cos 2\pi u(x_0+\Delta_x) - uV_r \sin 2\pi u(x_0+\Delta_x)\right]$$

$$= 2\pi\int_{-\frac{b_u}{2}}^{\frac{b_u}{2}} du\left[uV_i\cos 2\pi ux_0\cos 2\pi u\Delta_x - uV_i \sin 2\pi ux_0 \sin 2\pi u\Delta_x\right.$$
$$\left. - uV_r \sin 2\pi ux_0 \cos 2\pi u\Delta_x - uV_r \cos 2\pi ux_0 \sin 2\pi u\Delta_x\right].$$

If we make the assumption that Δ_x is small, we can expand to first order in Δ_x to get

$$0 = \int_0^{\frac{b_u}{2}} du\left[uV_i\cos 2\pi ux_0 - 2\pi\Delta_x u^2 V_i \sin 2\pi ux_0\right.$$
$$\left. - uV_r \sin 2\pi ux_0 - 2\pi\Delta_x u^2 V_r \cos 2\pi ux_0\right].$$

We can now solve for Δ_x:

$$\Delta_x = \frac{\int_0^{\frac{b_u}{2}} du\, u\left[V_i\cos 2\pi ux_0 - V_r \sin 2\pi ux_0\right]}{2\pi\int_0^{\frac{b_u}{2}} du\, u^2\left[V_i \sin 2\pi ux_0 + V_r\cos 2\pi ux_0\right]}$$

As an example, consider the case $V(u)=\cos\pi u$, truncated at $|u|=1$. We have then, for the point source at $x_0=.5$,

$$\Delta_x = \frac{-\int_0^1 du\, u\cos\pi u \sin\pi u}{2\pi\int_0^1 du\, u^2\cos^2\pi u}$$

$$= \frac{-\frac{u^2}{2}\frac{1}{2\pi}\sin^2\pi u\Big|_0^1 + \frac{\pi}{2}\int_0^1 du\, u^2\left[\cos^2\pi u - \sin^2\pi u\right]}{2\pi\int_0^1 du\, u^2\cos^2\pi u}$$

$$= \frac{1}{4}\left[1 - \frac{\left[\frac{u^3}{6} - \left(\frac{u^2}{4\pi} - \frac{1}{8\pi^3}\right)\sin 2\pi u - \frac{u\cos 2\pi u}{4\pi^2}\Big|_0^1\right]}{\left[\frac{u^3}{6} + \left(\frac{u^2}{4\pi} - \frac{1}{8\pi^3}\right)\sin 2\pi u + \frac{u\cos 2\pi u}{4\pi^2}\Big|_0^1\right]}\right]$$

$$= .06597$$

The exact peak shift is calculated as follows. The exact form for $\tilde{B}(x)$ is

$$\tilde{B}(x)=\int_{-\infty}^{\infty}dx'\,\frac{\sin 2\pi(x-x')}{\pi(x-x')}\,\frac{1}{2}\left[\delta(x-\tfrac{1}{2})+\delta(x+\tfrac{1}{2})\right]$$

$$=\operatorname{sinc} 2(x-\tfrac{1}{2})+\operatorname{sinc} 2(x+\tfrac{1}{2})$$

Searching for the peak iteratively gives the peak location at x=.56285 (to five places), and thus the peak shift is .06285, which agrees reasonably well (to about 5%) with our estimate based on the expansion to first order in the peak shift.

We now consider peak shifts which are due to averaging effects only. If V(u) is averaged with constant intervals over its entire domain, then

$$\hat{B}_\delta(x)=\sum_{n=-\infty}^{\infty}B(x-\tfrac{n}{T})\operatorname{sinc}T(x-\tfrac{n}{T})$$

Consider:

$$\frac{d}{dx}\hat{B}_\delta(x)=\sum_{n=-\infty}^{\infty}\frac{1}{dx}\left[B(x-\tfrac{n}{T})\frac{\sin\pi T(x-\frac{n}{T})}{\pi T(x-\frac{n}{T})}\right]$$

$$=\sum_{n=-\infty}^{\infty}\frac{dB(x')}{dx'}\Big|_{x'=x-\frac{n}{T}}\operatorname{sinc}T(x-\tfrac{n}{T})$$

$$+\sum_{n=-\infty}^{\infty}B(x-\tfrac{n}{T})\left[\frac{\cos\pi T(x-\frac{n}{T})}{(x-\frac{n}{T})}-\frac{\operatorname{sinc}T(x-\frac{n}{T})}{(x-\frac{n}{T})}\right].$$

Suppose now that $\frac{d}{dx}B(x_0)=0$. Then,

$$\frac{d}{dx}\hat{B}_\delta(x_0)=B(x_0)\left[\frac{\cos\pi Tx_0}{x_0}-\frac{\sin\pi Tx_0}{\pi Tx_0^2}\right]+\sum_{\substack{n=-\infty\\ n\neq 0}}^{\infty}\left\{B'(x_0-\tfrac{n}{T})\operatorname{sinc}T(x_0-\tfrac{n}{T})\right.$$

$$\left.+B(x_0-\tfrac{n}{T})\left[\frac{\cos\pi T(x_0-\frac{n}{T})}{(x_0-\frac{n}{T})}-\frac{\operatorname{sinc}T(x_0-\frac{n}{T})}{(x_0-\frac{n}{T})}\right]\right.$$

The terms in the sum are seen to represent possible aliasing effects

which, of course, can themselves cause peak shifts. In particular, let us now suppose that $B(x)$ is a band-limited function in $|x| \leq L_x$. Then, if we consider $|x_0| \leq L_x$, all terms in the sum over non-zero n are seen to vanish provided that $T \leq T_{NI}$, since if we average at intervals as small as or smaller than the Nyquist interval, then there will be no aliasing effects to influence peak shifting.

With these qualifications, we may write

$$\frac{d}{dx}\hat{B}_\delta(X_0) = B(X_0)\left[\frac{\cos \pi T X_0}{X_0} - \frac{\sin \pi T X_0}{\pi T X_0^2}\right].$$

In this case, then if $\hat{B}_\delta(x_0)$ is to be a relative extremum point coincident with a relative extremum in $B(x)$, we must satisfy one of the two following conditions:

1. $B(x_0) = 0$

2. $\frac{\cos \pi T X_0}{X_0} = \frac{\sin \pi T X_0}{\pi T X_0^2} \Longrightarrow \tan \pi T X_0 = \pi T X_0.$

Note that as $T \to 0$, the condition $\tan \pi T X_0 = \pi T X_0$ becomes satisfied, being exact in the limit $T=0$, as required, for any x_0. Note that this transcendental equation has an infinite number of possible solutions for x_0. If a peak in $B(x)$ occurs at one of these solutions, for a given value of T, then the corresponding peak in $\hat{B}_\delta(x)$ will also occur at x_0. Note that this result predicts that the peak shift oscillates in such a way as to be zero for those values of x_0 which satisfy condition 2 above, for a given fixed value of T.

If $x_0=0$, we must consider the following limit:

$$\lim_{x_0\to 0} \frac{1}{x_0}\left[\cos \pi T x_0 - \frac{\sin \pi T x_0}{\pi T x_0}\right]$$

Using L'Hospital's rule gives

$$\lim_{x_0\to 0} \frac{\cos \pi T x_0 - \mathrm{sinc}\, T x_0}{x_0} = \lim_{x_0\to 0} \frac{-\pi T \sin \pi T x_0 - \frac{d}{dx}\left[\mathrm{sinc}\, T x_0\right]}{1} = 0.$$

since the slope of the sinc function is zero when its argument is zero. From this we conclude that averaging with fixed $T\leq T_{NI}$, so that aliasing effects do not occur, will not produce a peak shift in a peak at the origin. This result resembles the fact that truncation alone does not produce a shift in a peak at the origin.

For $x_0\neq 0$, let us suppose that

$$\frac{d}{dx}\hat{B}_\delta(x_0+\Delta_x)=0 \quad \text{if} \quad \frac{d}{dx}B(x_0)=0.$$

Then

$$\frac{d}{dx}\hat{B}_\delta(x_0+\Delta_x)=0 = B(x_0+\Delta_x)\left[\frac{\cos \pi T(x_0+\Delta_x)}{x_0+\Delta_x} - \frac{\mathrm{sinc}\, T(x_0+\Delta_x)}{x_0+\Delta_x}\right]$$

which implies

$$\frac{\cos \pi T x_0 \cos \pi T \Delta_x - \sin \pi T x_0 \sin \pi T \Delta_x}{x_0+\Delta_x} = \frac{\sin \pi T x_0 \cos \pi T \Delta_x + \cos \pi T x_0 \sin \pi T \Delta_x}{\pi T (x_0^2 + 2x_0\Delta_x + \Delta_x^2)}$$

Expanding to first order in peak shift Δ_x, which we assume to be small, gives

$$\frac{\cos \pi T X_0 - \pi T \Delta_x \sin \pi T X_0}{X_0 + \Delta_x} = \frac{\sin \pi T X_0 + \pi T \Delta_x \cos \pi T X_0}{\pi T (X_0^2 + 2 X_0 \Delta_x)}.$$

Rearranging, and neglecting terms in Δ_x higher than first order gives

$$\Delta_x = \frac{X_0 \sin \pi T X_0 - \pi T X_0^2 \cos \pi T X_0}{\pi T X_0 \cos \pi T X_0 - (\pi^2 T^2 X_0^2 + 1) \sin \pi T X_0}.$$

As an example, consider the transform pair

$$V(u) = \left(1 + \frac{iu}{\sqrt{\pi}}\right) e^{-u^2} \supset (\sqrt{\pi} + \pi x) e^{-\pi^2 x^2} = B(x).$$

Now, $V(|u| \geq 3.5) \leq 10^{-5}$, so we effectively are averaging over the full visibility function if we truncate at $|u| = 3.5$. Since $B(|x| \geq 1) \leq 10^{-4}$, the "effective" Nyquist interval is $T_{NI} \simeq .5$. We choose a fairly gross averaging interval $T = 1$. The exact peak in $B(x)$ is calculated to be $x_0 = .07879$. The peak in $\hat{B}_\delta(x)$ can be determined by searching on the computer. and is $x_0 = .0685$, to four places, giving $\hat{\Delta}_x = -.01029$ for the true peak shift. Our equation predicts $\Delta_x = -.01976$, giving the peak at $x = .059$. Δ_x is a good estimate for $\hat{\Delta}_x$ but is off by a factor of 1.92 as opposed to the previous case for shifts due to truncation only, which agreed to within 5% with the true shift.

We now consider peak shifts resulting from symmetric truncation and averaging. For the case of averaging a symmetrically

truncated visibility function, we have

$$\hat{B}_\delta(x) = \mathcal{F}^{-1}\left\{ \bar{\mathcal{V}}(u)\right\} = \sum_{n=-N}^{N} T\left[\bar{V}_n\right] e^{-i2\pi u_n x}$$

$$= \sum_{n=-N}^{N} e^{-i2\pi u_n x} \int_{u_n - \frac{T_n}{2}}^{u_n + \frac{T_n}{2}} du\, V(u)$$

Then,

$$\frac{d}{dx}\hat{B}_\delta(x) = \sum_{n=-N}^{N} (-i2\pi u_n)\, e^{-i2\pi u_n x} \int_{u_n - \frac{T_n}{2}}^{u_n + \frac{T_n}{2}} du\, V(u).$$

Treating the value u_n as constant independent of the u integration, we may write

$$\frac{d}{dx}\hat{B}_\delta(x) = -2\pi \sum_{n=-N}^{N} u_n \int_{u_n - \frac{T_n}{2}}^{u_n + \frac{T_n}{2}} du \Big\{ \left(V_r \sin 2\pi u_n x - V_i \cos 2\pi u_n x\right) + i\left(V_i \sin 2\pi u_n x + V_r \cos 2\pi u_n x\right)\Big\}.$$

Noting that u_n is odd in n with $u_0=0$, V_r is even in u and V_i is odd in u, we see that the sum over integrals can be written as

$$\frac{d}{dx}\hat{B}_\delta(x) = -4\pi \sum_{n=1}^{N} u_n \int_{u_n - \frac{T_n}{2}}^{u_n + \frac{T_n}{2}} du \left(V_r \sin 2\pi u_n x - V_i \cos 2\pi u_n x\right).$$

As before, we suppose that $\frac{d}{dx} B(x_0)=0$ and that $\frac{d}{dx}\hat{B}_\delta(x_0+\Delta_x)=0$. Then,

$$\frac{d}{dx}\hat{B}_\delta(x_0+\Delta_x) = 0 = -4\pi \sum_{n=1}^{N} u_n \int_{u_n - \frac{T_n}{2}}^{u_n + \frac{T_n}{2}} du \Big(V_r \sin 2\pi u_n (x+\Delta_x) - V_i \cos 2\pi u_n (x_0+\Delta_x)\Big)$$

which implies

$$0 = \sum_{n=1}^{N} u_n \int_{u_n - \frac{T_n}{2}}^{u_n + \frac{T_n}{2}} du \Big[V_r\left(\sin 2\pi u_n x_0 \cos 2\pi u_n \Delta_x + \cos 2\pi u_n x_0 \sin 2\pi u_n \Delta_x\right) - V_i\left(\cos 2\pi u_n x_0 \cos 2\pi u_n \Delta_x - \sin 2\pi u_n x_0 \sin 2\pi u_n \Delta_x\right)\Big]$$

Assuming that the peak shift in small, we expand to first order in Δ_x and simplify to get

$$\Delta_x = \frac{\sum_{n=1}^{N} u_n \int_{u_n - \frac{T_n}{2}}^{u_n + \frac{T_n}{2}} du \left(V_r \sin 2\pi u_n x_o - V_i \cos 2\pi u_n x_o \right)}{-2\pi \sum_{n=1}^{N} u_n^2 \int_{u_n - \frac{T_n}{2}}^{u_n + \frac{T_n}{2}} du \left(V_i \sin 2\pi u_n x_o + V_r \cos 2\pi u_n x_o \right)}$$

As an example for this case, we consider

$$V(u) = e^{-|u|} \cos \pi u \supset \frac{1}{1+[2\pi(.5-x)]^2} + \frac{1}{1+[2\pi(.5+x)]^2} = B(x)$$

We want to truncate a fair amount of V(u) and average with $T > T_{NI}$. We choose truncation limits at $|u|=1.5$, and use $T=.6$, since $V(|u| \geq 1.5) \leq .2231$ and $B(|x| \geq 7.2) \leq .001$ implies $T_{NI}=.0694$ as the effective Nyquist interval. The true peak is at $x_o=.49939$ and the peak in $\hat{B}_\delta(x)$ is at $\hat{x}_o=.49877$, both found by iterative search to five places. Our equation for peak shift gives an estimate of $\Delta_x=-.0002374$, whereas the exact peak shift is -.00063. Agreement here is to within a factor of 2.6. Our equation gives an order of magnitude estimate.

In a real experiment, one would not know the true visibility and brightness functions, but would rather have only the average values of the visibility function as data. For the cases of averaging over the entire visibility function and averaging a symmetrically truncated V(u), our equations involve only integrations over the visibility function, which are just equal to the average

value (which we have as data) times the knownvalue of the averaging interval. We can thus estimate a margin of error for all peaks in the brightness function generated from the average value data. For the case of truncation only, we cannot determine the integrals (which now contain other factors of u) from the available data; however, this case is not of significant importance since experimental data will be in terms of average values of the visibility function.

4.6 Irregular Averaging Intervals

In the development of the averaging theorems in this chapter and in the discussion of peak shifts, we have used the simplifying assumption that T was a fixed averaging interval size. We now want to consider the generalization to the case where T is a variable parameter.

For the case where V(u) is averaged over its entire domain with irregular averaging intervals with epoch at the origin, we have

$$\bar{\gamma}(u) = \sum_{n=-\infty}^{\infty} T_n \left[\bar{V}_n\right] \delta(u-u_n)$$

where the midpoint of the n^{th} interval is now given by

$$u_n = \begin{cases} \frac{T_0}{2} + \sum_{\sigma=1}^{n-1} T_\sigma + \frac{T_n}{2} & : n>0 \\ 0 & : n=0 \\ -\left[\frac{T_0}{2} + \sum_{\sigma=-1}^{n+1} T_\sigma + \frac{T_n}{2}\right] & : n<0 \end{cases}$$

Then,

$$\hat{B}_\delta(x) = \sum_{n=-\infty}^{\infty} T_n \int_{-\infty}^{\infty} du\, e^{-i2\pi ux} \left[\int_{-\infty}^{\infty} dx'\, B(x')\, \mathrm{sinc}\, T_n x'\, e^{i2\pi u_n x'} \right] \delta(u-u_n)$$

$$= \sum_{n=-\infty}^{\infty} T_n \int_{-\infty}^{\infty} dx'\, B(x')\, \mathrm{sinc}\, T_n x'\, e^{-i2\pi u_n (x-x')} .$$

Because $u_n \neq nT$ for irregular intevals, we cannot replace the present sum by a sum over delta functions and thereby simplify the integral, as was possible for constant T.

For the case where V(u) is truncated symmetrically and averaged with irregular intervals, we get

$$\hat{B}_\delta(x) = \sum_{n=-N}^{N} T_n \int_{-\infty}^{\infty} dx'\, B(x')\, \mathrm{sinc}\, T_n x'\, e^{-i2\pi u_n (x-x')} .$$

In particular, for the important case $T_n = T_{-n}$, this can be simplified:

$$\hat{B}_\delta(x) = T_0 \int_{-\infty}^{\infty} dx'\, B(x')\, \mathrm{sinc}\, T_0 x' + 2\sum_{n=1}^{N} T_n \int_{-\infty}^{\infty} dx'\, B(x')\, \mathrm{sinc}\, T_n x' \cdot \cos 2\pi u_n (x-x')$$

$$= T_0 \int_{-\infty}^{\infty} dx'\, B(x')\, \mathrm{sinc}\, T_0 x' + 2\sum_{n=1}^{N} T_n \cos 2\pi u_n x \int_{-\infty}^{\infty} dx' B(x') \cdot \mathrm{sinc}\, T_n x' \cos 2\pi u_n x' + 2\sum_{n=1}^{N} T_n \sin 2\pi u_n x \int_{-\infty}^{\infty} dx' B(x')\, \mathrm{sinc}\, T_n x' \cdot \sin 2\pi u_n x'$$

$$= \int_{-\infty}^{\infty} dx'\, B(x')\, \frac{\sin \pi T_0 x'}{\pi x'} + \sum_{n=1}^{N} \left\{ \cos 2\pi u_n x \int_{-\infty}^{\infty} dx'\, \frac{B(x')}{\pi x'} \left[\sin k_n^+ x' + \sin k_n^- x' \right] + \sin 2\pi u_n x \int_{-\infty}^{\infty} dx'\, \frac{B(x')}{\pi x'} \left[\cos k_n^- x' - \cos k_n^+ x' \right] \right\}$$

where

$$k_n^+ \equiv \pi T_n + 2\pi u_n = \pi \left[T_0 + 2\sum_{\sigma=1}^{n} T_\sigma \right]$$

$$k_n^- \equiv \pi T_n - 2\pi u_n = -\pi \left[T_0 + 2\sum_{\sigma=1}^{n-1} T_\sigma \right] .$$

For irregular intervals, we have seen that only the bounds on the index n distinguish the cases of averaging over the entire V(u) and averaging a symmetrically truncated V(u). Therefore, we need to discuss the generalization of the peak shift equation only for averaging a symmetrically truncated visibility function. We will make the further restriction that $T_n=T_{-n}$ which will often be the relevant case (along both the u and v axes) for the radio interferometer system in which we are interested. It is obvious from a review of the method used to derive the peak shift Δ_x for the case of averaging with fixed T over a symmetrically truncated visibility function that the appropriate generalization for irregular intervals is just the previous result

$$\Delta_x = \frac{\sum_{n=1}^{N} u_n \int_{u_n-\frac{T_n}{2}}^{u_n+\frac{T_n}{2}} du \left(V_r \sin 2\pi u_n x_o - V_i \cos 2\pi u_n x_o\right)}{-2\pi \sum_{n=1}^{N} u_n^2 \int_{u_n-\frac{T_n}{2}}^{u_n+\frac{T_n}{2}} du \left(V_i \sin 2\pi u_n x_o + V_r \cos 2\pi u_n x_o\right)}$$

with $u_n \neq nT$ now.

4.7 Generalizations to Two Dimensions

The generalization of our 1-D results to 2-D is entirely straightforward. We will illustrate the procedure for one theorem and then simply state the other results. The epoch of averaging is always at the origin. We will assume that the cell sizes are irregular, and state the simplified form for constant cell sizes if one exists.

Theorem 4.6: Each average value of V(u,v) can be expressed in terms of a definite integral over the true source brightness function:

$$[\bar{V}_{n,m}] = \int_{-\infty}^{\infty} dx \; \mathrm{sinc}\, T_{u,n} x \, e^{i2\pi u_n x} \int_{-\infty}^{\infty} dy \; \mathrm{sinc}\, T_{v,m} y \, e^{i2\pi v_m y} B(x,y).$$

Proof: The average value of V(u,v) in the $(n,m)^{th}$ cell is

$$[\bar{V}_{n,m}] = \frac{1}{T_{u,n} T_{v,m}} \int_{u_n - \frac{T_{u,n}}{2}}^{u_n + \frac{T_{u,n}}{2}} du \int_{v_m - \frac{T_{v,m}}{2}}^{v_m + \frac{T_{v,m}}{2}} dv \; V(u,v)$$

where the cell midpoint coordinates are (u_n, v_m):

$$u_n = \begin{cases} \frac{T_{u,0}}{2} + \sum_{\sigma=1}^{n-1} T_{u,\sigma} + \frac{T_{u,n}}{2} : n > 0 \\ 0 : n = 0 \\ -\left[\frac{T_{u,0}}{2} + \sum_{\sigma=-1}^{n+1} T_{u,\sigma} + \frac{T_{u,n}}{2}\right] : n < 0 \end{cases} \qquad v_m = \begin{cases} \frac{T_{v,0}}{2} + \sum_{\sigma=1}^{m-1} T_{v,\sigma} + \frac{T_{v,m}}{2} : m > 0 \\ 0 : m = 0 \\ -\left[\frac{T_{v,0}}{2} + \sum_{\sigma=-1}^{m+1} T_{v,\sigma} + \frac{T_{v,m}}{2}\right] : m < 0 \end{cases}$$

Using

$$V(u,v) = \int_{-\infty}^{\infty} dx \int_{-\infty}^{\infty} dy \; e^{i2\pi(ux+vy)} B(x,y)$$

we write

$$[\bar{V}_{n,m}] = \frac{1}{T_{u,n} T_{v,m}} \int_{u_n - \frac{T_{u,n}}{2}}^{u_n + \frac{T_{u,n}}{2}} du \int_{v_m - \frac{T_{v,m}}{2}}^{v_m + \frac{T_{v,m}}{2}} dv \left[\int_{-\infty}^{\infty} dx \int_{-\infty}^{\infty} dy \; e^{i2\pi(ux+vy)} B(x,y) \right]$$

$$= \frac{1}{T_{u,n} T_{v,m}} \int_{-\infty}^{\infty} dx \int_{-\infty}^{\infty} dy \; B(x,y) \left[\int_{u_n - \frac{T_{u,n}}{2}}^{u_n + \frac{T_{u,n}}{2}} du \int_{v_m - \frac{T_{v,m}}{2}}^{v_m + \frac{T_{v,m}}{2}} dv \; e^{i2\pi(ux+vy)} \right]$$

$$= \frac{1}{T_{u,n} T_{v,m}} \int_{-\infty}^{\infty} dx \int_{-\infty}^{\infty} dy \; B(x,y) \, e^{i2\pi(u_n x + v_m y)} \frac{\sin \pi T_{u,n} x}{\pi x} \frac{\sin \pi T_{v,m} y}{\pi y}$$

■

For fixed cell sizes, $u_n=nT_u$, $v_m=mT_v$. We now state the other generalizations to 2-D.

The effect of averaging V(u,v) over its entire domain with fixed cell size is given by

$$\hat{B}_c(x,y)=\sum_{n=-\infty}^{\infty}\sum_{m=-\infty}^{\infty} B\left(x-\frac{n}{T_u},y-\frac{m}{T_v}\right)\,\mathrm{sinc}\,T_u\left(x-\frac{n}{T_u}\right)\,\mathrm{sinc}\,T_v\left(y-\frac{m}{T_v}\right).$$

For irregular cell sizes, the result is

$$\hat{B}_c(x,y)=\sum_{n=-\infty}^{\infty}T_{u,n}\sum_{m=-\infty}^{\infty}T_{v,m}\int_{-\infty}^{\infty}dx'\,\mathrm{sinc}\,T_{u,n}x'\,e^{-i2\pi u_n(x-x')}\cdot\int_{-\infty}^{\infty}dy'\,\mathrm{sinc}\,T_{v,m}y'\,e^{-i2\pi v_m(y-y')}B(x',y').$$

If V(u,v) is truncated symmetrically in u and v and averaged with irregular cell sizes, we simply change the infinite limits for the n and m summations to (-N to N) and (-M to M), respectively. (Note that averaging the truncated V(u,v) with fixed T_u and T_v does not simplify this result except to remove the cell size ($T_u\cdot T_v$) from the summation.) For the case where $T_{u,n}=T_{u,-n}$ and $T_{v,m}=T_{v,-m}$, we have

$$\hat{B}_\delta(x,y) = \int_{-\infty}^{\infty} dx' \frac{\sin \pi T_{u,0} x'}{\pi x'} \int_{-\infty}^{\infty} dy' \frac{\sin \pi T_{v,0} y'}{\pi y'} B(x',y')$$

$$+ \sum_{n=1}^{N} \sum_{m=1}^{M} \Bigg\{ \cos 2\pi u_n x \cos 2\pi v_m y \int_{-\infty}^{\infty} dx' \frac{\sin k_n^+ x' + \sin k_n^- x'}{\pi x'}$$

$$\cdot \int_{-\infty}^{\infty} dy' \frac{\sin k_m^+ y' + \sin k_m^- y'}{\pi y'} B(x',y') + \cos 2\pi u_n x \sin 2\pi v_m y$$

$$\cdot \int_{-\infty}^{\infty} dx' \frac{\sin k_n^+ x' + \sin k_n^- x'}{\pi x'} \int_{-\infty}^{\infty} dy' \frac{\cos k_m^- y' - \cos k_m^+ y'}{\pi y'} B(x',y')$$

$$+ \sin 2\pi u_n x \cos 2\pi v_m y \int_{-\infty}^{\infty} dx' \frac{\cos k_n^- x' - \cos k_n^+ x'}{\pi x'} \int_{-\infty}^{\infty} dy' \frac{\sin k_m^+ y' + \sin k_m^- y'}{\pi y'}$$

$$\cdot B(x',y') + \sin 2\pi u_n x \sin 2\pi v_m y \int_{-\infty}^{\infty} dx' \frac{\cos k_n^- x' - \cos k_n^+ x'}{\pi x'}$$

$$\cdot \int_{-\infty}^{\infty} dy' \frac{\cos k_m^- y' - \cos k_m^+ y'}{\pi y'} B(x',y') \Bigg\}$$

where

$$k_n^+ \equiv \pi \left[T_{u,0} + 2 \sum_{\sigma=1}^{n} T_{u,\sigma} \right] \qquad k_m^+ \equiv \pi \left[T_{v,0} + 2 \sum_{\sigma=1}^{m} T_{v,\sigma} \right]$$

$$k_n^- \equiv -\pi \left[T_{u,0} + 2 \sum_{\sigma=1}^{n-1} T_{u,\sigma} \right] \qquad k_m^- \equiv -\pi \left[T_{v,0} + 2 \sum_{\sigma=1}^{m-1} T_{v,\sigma} \right]$$

We may express the peak shift in two dimensions by (Δ_x, Δ_y) where the x and y components independently satisfy the 1-D peak shift equation for irregular averaging intervals given in the previous section. Note that this result explains why there was no peak shift in the y-direction in the model source study since both peaks occurred at y=0 values, and we found that peaks at the origin do not displace.

4.8 Development of an Algorithm

Having examined the effects on the brightness function

of truncating and averaging the visibility function, we now attempt to develop an algorithm which uses the relation between the average values $[V_{n,m}]$ and the exact brightness function B(x,y) to obtain a better estimate of B(x,y) than does the standard Fourier inversion method. The advantage to this approach lies in the fact that, although the fourier inversion method disregards the fact that the visibility function has been averaged, an algorithm incorporating this information might be capable of giving higher resolution than one which disregards it. The algorithm which we will develop here is by no means the only approach to the problem, nor is it necessarily the best; however, it may be a useful alternative to the standard inversion method, and as such deserves consideration. We will develop the basic concept in 1-D and then generalize to the two dimensional case where V(u,v) is averaged over a rectangular grid.

We have seen that the average value of V(u) in the n^{th} interval can be expressed as

$$[\bar{V}_n] = \int_{-\infty}^{\infty} dx\ B(x)\ \frac{\sin \pi T_n x}{\pi T_n x}\ e^{i2\pi u_n x}$$

Because the true source brightness function, B(x), appears in the integrand of a definite integral, we cannot invert the equation to solve for B(x). An approximation is therefore necessary.

Since we are concerned with band-limited functions, let us

assume that B(x) is band-limited to the interval $[-L_x, L_x]$. We can then expand B(x) in the complex Fourier series form

$$B(x) = \sum_{n=-\infty}^{\infty} C_n \, e^{-i\frac{2\pi n x}{2L_x}}$$

where the C_n may be complex, and B(x) is of course a real function. If we substitute this Fourier series for B(x) into the definite integral, we would be able to calculate the definite integral's value, with the integration limits now set at $-L_x$ and L_x. Although we can now compute the value of the definite integral, we are still not able to evaluate the infinite number of Fourier coefficients to deduce B(x) exactly. What we propose to do, then, is to convert the (2N+1) complex (in general) average values of the visibility function into the first (2N+1) complex Fourier coefficients in the expansion for B(x).

Let $\bar{B}(x)$ denote the approximation to B(x) determined by this method. Then

$$\bar{B}(x) = \sum_{p=-N}^{N} C_p \, e^{-i\frac{2\pi p x}{2L_x}} \approx B(x)$$

Inserting $\bar{B}(x)$ for B(x) in the definite integral gives

$$[\bar{V}_n] = \int_{-L_x}^{L_x} dx \sum_{p=-N}^{N} C_p \, e^{-i\frac{2\pi p x}{2L_x}} \, \mathrm{sinc}\, T_n x \, e^{i2\pi u_n x}$$

$$= \sum_{p=-N}^{N} C_p \int_{-L_x}^{L_x} dx \, \frac{\sin \pi T_n x}{\pi T_n x} \, e^{-i2\pi x\left(\frac{p}{2L_x} - u_n\right)}$$

We have (2N+1) equations for the (2N+1) values $[V_n]$, $n \in [-N, N]$. Since the definite integral is just a number, we call it $I_{p,n}$. We therefore

can write

$$[\bar{V}_n] = \sum_{p=-N}^{N} C_p \, I_{p,n}$$

We have a system of (2N+1) linear equations in the (2N+1) unknowns C_p. Hence, we have the matrix problem

$$\begin{pmatrix} [\bar{V}_{-N}] \\ \vdots \\ [\bar{V}_N] \end{pmatrix} = \begin{pmatrix} I_{-N,-N} & I_{-N,-N+1} & \cdots \\ \vdots & \vdots & \\ & & \end{pmatrix} \begin{pmatrix} C_{-N} \\ \vdots \\ C_N \end{pmatrix}$$

and we can obtain the required Fourier coefficients:

$$\begin{pmatrix} C_{-N} \\ \vdots \\ C_N \end{pmatrix} = \left(I_{p,n} \right)^{-1} \begin{pmatrix} [\bar{V}_{-N}] \\ \vdots \\ [\bar{V}_N] \end{pmatrix}$$

The matrix elements are determined as follows:

$$I_{p,n} = \int_{-L_x}^{L_x} dx \, \frac{\sin \pi T_n x}{\pi T_n x} \, e^{-i 2\pi x \left(\frac{p}{2L_x} - u_n \right)}$$

$$= \int_{-L_x}^{L_x} dx \, \frac{\sin \pi T_n x}{\pi T_n x} \cos 2\pi x \left(\frac{p}{2L_x} - u_n \right) - i \int_{-L_x}^{L_x} dx \, \frac{\sin \pi T_n x}{\pi T_n x} \sin 2\pi x \left(\frac{p}{2L_x} - u_n \right).$$

The imaginary portion has an odd integrand integrated over symmetric limits and therefore vanishes. Using a trigonometric identity gives

$$I_{p,n} = \frac{1}{2\pi T_n} \int_{-L_x}^{L_x} dx \left(\frac{\sin \alpha_{p,n} x}{x} + \frac{\sin \beta_{p,n} x}{x} \right)$$

$$= \frac{1}{\pi T_n} \int_{0}^{L_x} dx \left(\frac{\sin \alpha_{p,n} x}{x} + \frac{\sin \beta_{p,n} x}{x} \right)$$

where

$$\alpha_{p,n} \equiv \left[\pi T_n + 2\pi \left(\frac{p}{2L_x} - u_n \right) \right], \quad \beta_{p,n} \equiv \left[\pi T_n - 2\pi \left(\frac{p}{2L_x} - u_n \right) \right].$$

The integral cannot be given in closed form; the series result is

$$I_{p,n} = \frac{1}{\pi T_n} \sum_{r=0}^{\infty} \frac{(-1)^r}{(2r+1)(2r+1)!} \left[(\alpha_{p,n} L_x)^{2r+1} + (\beta_{p,n} L_x)^{2r+1} \right]$$

The matrix elements $I_{p,n}$ are real numbers, and we can therefore separate the problem in complex parameters into real and imaginary parts:

$$\begin{pmatrix} [\bar{V}_{-N}]_r \\ \vdots \\ [\bar{V}_N]_r \end{pmatrix} = \begin{pmatrix} I_{p,n} \end{pmatrix} \begin{pmatrix} \mathrm{Re}\{C_{-N}\} \\ \vdots \\ \mathrm{Re}\{C_N\} \end{pmatrix}$$

and

$$\begin{pmatrix} [\bar{V}_{-N}]_i \\ \vdots \\ [\bar{V}_N]_i \end{pmatrix} = \begin{pmatrix} I_{p,n} \end{pmatrix} \begin{pmatrix} \mathrm{Im}\{C_{-N}\} \\ \vdots \\ \mathrm{Im}\{C_N\} \end{pmatrix}$$

The series which results from the above integration must be checked for convergence. (The alternating theorem definition and theorems which we will cite here are taken from Marsden and Weinstein, 1980. B the algebraic sum rule, we can treat the composite series in $[(\alpha_{p,n}L_x)^{2r+1}+(\beta_{p,n}L_x)^{2r+1}]$ as two separate series, and provided each converges separately, then the composite series converges to the sum of the individual series. Consider the following limit:

$$\lim_{r\to\infty}\left|\frac{(-1)^r}{(2r+1)(2r+1)!}\,(\alpha_{p,n}L_x)^{2r+1}\right|$$

$$=\left[\lim_{r\to\infty}\frac{1}{2r+1}\right]\cdot\left[\lim_{r\to\infty}\frac{(\alpha_{p,n}L_x)^{2r+1}}{(2r+1)!}\right].$$

Both of these limits are zero (see Hildebrand, 1976, for verification of the second limit). The same result is obtained for the series in $(\beta_{p,n}L_x)^{2r+1}$. Since each of the separate series alternates in sign and the summation terms in both have the limit zero as $r\to\infty$, then both of these series satisfy the definition of an alternating series. We are therefore assured of convergence by a theorem which states that all alternating series are convergent. Additionally, another theorem insures that if we use only a partial sum to represent the series (as we will have to for practical calculations), then the error resulting from using the partial sum will be no greater than the first omitted term.

We must now address the problem that this method, which we will call the "matrix method", presupposed a knowledge of the true source extent L_x in order to calculate the matrix elements $I_{p,n}$. In the realistic case, L_x is one of the parameters which would be determined <u>from</u> the interferometric observations. To compensate for this difficulty, we propose that a zeroth order estimate for L_x be used initially in the calculations. This estimate may be based on a lower resolution observation capable of yielding a close estimate for L_x while still being unable to resolve the source structure. Using the zeroth order estimate $L_x^{(o)}$, we determine the

C_p's and hence deduce $\bar{B}^{(0)}(x)$. Now the definite integral theorem states that

$$\int_{-L_x}^{L_x} dx\ B(x) = V(0).$$

We can define an approximate definite integral relation by

$$\int_{-L_x^{(1)}}^{L_x^{(1)}} dx\ B^{(0)}(x) = [\bar{V}_0]$$

form which we can deduce a better estimate for the true source extent, $L_x^{(1)}$. Using $L_x^{(1)}$, we can determine $\bar{B}^{(1)}(x)$ from the matrix method. This process may be continued iteratively until we satisfy the approximate definite integral relation to within some error bound (assuming, of course, that the iterative scheme converges).

During initial 1-D trial cases using the matrix method, it was found that cases in which irregular averaging intervals were used, especially when the interval sizes differed by factors not near unity, gave totally incorrect results. It is believed that the cause of this phenomenon lies in the fact that a "frequency" factor $\frac{n}{2L_x}$ was assumed in the Fourier expansion for B(x). Now, $\{\frac{n}{2L_x}\}$ are the natural set of frequencies required to expand a function B(x) which is band-limited in the inteval $[-L_x, L_x]$. However, we are required to sample or average V(u) at the Nyquist interval, $T_{NI} = \frac{1}{2L_x}$, in order to produce this natural set of frequencies for the expansion of the band-limited function B(x). This is just the logic involved in the proof of the Sampling Theorem. By using a set of averaging intervals of different sizes, we are, in essence,

"confusing" the frequency information from which we are attempting to derive the fourier series coefficients, C_p.

To circumvent this difficulty, it is possible to reformulate the problem into one using averaging intevals whose sizes are fixed at the Nyquist interval. Thus, given a set of data containing average values of V(u) over irregular intervals, we can convert the data into an appropriate form for use in the matrix method.

The proposed reformulation algorithm proceeds as follows. First, we examine the truncation limits to see if an integral number of Nyquist intervals, with epoch at the origin, will fit in between these limits. If this does not occur, we symmetrically extend the truncation limits so as to satisfy this requirement. In the extension region, we assign a zero value for the average visibility. (Assigning a zero value for the average vixibility in the extension region is similar to other methods where zero values are implicitly or explicitly assigned to portions of the u-v plane for which data is not available; however, other techniques, such as assigning a data value based on a Gaussian taper, may be more advantageous. These possibilities have not been investigated here, but further study should include considerations of alternative data extension techniques.) We will say that the original data set index n runs $n \epsilon [-N,N]$, where it is understood that N accounts for the domain extension, if it was necessary. We now "reaverage" the average values of the visibility function to obtain Nyquist interval average values.

Consider the k^{th} Nyquist interval, with indexing scheme in k similar to the indexing scheme in n for the data values. Let there be J_k original data intervals lying wholly or partly in the k^{th} Nyquist interval. Denoting $\bar{V}_k$ as the average value in the k^{th} Nyquist interval whose midpoint is u_k, we have

$$\bar{V}_k = \frac{1}{T_{NI}} \int_{u_k - \frac{T_{NI}}{2}}^{u_k + \frac{T_{NI}}{2}} du\, V(u)$$

$$= \sum_{n=n_k}^{J_k} \frac{T_n}{T_{NI}} \int_{u_n - \frac{T_n}{2}}^{u_n + \frac{T_n}{2}} du\, V(u)$$

$$= \sum_{n=n_k}^{J_k} \frac{T_n}{T_{NI}} [\bar{V}_n]$$

where n_k is the lowest index number (in the possibly extended set $n \epsilon [-N,N]$) for an original averaging interval which is contained wholly or partly in the k^{th} Nyquist interval. Using the original $[V_n]$ data values in this equation, we compute the values for the "reaveraged" data set $\bar{V}_k$.

Now, we can also write our expression for $[V_n]$ in terms of $\bar{B}(x)$ for the terms in the sum:

$$\bar{V}_k = \frac{1}{T_{NI}} \sum_{n=n_k}^{J_k} T_n \int_{-L_x}^{L_x} dx'\, B(x') \operatorname{sinc} T_n x' \, e^{i 2\pi u_n x'}$$

Let there be (2K+1) Nyquist intervals so that $k \epsilon [-K,K]$. The Fourier expansion for B(x) is

$$B(x) = \sum_{p=-\infty}^{\infty} C_p \, e^{-i \frac{2\pi p x}{2L_x}}$$

and we can obtain (2K+1) coefficients from the (2K+1) Nyquist interval average values of V(u):

$$\bar{B}(x) = \sum_{p=-K}^{K} C_p \, e^{-i\frac{2\pi p x}{2L_x}} \approx B(x).$$

Using this expression for B(x) in the integral gives

$$\bar{V}_k = \frac{1}{T_{NI}} \sum_{n=n_k}^{J_k} T_n \sum_{p=-K}^{K} C_p \int_{-L_x}^{L_x} dx' \, \mathrm{sinc}\, T_n x' \, e^{-i2\pi x'\left(\frac{p}{2L_x} - u_n\right)}$$

$$= \frac{1}{T_{NI}} \sum_{n=n_k}^{J_k} T_n \left\{ \sum_{p=-K}^{K} I_{p,n} C_p \right\}$$

where, as done previously,

$$I_{p,n} = \frac{1}{\pi T_n} \sum_{r=0}^{\infty} \frac{(-1)^r}{(2r+1)(2r+1)!} \left[(\alpha_{p,n} L_x)^{2r+1} + (\beta_{p,n} L_x)^{2r+1} \right]$$

and

$$\alpha_{p,n} \equiv \pi T_n + 2\pi\left(\frac{p}{2L_x} - u_n\right), \qquad \beta_{p,n} \equiv \pi T_n - 2\pi\left(\frac{p}{2L_x} - u_n\right).$$

Now, since the sum over n here is independent of the sum over p, we can write

$$\bar{V}_k = \sum_{p=-K}^{K} C_p \left[\frac{1}{T_{NI}} \sum_{n=n_k}^{J_k} T_n I_{p,n} \right]$$

$$= \sum_{p=-K}^{K} C_p I'_{p,k}$$

where we define

$$I'_{p,k} \equiv \frac{1}{T_{NI}} \sum_{n=n_k}^{J_k} T_n I_{p,n}.$$

We have now completely reformulated the original problem into a form in which the frequency confusion problem for irregular averaging intervals has been circumvented. We again have a linear system, but now with (2K+1) equations in the (2K+1) unknown C_p.

For the generalization to two dimensions, we start with the previous result

$$[\bar{V}_{n,m}] = \int_{-\infty}^{\infty} dx \; \mathrm{sinc}\, T_{u,n} x \, e^{i2\pi u_n x} \int_{-\infty}^{\infty} dy \; \mathrm{sinc}\, T_{v,m} y \, e^{i2\pi v_m y} B(x,y)$$

We initially suppose that all averaging cells are fixed at the Nyquist cell size. Let there be (2N+1) by (2M+1) cells inside the truncation limits. The appropriate approximation to B(x,y) is now

$$\bar{B}(x,y) = \sum_{p=-N}^{N} \sum_{q=-M}^{M} C_{p,q} e^{-i\frac{2\pi p x}{2L_x}} e^{-i\frac{2\pi q y}{2L_y}} \approx B(x,y).$$

Using this expression for B(x,y) in the previous integral gives

$$[\bar{V}_{n,m}] = \sum_{p=-N}^{N} \sum_{q=-M}^{M} C_{p,q} \left[\int_{-\infty}^{\infty} dx \; \mathrm{sinc}\, T_{u,n} x \, e^{-i2\pi x\left(\frac{p}{2L_x} - u_n\right)} \right] \cdot \left[\int_{-\infty}^{\infty} dy \; \mathrm{sinc}\, T_{v,m} y \, e^{-i2\pi y\left(\frac{q}{2L_y} - v_m\right)} \right].$$

Each integral is recognized as being of the same form as the previously considered 1-D integral. We therefore define

$$I_{n,m,p,q} \equiv I_{p,n} I_{q,m},$$

$$I_{p,n} \equiv \frac{1}{\pi T_{u,n}} \sum_{r=0}^{\infty} \frac{(-1)^r}{(2r+1)(2r+1)!} \left[(\alpha_{p,n} L_x)^{2r+1} + (\beta_{p,n} L_x)^{2r+1} \right],$$

$$I_{q,m} \equiv \frac{1}{\pi T_{v,m}} \sum_{r=0}^{\infty} \frac{(-1)^r}{(2r+1)(2r+1)!} \left[(\alpha_{q,m} L_y)^{2r+1} + (\beta_{q,m} L_y)^{2r+1} \right],$$

where

$$\alpha_{p,n} \equiv \pi T_{u,n} + 2\pi\left(\frac{p}{2L_x} - u_n\right) \qquad \alpha_{q,m} \equiv \pi T_{v,m} + 2\pi\left(\frac{q}{2L_y} - v_m\right)$$

$$\beta_{p,n} \equiv \pi T_{u,n} - 2\pi\left(\frac{p}{2L_x} - u_n\right) \qquad \beta_{q,m} \equiv \pi T_{v,m} - 2\pi\left(\frac{q}{2L_y} - v_m\right)$$

We can formulate a matrix equation by trating (n,m) and (p,q) as the two indices [ ]:

$$\begin{pmatrix} [\bar{V}_{-N,-M}] \\ \vdots \\ [\bar{V}_{n,m}] \\ \vdots \\ [\bar{V}_{N,M}] \end{pmatrix} = \begin{pmatrix} I_{(-N,-M),(-N,-M)} & \cdots & \cdots \\ \vdots & & \vdots \\ \cdots & I_{(n,m)(p,q)} & \cdots \\ \vdots & & \vdots \end{pmatrix} \begin{pmatrix} C_{-N,-M} \\ \vdots \\ C_{p,q} \\ \vdots \\ C_{N,M} \end{pmatrix}$$

The solution to this 2-D problem therefore proceeds in a manner directly analogous to the 1-D case, including iterative refinements for L_x and L_y.

The reformulation algorithm also proceeds in direct analogy to the 1-D case. Let there be (2K+1)·(2L+1) Nyquist cells inside the truncation limits. The truncation limits may have had to have been extended along the u and/or v axes, as previously discussed for the u axis in the 1-D case. We will say that the original data set indices run as $n\epsilon[-N,N]$, $m\epsilon[-M,M]$, where it is understood that N and M account for the domain extension, if it was necessary. Index $k\epsilon[-K,K]$ is the Nyquist cell reference index along the u axis, and $l\epsilon[-L,L]$ is the Nyquist cell reference index along the v axis. Let $\bar{V}_{k,l}$ denote the average value of V(u,v) in the $(k,l)^{th}$ Nyquist cell. We "reaverage" the average value data into Nyquist cells:

$$\bar{V}_{k,l} = \sum_{n=n_k}^{J_k} \sum_{m=m_l}^{G_l} \frac{T_{u,n} T_{v,m}}{T_{u,NI} T_{v,NI}} [\bar{V}_{n,m}]$$

Here, n_k and m_l are the lowest values of n and m such that the $(n_k,m_l)^{th}$ cell in the original (possibly extended) data set lies wholly or partly in the $(k,l)^{th}$ Nyquist cell. Similarly, J_k and G_l are the highest values of n and m such that the $(J_k,G_l)^{th}$ cell in the original (possibly extended) data set lies wholly or partly in the $(k,l)^{th}$ Nyquist cell. Then, using the analogous procedure as we discussed for the 1-D case, we have

$$\bar{V}_{k,l} = \sum_{n=n_k}^{J_k} \sum_{m=m_l}^{G_l} \frac{T_{u,n}\, T_{v,m}}{T_{u,NI}\, T_{v,NI}} \sum_{p=-K}^{K} \sum_{q=-L}^{L} C_{p,q}\, I_{p,n}\, I_{q,m}$$

$$= \sum_{p=-K}^{K} \sum_{q=-L}^{L} C_{p,q}\, I'_{k,l,p,q}$$

where we define, $I'_{k,l,p,q} \equiv I'_{p,k}\, I'_{q,l}$,

$$I'_{p,k} \equiv \sum_{n=n_k}^{J_k} \frac{T_{u,n}}{T_{u,NI}}\, I_{p,n} \quad , \quad I'_{q,l} \equiv \sum_{m=m_l}^{G_l} \frac{T_{v,m}}{T_{v,NI}}\, I_{q,m}$$

We formulate a matrix problem here by grouping indices:

$$\bar{V}_{k,l} = \sum_{(p,q)=(-K,-L)}^{(K,L)} C_{(p,q)}\, I'_{(k,l),(p,q)}$$

where

$$I'_{(k,l),(p,q)} \equiv I'_{p,k}\, I'_{q,l}$$

Solving this linear system for the $C_{(p,q)}$ vector gives us $\bar{B}(x,y)$. Note that a suitable index contraction scheme is:

$$(k,l) = (k-1)\, K + l$$
$$(p,q) = (p-1)\, P + q \ .$$

CHAPTER 5

APPLICATION OF THE MATRIX ALGORITHM

In this chapter, we apply the matrix algorithm to several one-dimensional test cases. Development of a suitable Fortran source code for the implementation of the two-dimensional algorithm has been in progress, but as yet has not been completely debugged. An advantage to the presentation of some one-dimensional test cases is that the results may be graphically displayed without excessive computer time necessary to generate a sufficient density of points for plotting, as would be required for a decent plot of a 2-D test case. Additionally, numerical evaluation of the convolution integrals needed to study truncation effects can be performed faster and to higher accuracy for one-dimensional examples than for two-dimensional cases. After presenting the test cases, the limitations of the algorithm will be pointed-out, and we conclude with a brief discussion of a possible direct application to averaging along curvilinear tracks in the u-v plane.

5.1 Application to Test Cases

The Fortran source code for the implementation of the 1-D matrix algorithm is presented as Program B of the Appendix. Evaluation of $\tilde{B}(x)$ and $\hat{B}_\delta(x)$ was performed in a manner similar to that used for the 2-D model study (see Program A of the Appendix). The only significant difference was that the numerical integration required

to compute $\tilde{B}(x)$ used the average value of the two integrand values at each end of an integration mesh interval times the interval's length instead of the integrand's value at the interval's midpoint times the interval. Since the 1-D program to determine $\tilde{B}(x)$ and $\hat{B}_{\delta}(x)$ is considerably simpler than, but analogous to the 2-D case, the 1-D program is not included in the Appendix.

Four simple brightness functions were used as test functions, and each was studied for two averaging schemes applied to their respective visibility functions. The averaging schemes, designated A and B, were as follows:

Averaging Scheme A

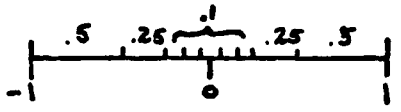

Averaging Scheme B

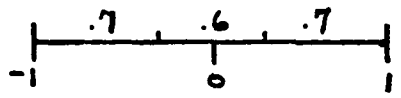

Table 5.1 presents the parameters of interest for thetest functions. Averaging scheme A uses intervals which are all smaller than the Nyquist interval for test functions 2 and 4. Utilization of the matrix algorithm is intended primarily for cases where the effects of averaging are significant, i.e., where the averaging intervals are larger than the Nyquist interval; averaging scheme B uses intervals which are larger than the Nyquist interval for all of the 4 test functions.

Figures 5.1 through 5.8 provide comparative illustrations

TABLE 5.1 1-D Source Characteristics

Case	Brightness Function	$B(\lvert x\rvert \gtrsim X_c) \lesssim .001$	T_{NI}	Peak Location	Visibility Function	Truncation Limits	Averaging Scheme -- Estimate for L_x Used in Matrix Calculation
1	$B(x)=.5[\delta(x+.5)+\delta(x-.5)]$	N/A	N/A	$x=\pm.5$	$V(u)=\cos \pi u$	$\lvert u\rvert=1$	A - 1.25 B - 1.
2	$B(x)=\begin{cases}1-\lvert x\rvert, & \lvert x\rvert\leq 1\\ 0 & \lvert x\rvert>1\end{cases}$	$x_c=1.$	.5	x=0	$V(u)=\text{sinc}^2 u$	$\lvert u\rvert=1$	A - 1.25 B - 1.
3	$B(x)=\text{sinc}^2 x$	$x_c=10.5$	.0476	x=0 and where $x=\frac{\text{TAN}\pi X}{\pi}$	$V(u)=\begin{cases}1-\lvert u\rvert, & \lvert u\rvert\leq 1\\ 0 & \lvert u\rvert>1\end{cases}$	$\lvert u\rvert=1$	A - 1.25 B - 1.
4	$B(x)=\sqrt{\pi}e^{-\pi^2 x^2}$	$x_c=.87$	.575	x=0	$V(u)=e^{-u^2}$	$\lvert u\rvert=1$	A - 1.25 B - 1.

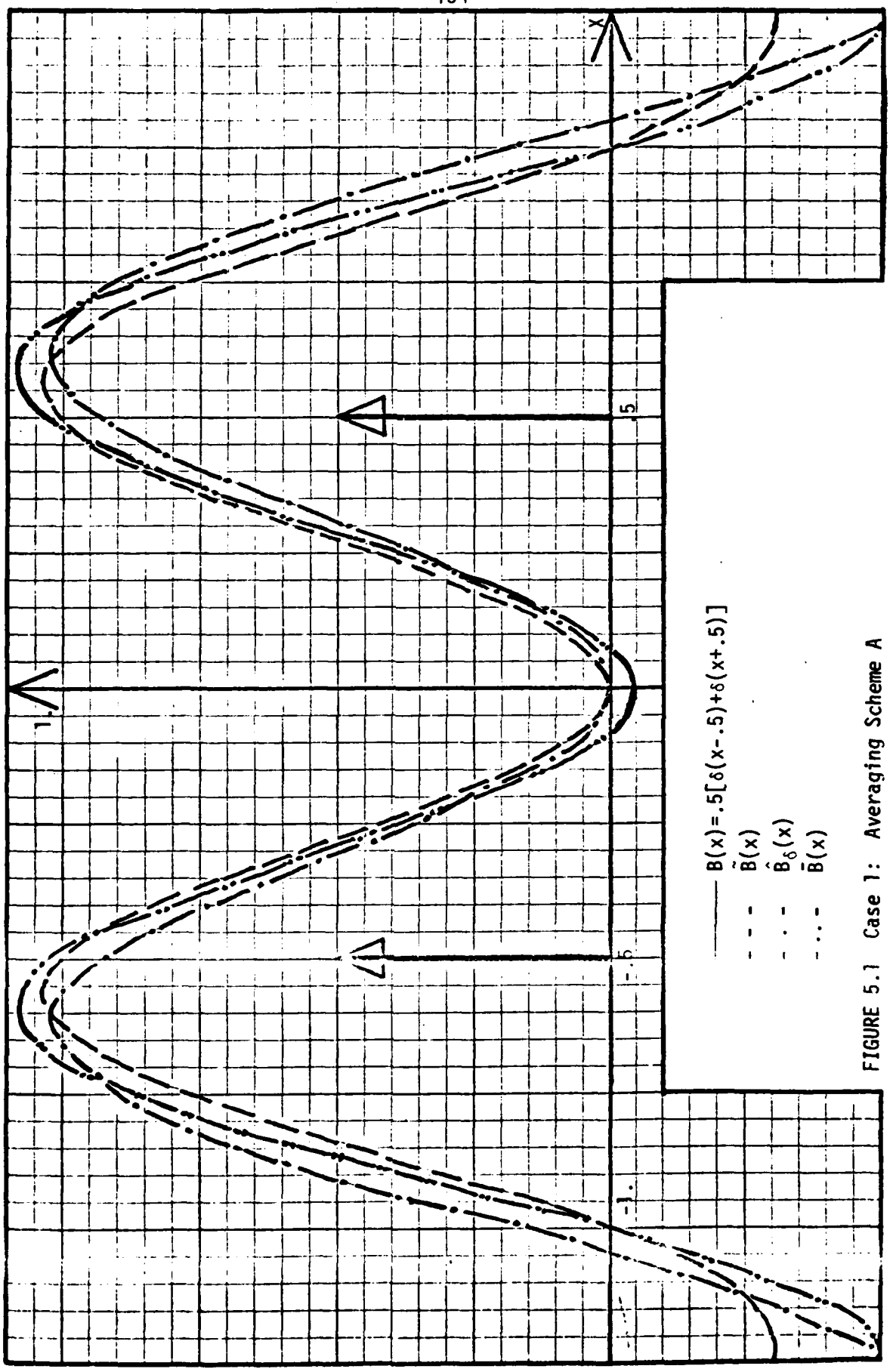

FIGURE 5.1 Case 1: Averaging Scheme A

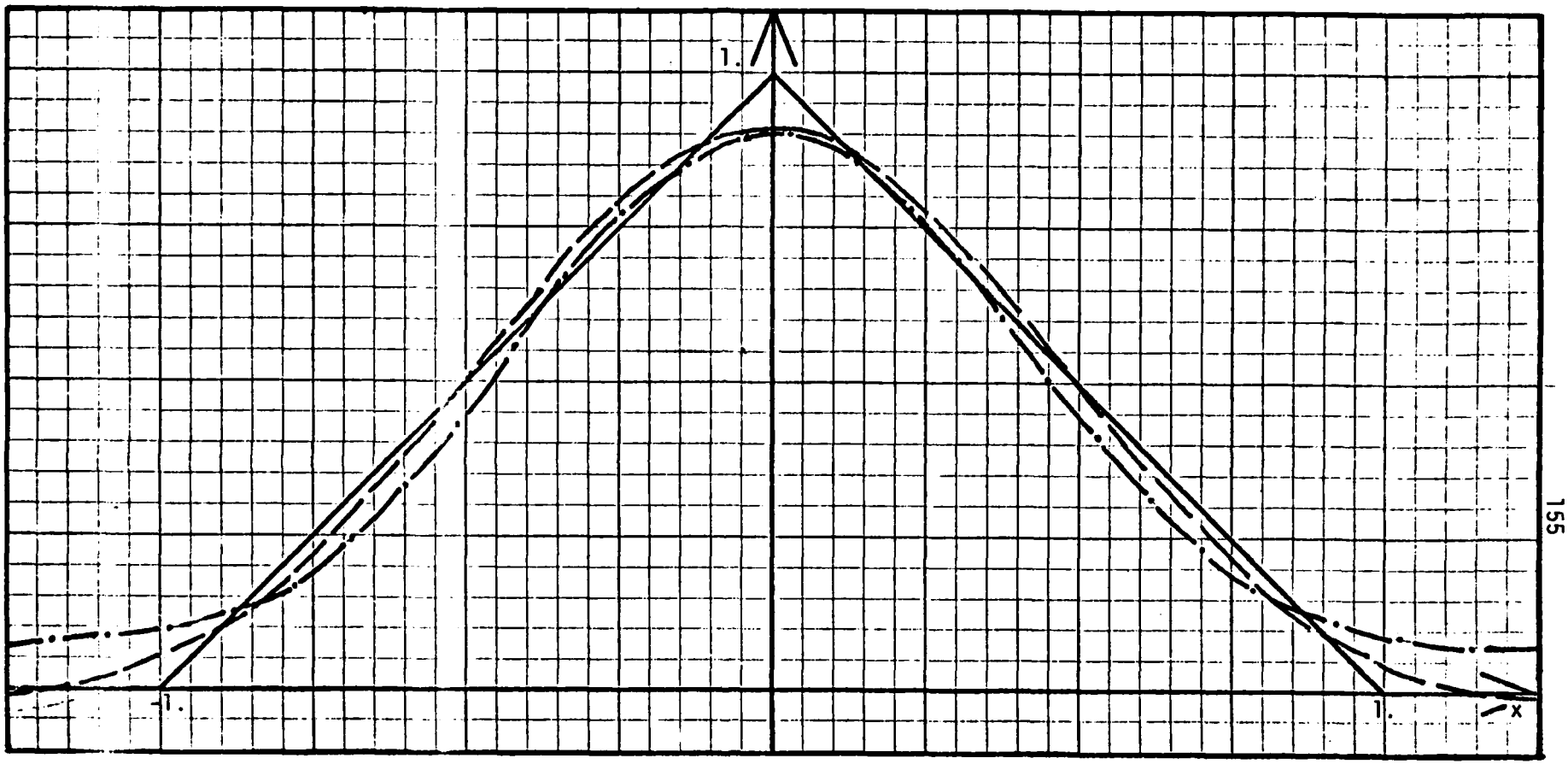

_____ $B(x) = 1-|x|, |x| \leq 1$

- - - $\tilde{B}(x)$: $\bar{B}(x)$ is coincident with $\tilde{B}(x)$

- . - $\hat{B}_{\delta}(x)$

FIGURE 5.2 Case 2: Averaging Scheme A

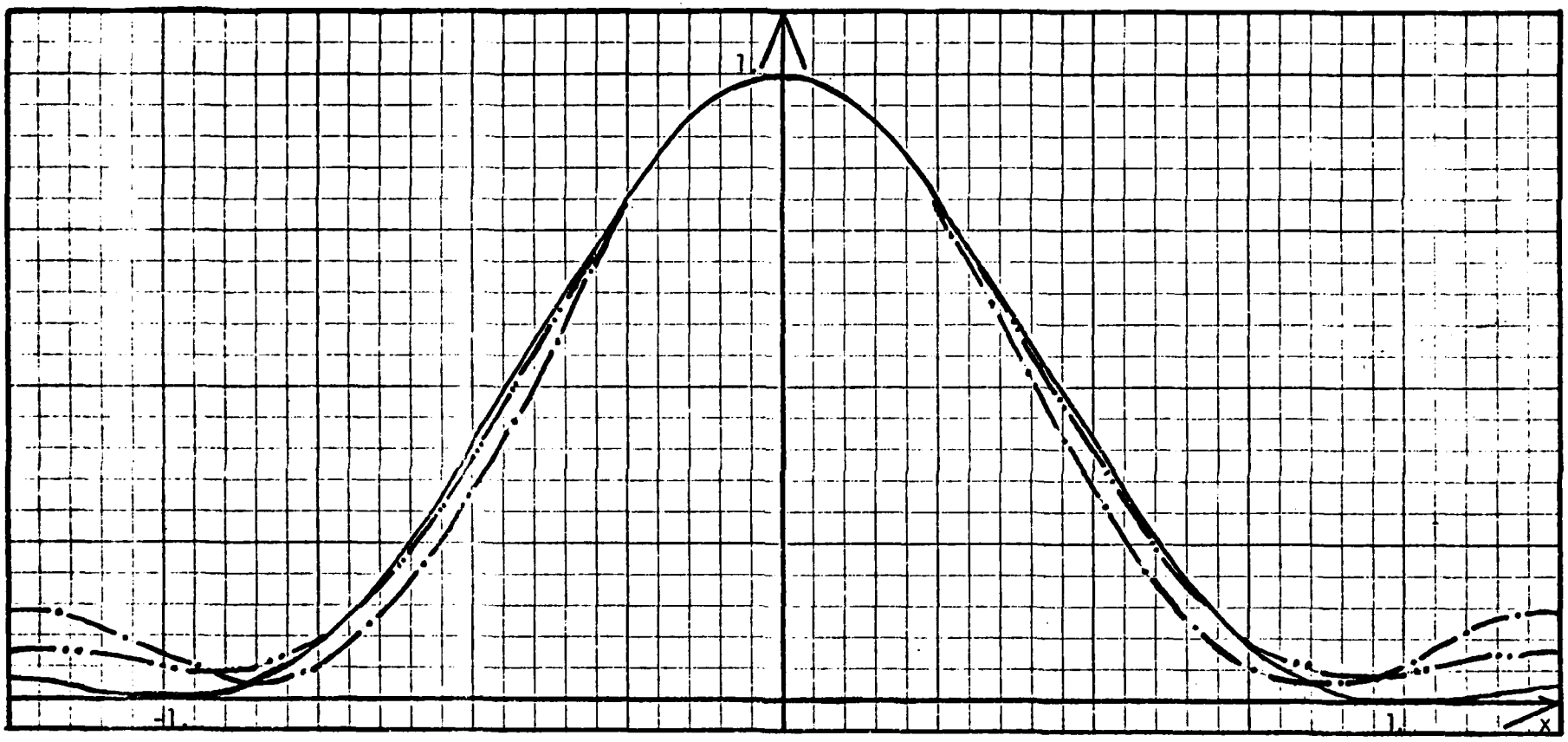

_____ $B(x) = \text{sinc}^2 x$: $\tilde{B}(x)$ is coincident with $B(x)$ since $V(\omega)$ is not truncated

- · - $\hat{B}_\delta(x)$
- ·· - $\bar{B}(x)$

} Coincident with $B(x)$ for $|x| < .25$

FIGURE 5.3 Case 3: Averaging Scheme A

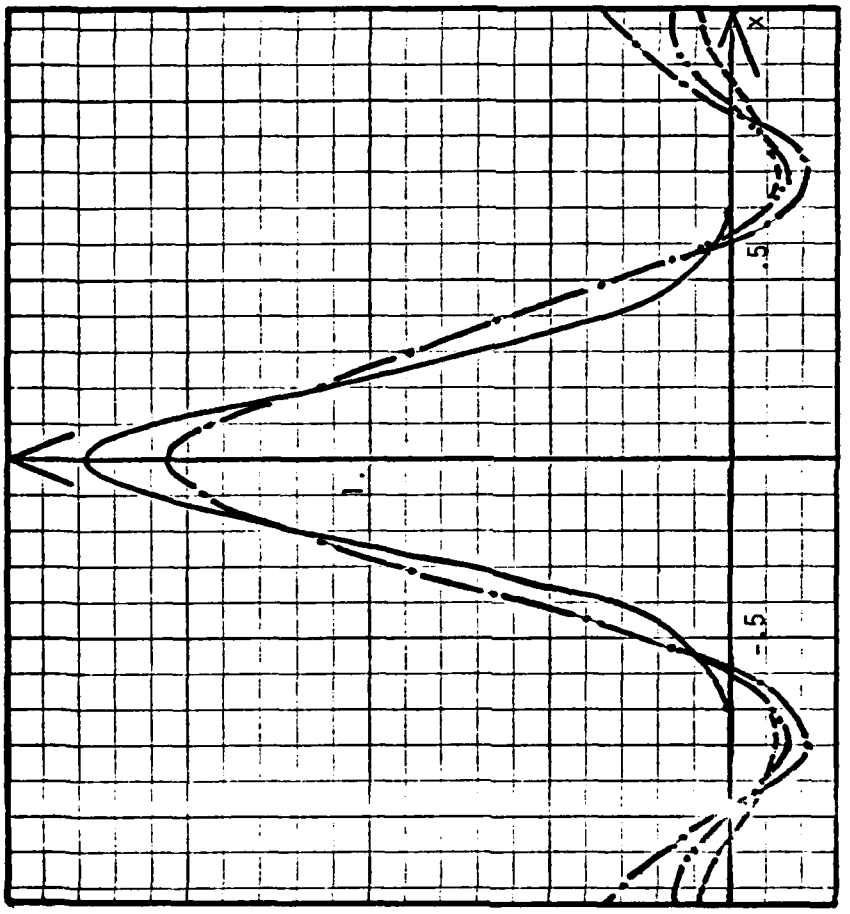

FIGURE 5.4 Case 4: Averaging Scheme A

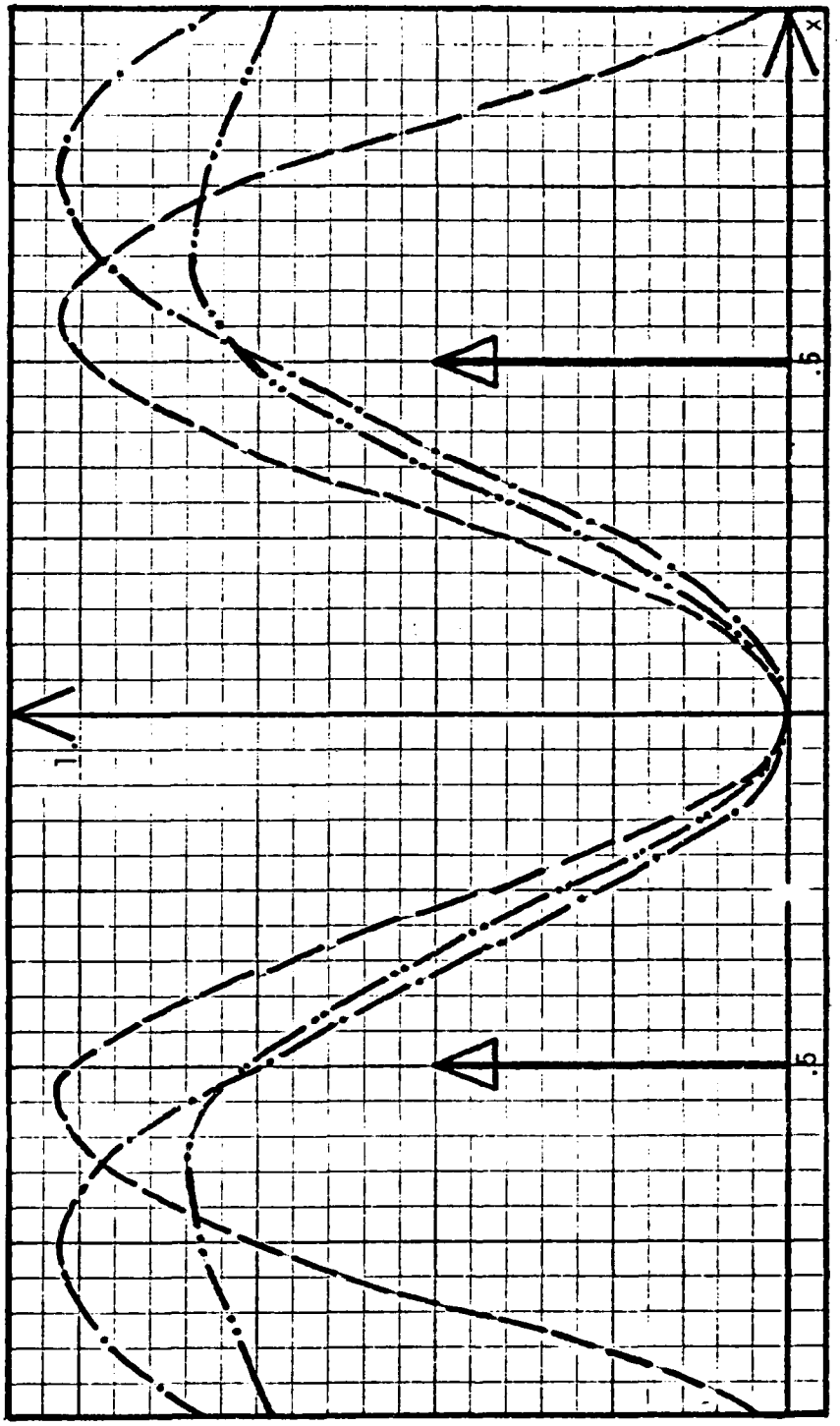

——— $B(x) = .5[\delta(x+.5) + \delta(x+.5)]$

- - - $\tilde{B}(x)$

- . - $\hat{B}_\delta(x)$

-.-.- $\bar{B}(x)$

FIGURE 5.5 Case 1: Averaging Scheme B

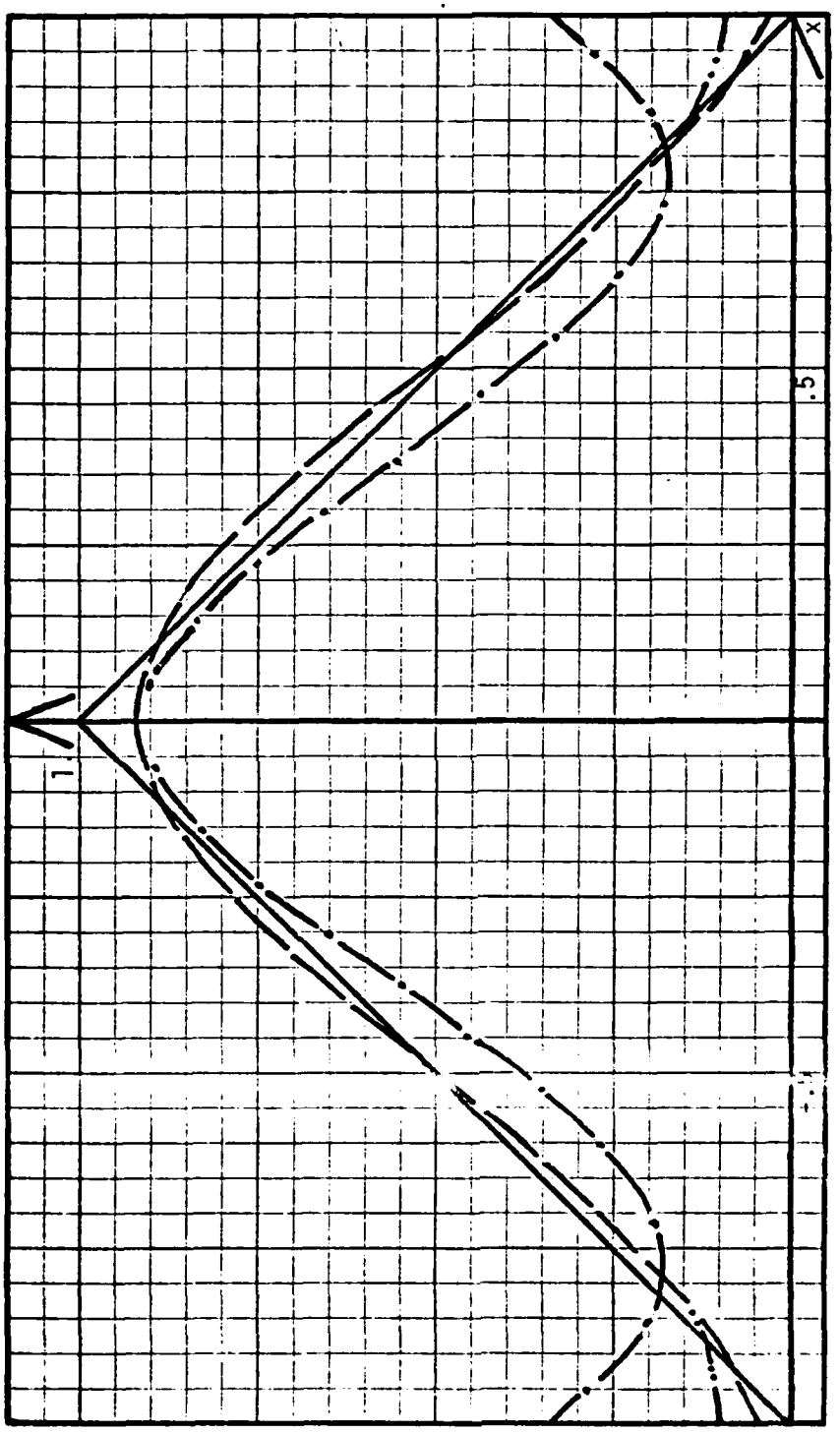

—— $B(x) = 1-|x|, \quad |x| \leq 1$

- - - $\tilde{B}(x)$

- . - $\hat{B}_{\delta}(x)$

- . . - $B(x)$: Coincides with $\tilde{B}(x)$ for $|x| < .8$

FIGURE 5.6 Case 2: Averaging Scheme B

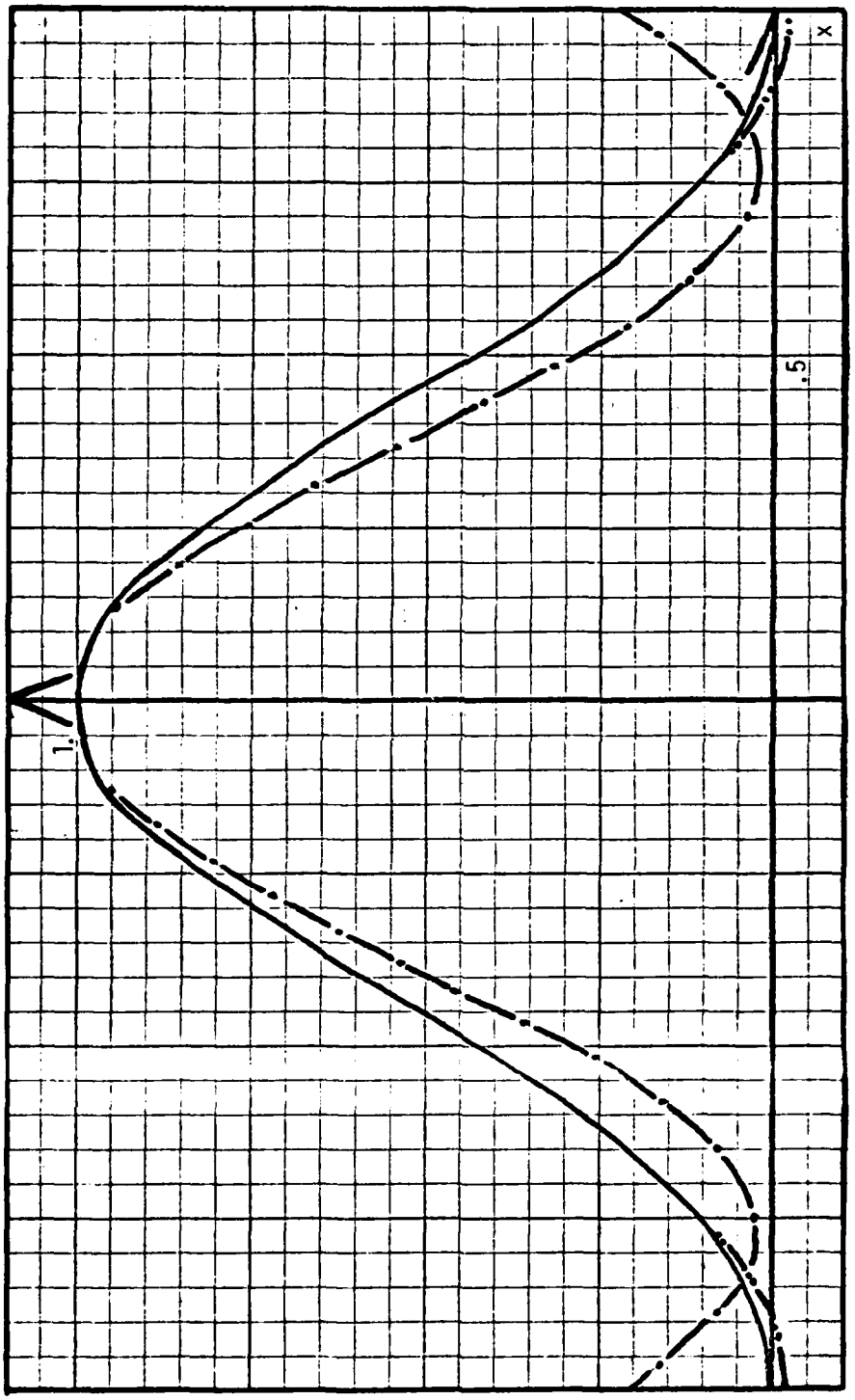

—— $B(x) = \text{sinc}^2 x$: $\tilde{B}(x)$ coincidnet with B(x) since V(u) is not truncated

- - - $\hat{B}_\delta(x)$

- ·- · $\bar{B}(x)$: Coincident with B(x) for $|x|<.8$

FIGURE 5.7 Case 3: Averaging Scheme B

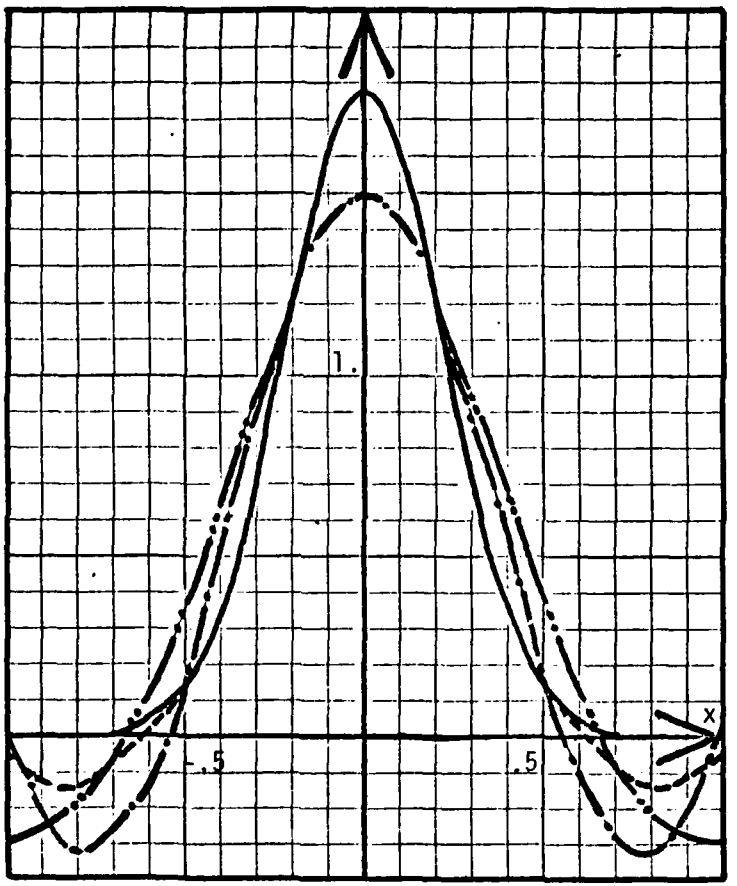

——— $B(x) = \sqrt{\pi}\, e^{-\pi 2x^2}$

- - - $\tilde{B}(x)$: Coincident with B (x) for $x \lesssim .5$

- . - $\hat{B}_\delta(x)$

- . . - $\bar{B}(x)$

FIGURE 5.8 Case 4: Averaging Scheme B

of $B(x)$, $\tilde{B}(x)$, $\bar{B}(x)$ and $\hat{B}_\delta(x)$ for the eight test cases which were examined. Results are illustrated only within the bounds of the estimated source extent L_x which was assumed for each model source in order to apply the matrix algorithm.

5.2 Observations and Discussion

For averaging scheme A, it is clearly seen from the figures that $\bar{B}(x)$ surpasses $\hat{B}_\delta(x)$ in estimating the true brightness fuction $B(x)$. For the case of two point sources, we also see that the peaks in $\bar{B}(x)$ are closer to the true point source locations in $B(x)$ than are the corresponding peaks in $\hat{B}_\delta(x)$; thus it appears that $\bar{B}(x)$ givesa smaller peak shift than does $\hat{B}_\delta(x)$. We should note that the matrix algorithm does not yield a non-negative estimate for $B(x)$.

The estimated source extent L_x was chosen as 1.25 for all four cases using averaging scheme A. This then sets the Nyquist interval $T_{NI}=.4$, and a domain extension was not required to apply the matrix algorithm since five Nyquist intervals with an epoch of averaging at the origin fit inside the [illegible] limits. Note that the chosen estimate for L_x is not the true source extent (or even an effective source extent based on our previously specified criterion) and it therefore appears that the matrix algorithm is not very sensitive to the source extent estimation, provided that domain extension is not required.

An estimated source extent of 1. was chosen for use with averaging scheme B. This value for L_x set the Nyquist interval at .5, and a domain extension at .25 was then required at both truncation limits in order to have the epoch of averaging at the origin. For these four cases, the choice as to whether $\hat{B}_\delta(x)$ or $\bar{B}(x)$ gives the better estimate for B(x) is not as clear as the previous four cases. Averaging scheme B used averaging intervals which were larger than the effective Nyquist interval for all four test functions. The peak shift in $\hat{B}_\delta(x)$ for the case of the two point sources is quite severe, and $\bar{B}(x)$ yielded a smaller peak shift than $\hat{B}_\delta(x)$. However, $\bar{B}(x)$ has flattened-out in comparison to $\hat{B}_\delta(x)$ and in this way $\bar{B}(x)$ is less representative of the true source than is $\hat{B}_\delta(x)$. Thus, we have a trade-off in this case, with $\bar{B}(x)$ providing a better estimate to the locations of the point sources but with $\hat{B}_\delta(x)$ providing a better resemblance to the symmetric nature of the true point sources. The most probable cause of the flattening in $\bar{B}(x)$ is the fairly severe domain extension and the assignment of a zero value for the average visibility in the domain extension region, since the required extension here was 25% of the estimated source extent.

For the test function $B(x)=1-|x|$ and $B(x)=\text{sinc}^2 x$, the matrix algorithm clearly gave a better estimate for the true brightness function than did $\hat{B}_\delta(x)$. For these two test functions, the corresponding visibility functions have small or zero values in the domain extension regions, and the assignment of a zero value for the

averages visibility in the domain extension regions was therefore not a bad assumption. Note also the severe effect of aliasing in $\hat{B}_\delta(x)$ in Figures 5.6 and 5.7. $\bar{B}(x)$ does not show this severe aliasing effect.

For the Gaussian test function, we see that $\bar{B}(x)$ is clearly worse in estimating $B(x)$ than is $\hat{B}_\delta(x)$. $\bar{B}(x)$ has broadened-out in comparison to $\hat{B}_\delta(x)$. Again, the likely cause for the poor estimate given by $\bar{B}(x)$ is the fact that the visibility function has non-negligible values in the domain extension regions, and the assignment of zero average visibility in the domain extension regions is therefore a bad assumption for this case.

From the rather limited survey of test functions which has thus far been conducted, we can make the following tentative conclusions, which require further analysis to fully justify them. First, it appears that the matrix algorithm reduces the size of the peak shift interval, and therefore $\bar{B}(x)$ provides a better estimate for the locations of the peaks in the true brightness function than does $\hat{B}_\delta(x)$. The matrix algorithm does not appear to be very sensitive to the estimation of L_x if such an estimate does not require a domain extension. However, the matrix algorithm does appear to be sensitive to estimates for L_x which require domain extension if the visibility function has non-negligible values in the extension regions and a zero value for the average visibility is assigned in the extension regions. A possible remedy for this

problem might be to assign a value for the average visibility in the extension region based on a Gaussian taper rather than the arbitrary assignment of a zero value. Finally, we have seen that the matrix algorithm does not always provide a non-negative estimate for the value of the brightness function, and therefore $\bar{B}(x)$ as well as $\hat{B}_\delta(x)$ sometimes fail to yield physically meaningful (i.e., non-negative) values for the brightness of a real source.

5.3 Limitation of the Matrix Algorithm

In this section, we will discuss problems with and possible limitations of the matrix algorithm.

From the test functions which were examined, it can be seen that reasonable estimates for L_x appear to be sufficient for the calculation of the matrix elements. The estimate for L_x determines the effective Nyquist interval and thereby also determines the amount of domain extension required to reformulate the data into Nyquist intervals with an epoch of averaging at the origin. The present algorithm was designed specifically for an averaging epoch at the origin; for the case where two averaging intervals meet at the origin, singularities were found to occur and the algorithm breaks down. Furthermore, as indicated by Figure 5.8, the domain extension may be sufficiently radical so as to cause the matrix algorithm to yield a poorer estimate for B(x) than does the standard Fourier inversion method. Using an average value based on a Gaussian

taper in the domain extension regions may be of some benefit here, and in any extent should give a better estimate for B(x) than does the arbitrary assignment of a zero average value in the domain extension regions, which was the technique used in the present study.

Another problem concerns the use of the matrix algorithm for cases where the number of Nyquist intervals in the reformulated problem exceeds about seven intervals. It was found that, in such cases, some of the matrix elements become very large and the order of magnitude differences between some elements was as high as 10^7. For cases where the matrix elements have such a wide range of values, the matrix inversion process often breaks down (at least for the two different inversion methods which were tried in this study). Additionally, accuracy problems were encountered, especially for cases where the number of Nyquist intervals exceeded about seven intervals. Each matrix element is calculated by an iterative process, and accuracy may be lost in the calculation of individual elements as well as in the matrix inversion process. These inaccuracies generally result in poorly determined values for the Fourier series coefficients for $\bar{B}(x)$. For example, if V(u) is a real function, then we expect the Fourier series coefficients for $\bar{B}(x)$ to be real and symmetric (i.e., $C_p=C_{-p}$); however, the symmetry between corresponding coefficients is often lost due to the accuracy problems, and $\bar{B}(x)$ undesirably becomes a complex function. Modifying the Fortran program to operate in double-precision and perhaps using

better matrix inversion techniques may help alleviate the accuracy problems.

The 2-D matrix algorithm will undoubtably be even more sensitive to accuracy problems than the 1-D case, expecially for those problems related to the matrix inversion. If there are N^2 Nyquist cells in the reformulated problem (N intervals along both the u and v axes), then the matrix which must be inverted will have N^4 elements. Accurate inversion of a large matrix then becomes a further problem to be considered.

For successful application of the matrix algorithm to "real-world" data, the above cited problems would have to be adequately alleviated. At this time it is uncertain whether or not the algorithm, in its present form, will be capable of application to a general 2-D case because of its present numerical problems. Thus, although the results illustrated in Figures 5.1 through 5.8 are encouraging, one must keep in mind that application of the algorithm to more complicated cases and to 2-D functions may become intractable. The results presented here should be taken as encouraging evidence for the feasibility of an inversion technique for an averaged visibility function which yields a better estimate to the true source brightness function than does the standard Fourier inversion method.

5.4 The Problem of Curvilinear Tracks

Direct application of the matrix algorithm to averaging along a curvilinear track may be possible. Time has not permitted a detailed analysis or model study for this technique, and we therefore confine ourselves to a brief speculative discussion (admittedly lacking details) of a possible approach to this problem. If such an algorithm could be developed, it would offer the advantage of dealing directly with the experimental data obtained along tracks in the u-v plane without the preliminary requirement of "gridding" the data into rectangular cells.

We have seen that the response of the interferometer is a sequence of average values of the visibility function along a curvilinear track in the u-v plane which is determined by the relative motion of the baseline vector with respect to the source vector. For the case of an interferometer with two elements on the earth's surface the track is elliptical, whereas for a system incorporating elements on satellites the curvilinear track is not a simple closed curve, although the "open-ended" trajectory in the u-v plane can be calculated as a function of time. For simplicity, we will consider the case of an elliptical track; the generalization to an arbitrary track replaces the elliptical curve by the appropriate relation $v=v(u)$.

Let $\mathcal{C}$ denote a curvilinear track in the u-v plane, which for simplicity we choose to be an ellipse:

$$\mathcal{C} \longrightarrow \frac{u^2}{a^2} + \frac{v^2}{b^2} = 1$$

The differential line element for this track is

$$ds = du\sqrt{\frac{a^2 + u^2(b^2-a^2)}{a^2-u^2}}$$

and the arclength s_j over the j^{th} averaging segment is

$$s_j = \int_{\mathcal{C}_j} ds = \int_{u_j}^{u_j+\Delta u_j} du\sqrt{\frac{a^2 + u^2(b^2-a^2)}{a^2-u^2}}.$$

Denote the average value of V(u,v) along the j^{th} averaging segment $\mathcal{C}_j$ by $[\bar{V}]_{s_j}$, so that

$$[\bar{V}]_{s_j} = \frac{1}{s_j}\int_{\mathcal{C}_j} ds\, V(u,v) = \frac{1}{s_j}\int_{\mathcal{C}_j} ds\left[\int_{-L_x}^{L_x}\int_{-L_y}^{L_y} dx\,dy\; e^{i2\pi(ux+vy)} B(x,y)\right]$$

where we have assumed a region-limited brightness function and replaced V(u,v) by the Fourier transform of its conjugate function. As above, we assume that B(x,y) has an exact Fourier expansion given by

$$B(x,y) = \sum_{p=-\infty}^{\infty}\sum_{q=-\infty}^{\infty} C_{p,q}\, e^{-i2\pi\left(\frac{px}{2L_x} + \frac{qy}{2L_y}\right)}$$

and that an approximation to B(x,y) is given by

$$\bar{B}(x,y) = \sum_{p=-P}^{P}\sum_{q=-Q}^{Q} C_{p,q}\, e^{-i2\pi\left(\frac{px}{2L_x} + \frac{qy}{2L_y}\right)} \approx B(x,y).$$

Substituting $\bar{B}(x,y)$ for $B(x,y)$ in the expression for $[\bar{V}]_{S_j}$ gives

$$[\bar{V}]_{S_j} = \frac{1}{S_j} \sum_{p=-P}^{P} \sum_{q=-Q}^{Q} C_{p,q} \int_{\mathcal{C}_j} ds \left[\int_{-L_x}^{L_x} dx\, e^{-i2\pi x\left(\frac{p}{2L_x} - u\right)} \right] \cdot \left[\int_{-L_y}^{L_y} dy\, e^{-i2\pi y\left(\frac{q}{2L_y} - v\right)} \right]$$

$$= \frac{1}{S_j} \sum_{p=-P}^{P} \sum_{q=-Q}^{Q} C_{p,q} \int_{\mathcal{C}_j} ds\, \frac{\sin 2\pi L_x\left(\frac{p}{2L_x} - u\right)}{\pi\left(\frac{p}{2L_x} - u\right)} \, \frac{\sin 2\pi L_y\left(\frac{q}{2L_y} - v\right)}{\pi\left(\frac{q}{2L_y} - v\right)} .$$

The line integral can be performed by expressing v in terms of u along the arc $\mathcal{C}_j$ and expressing ds in terms of du; we get

$$[\bar{V}]_{S_j} = \frac{1}{S_j} \sum_{p=-P}^{P} \sum_{q=-Q}^{Q} C_{p,q} \int_{u_j}^{u_j + \Delta u_j} du \sqrt{\frac{a^2 + u^2(b^2 - a^2)}{a^2 - u^2}} \cdot \frac{\sin 2\pi L_x\left(\frac{p}{2L_x} - u\right)}{\pi\left(\frac{p}{2L_x} - u\right)} \, \frac{\sin 2\pi L_y\left(\frac{q}{2L_y} - v(u)\right)}{\pi\left(\frac{q}{2L_y} - v(u)\right)} .$$

Contracting the indices p,q to a single index [(p,q)=(p-1)P+q] then let us formulate a matrix equation:

$$\begin{pmatrix} [\bar{V}]_{S_1} \\ \vdots \\ [\bar{V}]_{S_j} \\ \vdots \end{pmatrix} = \begin{pmatrix} I_{j,(p,q)} \end{pmatrix} \begin{pmatrix} C_1 \\ \vdots \\ C_{(p,q)} \\ \vdots \end{pmatrix}$$

where the matrix elements are given by

$$I_{j,(p,q)} = \frac{\int_{u_j}^{u_j + \Delta u_j} du \sqrt{\frac{a^2 + u^2(b^2 - a^2)}{a^2 - u^2}} \, \frac{\sin 2\pi L_x\left[\frac{p}{2L_x} - u\right]}{\pi\left[\frac{p}{2L_x} - u\right]} \, \frac{\sin 2\pi L_y\left[\frac{q}{2L_y} - \frac{b}{a}\sqrt{a^2 - u^2}\right]}{\pi\left[\frac{q}{2L_y} - \frac{b}{a}\sqrt{a^2 - u^2}\right]}}{\int_{u_j}^{u_j + \Delta u_j} du \sqrt{\frac{a^2 + u^2(b^2 - a^2)}{a^2 - u^2}}}$$

The integrals may be performed numerically. As discussed in the previous cases, we assume that a-priori estimates for L_x and L_y are available, and that an iterative refinement of the source extent may be possible if such a scheme converges.

A few comments are in order. We have attempted to outline a one-dimensional treatment for a 2-D Fourier transform because actual data is available along 1-D curvilinear tracks. The variable u was chosen arbitrarily here as the 1-D independent variable; actually, the variable chosen to be independent should probably have the smaller of the two Nyquist interval lengths (i.e., choose u if $T_{u,NI} < T_{v,NI}$). It will probably be necessary to reformulate the problem in some way as discussed above for the 1-D and 2-D cases with rectilinear averaging. Since only one variable is left independent, it may be necessary to use T_{NI} (the smaller of the two Nyquist interval lengths) instead of $\frac{1}{2L_x}$ and $\frac{1}{2L_y}$ in the expression for $\bar{B}(x,y)$, i.e.

$$\bar{B}(x,y) = \sum_{p=-P}^{P} \sum_{q=-Q}^{Q} C_{p,q}\, e^{-i2\pi T_{NI}(px+qy)}$$

Since the smaller of the two Nyquist intervals is used, aliasing effects should not occur along the x or y direction. The averaging scheme could then be reformulated in terms of the smaller Nyquist interval.

To check the feasibility and develop the details of a curvilinear track approach will require considerable further analysis and model studies.

CHAPTER 6

SUMMARY AND CONCLUSIONS

We have reviewed the origins of the basic Fourier transform relation between the brightness distribution function and the visibility functions. For VLBI systems in which some or all of the array elements are located on satellites, the interferometric response is a set of average values of the visibility function obtained along a curvilinear trajectory in the u-v plane. For a pair of interferometer elements on the earth, the trajectory through the u-v plane is elliptical; however, if one or both elements of the pair are on satellites, the trajectory is in general an open-ended curve. An advantage to the use of elements on satellites is that the curvilinear track in the u-v plane does not close back upon itself after completion of an orbit (due to the non-commensurate orbital periods for the two elements), and the track's coverage of the u-v plane therefore increases with time. In this way, observational data may be obtained over a large portion of the u-v plane inside the truncation limits, which are determined by the maximum baseline projection normal to the direction to the source.

Using interferometer elements on satellites provides the opportunity for longer baselines and hence higher resolution of source structure than is possible with elements on the earth. However, due to a number of factors which we have discussed, averaging of the visibility function along the track in the u-v plane becomes

a significant problem for systems which incorporate elements on satellites, and the brightness function which is derived from the observational data may be seriously distorted due to the influence of averaging effects.

The major goal of this thesis has been to elucidate and understand the effects on the brightness function due to truncating and averaging the visibility function. We first gained a qualitative appreciation for the nature of these effects by studying a model case. We then quantitatively analyzed these effects. Periodicity considerations were discussed, and we concluded that aliasing effect should not be severe unless the data are gridded onto a lattice with constant (or nearly constant) cell sizes which were larger than the Nyquist cell size. We then investigated the separate effects of averaging and truncation, as well as their combined effect.

The effect of symmetrically truncating the visibility function is to smooth the brightness function and to introduce "ringing", and this effect is concisely expressed by the convolution of the true brightness function with sinc factors whose widths are determined by the truncation limits. The effect of averaging the visibility function with constant averaging intervals was concisely expressed by multiplying the true brightness function by a sinc factor whose width is determined by the size of the averaging intervals, and periodically extending this function with a period

given by the inverse of the averaging interval size. Averaging and truncating the visibility function produces a brightness function which bears a combination of the individual influences cited above. We then examined these results to check for consistency in limiting cases, and also for the case of a linear visibility function for which averaging and sampling became identical.

It was found that averaging and truncating the visibility function produced shifts in the location of peaks in the brightness distribution function. This effect was analyzed and we produced a result capable of predicting the peak shift to first order. This result can be applied to actual experimental data; however, future work in this regard should consider expansions to higher order in peak shift and then use the computer to solve the resulting polynomial for the peak shift.

Since the basic theory of truncation and averaging effects was developed in one-dimension for fixed averaging interval size, we then generalized our results to include irregular averaging interval sizes, and we generalized to two-dimensions.

The ancillary goal of this thesis was to try to apply our knowledge and understanding of truncation and averaging effects to develop an algorithm which, by accounting for the effects of truncation and averaging, might possibly produce a better estimate for the true source brightness function than does the standard Fourier inversion method. We developed an algorithm in 1-D, and

subsequently generalized it to 2-D. We have called this method the matrix-algorithm because our particular application of the theorem relating an average value of the visibility function to the brightness function resulted in a matrix equation which, when solved, yielded a set of Fourier series coefficients for a function which approximated the true brightness function. The matrix algorithm was applied to a few test cases, and the results were compared with those of the standard Fourier inversion method. Unfortunately, the matrix algorithm did not produce the best estimate for the true brightness function on a consistent basis. It appeared that the domain extension, which is sometimes necessary in order to be able to use the matrix algorithm, was the cause of the poor results obtained in some cases. In those cases, the visibility function had non-negligible values in the domain extension region, and our crude assumption which assigned a zero value for the average visibility in the extension region apparently led to the poor estimate for the brightness function. Future investigations should try alternative techniques for assigning a value in the extension region; for example, a value based on a Gaussian taper may be useful.

The matrix algorithm was found to have some numerical difficulties when attempting to apply it to cases where the number of Nyquist intervals in the reformulated problem exceeded about seven intervals. A refined computer program may correct this difficiency, but if it cannot be corrected then the matrix algorithm will

not be feasible for "real-world" applications, and another approach should be considered.

The possibility of applying the matrix algorithm directly to averaging along a curvilinear track was briefly considered. A basic approach was sketched-out, but a definitive statement as to the feasibility and details of such a technique will require considerably more study than has been possible here. If such a technique could be developed, based either on the matrix algorithm or some other algorithm which accounts for truncation and averaging effects, it may possibly provide a much better estimate for the brightness function than does the method of gridding the data and applying the standard Fourier inversion method.

APPENDIX A

SYMBOL GLOSSARY

The following alphabetized list provides a summary of the major symbols used throughout this thesis. Symbols which are introduced in the text and used only for a short topic are not included here.

$\vec{b}$	Baseline vector for a two-element interferometer.
$B(x,y)$	Source brightness function.
$\tilde{B}(x.y)$	Brightness function which is the Fourier transform of a truncated visibility function.
$\hat{B}_{\delta}(x,y)$	Brightness function which is the standard Fourier transform of a truncated and averaged visibility function.
$\bar{B}(x,y)$	Brightness function obtained by matrix algorithn from truncated and averaged visibility function.
b_u, b_v	Extent of the visibility function inside the truncation limits in the u and v directions, respectiveîy.
c_u, c_v	Midpoint coordinates for the non-truncated portion of the visibility function.
$\delta(x,y)$	Two dimensional Dirac delta function, $(x,y) = (x)\ (y)$.
Δ_x, Δ_y	Peak shift values along the x and y directions, respectively; i.e., Δ_x indicates the distance along the x axis from a peak in the true source brightness function $B(x,y)$ at x_0 to the corresponding peak in $B(x,y)$ at $(x_0+\Delta_x)$.
$\mathcal{F}$	Fourier transform operator.
$\mathcal{F}^{-1}$	Inverse Fourier transform operator
$I_{p,n}$	Matrix used in the matrix algorithm whose elements are definite integrals over the source region.
i	$\sqrt{-1}$.
i, as subscript:	Imaginary part.

L_x, L_y	Distance from the origin along the x and y axes, respectively, to the region boundary of a region-limited brightness function. If B(x,y) is not truly a region-limited function, then an effective region boundary may be defined; here, we use the criterion that $B(x,y) \leq .001$ for all x,y outside the effective region boundary.
NI, as subscript:	Nyquist interval, i.e., $T_{u,NI}$ means that the averaging interval along the u axis is equal to the Nyquist interval.
r, as subscript:	Real part.
$\hat{s}_o$	Unit vector in direction of a point source or approximately in the direction of the centoid of an extended source.
$\hat{s}$	Unit vector in the direction in which the interferometer is pointed.
sinc x	$\text{sinc } x = \frac{\sin \pi x}{\pi x}$, after Bracewell (1978).
t_o	Integration time period.
$T_{u,n}, T_{v,m}$; $T_u, T_v; T$	Averaging interval size; subscripts u and v designate respective axis along which interval lies; subscripts n and m index a particular interval along the respective axis; no n or m index indicates that the averaging intervals all have the same length along the relevant axis; no subscripts at all indicates constant averaging interval for one dimension only.
u,v	Orthogonal components of the interferometric resolution.
u_n, v_m	Midpoint coordinates for the $(n,m)^{th}$ averaging cell (or the $(n,m)^{th}$ averaging arc for an elliptical track in the u-v plane).
u_{min}, v_{min}	Lower truncation limits along u and v axes, respectively.
V(u,v)	Visibility function; exact Fourier transform of B(x,y).
$\tilde{V}(u,v)$	Truncated visibility function.
$[\bar{V}_{n,m}]$	The average value of the visibility function in the $(n,m)^{th}$ cell.

$\bar{V}_{n,m}(u,v)$	The average value of $V(u,v)$ in the $(n,m)^{th}$ cell expressed as a function of u and v by using a delta function at the cell midpoint (standard representation).
$\bar{\mathcal{V}}(u,v)$	The function which represents the truncated and averaged visibility function; Fourier transform of $B_\delta(x,y)$; $\bar{\mathcal{V}}(u,v) \equiv \sum_{n,m} \bar{V}_{n,m}(u,v)$.
w	Width parameter for the model source.
x,y	Angular position coordinates for a celestial object; viewed as rectangular coordinate system on the plane of the sky; angular-rectangular conversion possible if distance to source is known.
x_o, y_o	Position coordinates for a peak in B(x,y).
*	Convolution product, if used as a superscript, denotes complex conjugation.
$\supset$	Indicates a Fourier transform pair: $V(u) \supset B(x)$.
III	Sampling function: $III(\frac{u}{T}) \equiv T \sum_{n=-\infty}^{\infty} \delta(u-nT)$, after Bracewell (1978).
$\Pi(u,v)$	2-D Box function, $\pi(u,v) \equiv \pi(u)\ \pi(v)$, where $\pi(u) \equiv \begin{cases} 1 & \lvert u\rvert < \frac{1}{2} \\ \frac{1}{2} & \lvert u\rvert = \frac{1}{2} \\ 0 & \lvert u\rvert > \frac{1}{2} \end{cases}$, after Bracewell, (1978).

APPENDIX B

Program A

```
      COMMON VREAVG(25,25),VIMAVG(25,25),TTUU(25),TTVV(25),UUN(25),
     & VVN(25),NUMAX,NVMAX
      DIMENSION XX(3),S(2),W(3)
      DIMENSION XUMIN(10),XUMAX(10),XVMIN(10),XVMAX(10)
      DIMENSION IMAX(10),TU(10,10),TV(10,10),NU(10,10),NV(10,10)
      DIMENSION IU(10),IV(10)
      DIMENSION BB(25,25)
      DIMENSION BTWID(41,41)
      VREAL(U,V)=(2./AAAA)*(COS(2.*PI*U))*(EXP(((-1.)*PI/AAAA)*
     & ((U**2)+(V**2))))
      VIMAG(U,V)=0*U*V
      B(X,Y)=EXP((-1.)*PI*AAAA*(((X-1.)**2)+(Y**2)))+
     & EXP((-1.)*PI*AAAA*(((X+1.)**2)+(Y**2)))
      AAAA=10.
      XL=4.
      YL=4.
      PI=3.1416
      K=
C
C
C
C TRUNCATION EFFECTS ONLY
      READ 2000,UMIN,UMAX,VMIN,VMAX
2000  FORMAT(4(E16.8))
      PRINT 2001,UMIN,UMAX,VMIN,VMAX
2001  FORMAT(6H UMIN=,E16.8,5X,5HUMAX=,E16.8,5X,5HVMIN=,E16.8,5X,
     & 5HVMAX=,E16.8)
C
C
      D=.1
      DEL=D**2
      NNN=(10./D)+.1
      PRINT 2002,NNN
2002  FORMAT(5H NNN=,I4,/////)
      PRINT 2003
2003  FORMAT(3X,2HX,11X,1HY,10X,7HB$(X,Y))
      DU=UMAX-UMIN
      DV=VMAX-VMIN
      DO 2005 IIXX=1,11
      IX=IIXX-1
      X=IX/4.
      DO 2005 IIYY=1,11
      IY=IIYY-1
      Y=IY/4.
      BTWID(IIXX,IIYY)=
      DO 2006 IXMID=1,NNN
      XMID=(-5.-(D/2.))+(IXMID*D)
      XL=X-XMID
      IF(XMID.NE.0)GO TO 2007
      XMID=.00000001
2007  SI=(SIN(PI*DU*XMID))/(PI*XMID)
      TU=(COS(PI*(UMAX+UMIN)*XMID))*SI
      YMID=(-5.-(D/2.))+(IYMID*D)
      YL=Y-YMID
      IF(YMID.NE.0)GO TO 2009
      YMID=.00000001
```

NUMERICALLY PERFORMS THE CONVOLUTION INTEGRAL FOR $B(x,y)$ [SYMMETRIC TRUNCATION ON-Y]

$XL = L_x$, $YL = L_y$

INTEGRATION MESH SIZE

```
LEVEL  21          MAIN          183   DATE = 80313          09/49/31
2009    F2=(SIN(PI*BV*YMID))/(PI*YMID)
        BTWID(IIXX,IIYY)=BTWID(IIXX,IIYY)+(DEL*F1*F2*(B(XL,YL)))
2008    CONTINUE
2006    CONTINUE
        PRINT 2010,X,Y,BTWID(IIXX,IIYY)
        WRITE(7,2010) X,Y,BTWID(IIXX,IIYY)
2010    FORMAT(1X,F7.3,4X,F7.3,1 X,E16.8)
 005    CONTINUE
2004    CONTINUE
C COMPARISON OF BTWID WITH B EXACT
        WRITE(7,9147)
 147    FORMAT(35HDCOOC ********COOOO**********COOOO)
        PRINT 128
        PRINT 128
         PRINT 128
        BTD=0
        BTSD=0
        XLINCR=.25
        YLINCR=.25
        SMAREA=(.25)**2
        DO 9711  I=1,11
        X=(I-1)*XLINCR
        DO 9711 J=1,11
        Y=(J-1)*YLINCR
        BTD=BTD+((B(X,Y)-BTWID(I,J))*SMAREA)
        BTSD=BTSD+(((B(X,Y)-BTWID(I,J))**2)*SMAREA)
        WRITE(7,9715) X,Y,BTD,BTSD
9715    FORMAT(2(F4.1),2(E16.8))
9711    CONTINUE
9710    CONTINUE
        PRINT 9815,BTD
9815    FORMAT(42H THE TOTAL DEVIATION OF BEXACT FROM BTWID=,E16.8)
        PRINT 9816,BTSD
9816    FORMAT(40H THE TOTAL SQUARED DEVIATION OF BEXAC FROM BTWID=,E16.8)
C END COMPARISON STEP
C USING ONLY 1 QUADRANT
C END TRUNCATION ONLY STUDY
        PRINT 128
        PRINT 128
        PRINT 128
        PRINT 128
        READ 100,DELTA,XMIN,YMIN,NX,NY,KMAX
 00     FORMAT(3F16.8,3I4)
        D2=DELTA**2
        READ 101,(XUMIN(I),XUMAX(I),XVMIN(I),XVMAX(I),IU(I),IV(I),
       & I=1,KMAX)
 01     FORMAT(4F16.8,2I4)
        DO 10 I=2,KMAX
        IIU=IU(ICOUNT)
        IIV=IV(ICOUNT)
        K=K+1
```

BTWID IS $\hat{B}(x,y)$

B EXACT IS $B(x,y)$

BEGINNING OF $\hat{B}_s(x,y)$ STUDY

KMAX = THE NUMBER OF INDIVIDUAL WITH SCANNING, HAS A EACH SEGMENT COMPLETE $\hat{B}_s(x,y)$ CALCULATION

```
LEVEL  21                    MAIN          184   DATE = 80313          09/40/ 1

C TV(K,J-1) IS INPUT AS HALF THE ACTUAL AVERAGING INTERVAL SIZE
C FOR THE V INTERVAL CENTERED AT V=
      READ 1 2,(TU(K,J),NU(K,J),J=1,IIU)
      READ 1 2,(TV(K,JJ),NV(K,JJ),JJ=1,IIV)
102   FORMAT(F16.8,I4)
133   CONTINUE
      PRINT 130,DELTA,NX,NY
130   FORMAT(7H DELTA=,F16.8,5X,25HX AND Y INTERVALS,.25 EA,,
     $ 3HNX=,I4,12X,3HNY=,I4)
      PRINT 131,KMAX
131   FORMAT(23H NUMBER OF DATA GROUPS=,I4)
      PRINT 128
      PRINT 128
128   FORMAT(//////////)
      DO 122 IGROUP=1,KMAX
      WRITE(7,145)
145   FORMAT(35H11111**********11111**********11111)
      IIU=IU(IGROUP)
      IIV=IV(IGROUP)
      JJ=1
      DO 701 I=1,IIU
      NSETU=NU(IGROUP,I)
      DO 701 J=1,NSETU
      TTUU(JJ)=TU(IGROUP,I)
      JJ=JJ+1
701   CONTINUE
700   CONTINUE
      NUMAX=JJ-1
      JJ=1
      DO 702 I=1,IIV
      NSETV=NV(IGROUP,I)
      DO 703 J=1,NSETV
      TTVV(JJ)=TV(IGROUP,I)
      JJ=JJ+1
703   CONTINUE
702   CONTINUE
      NVMAX=JJ-1
      PRINT 735,NUMAX,NVMAX
735   FORMAT(7H NUMAX=,I4,6H NVMAX=,I4)
      DO 107 IX=1,NX
      DO 160 IY=1,NY
      BE(IX,IY)=0
160   CONTINUE
107   CONTINUE
      UMIN=XUMIN(IGROUP)
      UMAX=XUMAX(IGROUP)
      VMIN=XVMIN(IGROUP)
      VMAX=XVMAX(IGROUP)
      PRINT 132,IGROUP
132   FORMAT(33H NEXT DATA GROUP SEQUENCE NUMBER=,I4)
      PRINT 134,UMIN,UMAX,VMIN,VMAX
134   FORMAT(21H NEW DATA GROUP,UMIN=,E16.8,4X,5HUMAX=,E16.8,4X,
     $5HVMIN=,E16.8,4X,5HVMAX=,E16.8)
      PRINT 135,(TU(IGROUP,L),NU(IGROUP,L),L=1,IIU)
      PRINT 161,(TV(IGROUP,LL),NV(IGROUP,LL),LL=1,IIV)
135   FORMAT(4H TU=,E16.8,5X,3HNU=,I4,28H NUMBER OF TIMES FOR THIS TU)
161   FORMAT(4H TV=,E16.8,5X,3HNV=,I4,28H NUMBER OF TIMES FOR THIS TV)
```

```
      PRINT 120
      PRINT 8...
303   FORMAT(2X,47H(* = SPECIFICATION OF THE AVERAGING INTERVAL,
     $  /*****,1 X,47H=*AVERAGE VALUE IN THIS INTERVAL*****)
      PRINT 301
301   FORMAT(6X,2HUN,13X,2HUC,13X,2HVM,13X,2HTV,15X,
     $ 13HVREAL AVERAGE,5X,13HVIMAG AVERAGE,/)
      UCHK=UMIN
      VCHK=VMIN
      DO 111 I1=1,IIU
      UCHK=UCHK+(TU(IGROUP,I1)*NU(IGROUP,I1))
111   CONTINUE
      DO 165 I2=1,IIV
      VCHK=VCHK+(TV(IGROUP,I2)*NV(IGROUP,I2))
165   CONTINUE
      CHK1=ABS(UMAX-UCHK)
      IF(CHK1.LT..1)GO TO 113
      PRINT 114,IGROUP
114   FORMAT(47H TU INTERVALS NOT COMMENSURATE WITH U RANGE,SET,I4)
      GO TO 115
113   CHK2=ABS(VMAX-VCHK)
      IF(CHK2.LT..1)GO TO 167
      PRINT 168,IGROUP
168   FORMAT(47H TV INTERVALS NOT COMMENSURATE WITH V RANGE,SET,I4)
      GO TO 115
167   UN=UMIN
      VM=VMIN
      UMID=UMIN+(DELTA/2.)
      UUMID=UMID
      VMID=VMIN+(DELTA/2.)
      VVMID=VMID
      LINC1=1
      LINC10=1
      DO 115 INC1=1,IIU
      TTU=TU(IGROUP,INC1)
      NU=TTU/DELTA+.1
      NSETU=NU(IGROUP,INC1)
      DO 116 INC2=1,NSETU
      UN=UN+(TTU/2.)
      DO 215 INC10=1,IIV
      TTV=TV(IGROUP,INC10)
      NV=TTV/DELTA+.1
      NSETV=NV(IGROUP,INC10)
      DO 216 INC20=1,NSETV
      VM=VM+(TTV/2.)
      IF(INC10.NE.1)GO TO 165
      IF(INC20.NE.1)GO TO 165
      SUMVR=0
      SUMVI=0
      VM=0.
      VVVMID=VVMID
      VMID=VMID-TTV
      VVMID=VMID
      NV2=NV*2
      DO 217 INCRV=1,NV2
      SUMVR=SUMVR+(D2*VREAL(UMID,VMID))
      SUMVI=SUMVI+(D2*VIMAG(UMID,VMID))
```

CHECKS THAT ALL INTERVALS ARE COMMENSURATE W/ ASSOCIATED TRUNCATION LIMITS

START OF CALCULATIONS TO DETERMINE $[\bar{V}]_{n,m}$ AND $\hat{B}_S(x,y)$

```
LEVEL  21                    MAIN          186  DATE = 8.313          79/09/21

      VMID=VMID+DELTA
1170  CONTINUE
      VMID=VVMID
      UMID=UMID+DELTA
1180  CONTINUE
      AVGVR=SUMVR/(TTU*2.*TTV)
      AVGVI=SUMVI/(TTU*2.*TTV)
      VVMID=VVVMID
      GO TO 188
185   SUMVR=0
      SUMVI=0
      DO 117 INCRU=1,NU
      DO 217 INCRV=1,NV
      SUMVR=SUMVR+(B2*VR=AL(UMID,VMID))
     1SUMVI=SUMVI+(B2*VIMAG(UMID,VMID))
      VMID=VMID+DELTA
217   CONTINUE
      VVMID=VVMID
      JMID=JMID+DELTA
117   CONTINUE
      AVGVR=SUMVR/(TTU*TTV)
      AVGVI=SUMVI/(TTU*TTV)
C LINC1 GOES 1 TO NUMAX
C LINC2 GOES 1 TO NVMAX
188   VRLAVG(LINC1,LINC2)=AVGVR
      VIMAVG(LINC1,LINC2)=AVGVI
      PRINT 802,UN,TTU,VM,TTV,AVGVR,AVGVI
802   FORMAT(2X,F10.6,5X,F10.6,5X,F10.6,5X,F10.6,10X,E16.8,5X,E16.8)
      WRITE(7,803) UN,TTU,VM,TTV,AVGVR,AVGVI
803   FORMAT(6(F12.8))
      X=XMIN
      DO 119 IX=1,NX                                   FORMS B_S(X,Y)
      Y=YMIN                                           BY SUMMATION
      DO 219 IY=1,NY                                   EACH AVERAGING
      FACCOS=COS((2.*PI)*((UN*X)+(VM*Y)))              CELL'S CENTRAL
      FACSIN=SIN((2.*PI)*((UN*X)+(VM*Y)))              BRIGHTNESS
      B3(IX,IY)=(2.*TTU*TTV*((AVGVR*FACCOS)+(AVGVI*FACSIN)))+B3(IX,IY)
      Y=Y+.25
219   CONTINUE                                         BB ⟶ B̂S
      X=X+.25
119   CONTINUE
      VVM(LINC1)=VM
      LINC1=LINC1+1
      IF(LINC1.NE.1)GO TO 187
      IF(LINC2.NE.1)GO TO 187
      VM=VM+TTV
      GO TO 186
187   VM=VM+(TTV/2.)
186   VMID=VVMID+TTV
      VVMID=VMID
      UMID=UUMID
216   CONTINUE
      UMID=UMID+(DELTA/2.)
      VVMID=VMID
      JMID=UUMID+TTU
      UUMID=JMID
```

```
      UUN(LINC1)=UN
      LINC1=LINC1+1
      UN=UN+(TTU/2.)
      LINC1=1
      VN=VMIN
116   CONTINUE
115   CONTINUE
C     OUTPUT ---------- PRINTS AND PUNCHES CARDS
      WRITE(7,146)                    GIVING THE VALUES OF
146   FORMAT(3H422222**********2222**********22222)   B_S(X,Y) AT THE
     1  PRINT 128                     POINTS IN THE
      X=XMIN                          X-Y PLANE WHERE
      DO 125 IX=1,NX                  B_S HAS CHANGED SIGN
      Y=YMIN
    1 DO 126 IY=1,NY
      PRINT 127,X,Y,BB(IX,IY)
127   FORMAT(5H B(X=,F5.2,3H,Y=,F5.2,2H)=,E16.8)
      WRITE(7,129) X,Y,BB(IX,IY)
129   FORMAT(3(E16.8))
      Y=Y+.25
126   CONTINUE
      X=X+.25
125   CONTINUE
      PRINT 128
      PRINT 128
      PRINT 128
      PRINT 128
C
C
C     THE FOLLOWING SECTIONS APPLY THE VARIOUS TESTS
C     TO B̂_S(X,Y) WHICH ARE DISCUSSED IN CHAPTER 3 OF
C     THIS THESIS
      PRINT 128
      PRINT 128
      PRINT 128
      PRINT 128
C DETERMINATION OF PEAKS
C WE USE THE HARWELL LIBRARY ROUTINE VA06A — SEE REFERENCES
      PRINT 128
      PRINT 128
     1  N=
      XX(1)=-1.
      XX(2)=.
      STEP=.05
     1  ACC=.1
      MAXFUN=1.00
      IPRINT=-1
      CALL VA06A(N,XX,F,G,STEP,ACC,MAXFUN,IPRINT,W)
      XCM1=XX(1)
      YCM1=XX(2)
      PKMAX=(-1.)*F
      PRINT 120,XCM1,YCM1,PKMAX
120   FORMAT(25H PEAK IN COMPONENT 1 AT (,E15.8,1H,,E15.
     1  8,11H) OF SIZE=, 1P,E15.8)
      XX(1)=1
      XX(2)=2
      CALL VA06A(N,XX,F,G,STEP,ACC,MAXFUN,IPRINT,W)
```

```
      XCM2=XX(1)
      YCM2=XX(2)
      BBMAX=(-1.)**I
      PRINT 1201,XCM2,YCM2,BBMAX
1201  FORMAT(25H PEAK IN COMPONENT 2 AT(,E16.8,1H,,E16.8,
     $ 21H) AND PEAK MAGNITUDE=,E16.8)
C
C
C
C VECTOR FROM PEAK 1 TO PEAK 2
      PRINT 128
      PRINT 1500
1500  FORMAT(36H VECTOR FROM LEFT PEAK TO RIGHT PEAK)
      DIST=SQRT((XCM2-XCM1)**2+(YCM2-YCM1)**2)
      THETA=ATAN((YCM2-YCM1)/(XCM2-XCM1))
      PRINT 1501,DIST,THETA
1501  FORMAT(42H VECTOR MAGNITUDE FOR SEPARATION OF PEAKS=,E16.8,10X,
     $ 24HVECTOR ANGLE WRT X AXIS=,F7.2)
      PRINT 128
      PRINT 128
C
C
C
C
C
C
C
C
C
C HALF WIDTH DETERMINATIONS
      BCKB=1
      HINC=.1
      B1HALF=.5*BB1MAX
      B2HALF=.5*BB2MAX
C
C
C
C
C
C
      PRINT 128
      PRINT 128
      YH1TRU=SQRT((ALOG(2.))/(AAAA*PI))
      YH2TRU=SQRT((ALOG(2.))/(AAAA*PI))
      XX(1)=XCM1
      XX(2)=YH1TRU
1805  CALL CALCBB(N,XX,BHALF,B)
      BCK1=((-1.)*BHALF)-B1HALF
      ABCK1=ABS(BCK1)
      IF(ABCK1.LT.1.) GO TO 1802
      IF(BCK1.GT.0)GO TO 1801
      IF(BCK3)1802,1802,1804
1802  XX(2)=(X(2)-HINC
```

AD-A093 792 ARMY MILITARY PERSONNEL CENTER ALEXANDRIA VA F/G 17/9
FOURIER TRANSFORMATION THEORY FOR AVERAGED FUNCTIONS, WITH APPL--ETC(U)
FEB 81 R J BONOMETTI

UNCLASSIFIED NL

END
DATE FILMED
2 81
DTIC

```
      BCKB=-1.
      GO TO 1815
1814  HINC=HINC/2.
      XX(2)=XX(2)-HINC
      BCKB=-1.
      GO TO 1815
1811  IF(BCKB)1816,1816,1818
1816  XX(2)=XX(2)+HINC
      BCKB=1.
      GO TO 1815
1818  HINC=HINC/2.
      XX(2)=XX(2)+HINC
      BCKB=1.
      GO TO 1815
1813  HINC=HINC/2.
      XX(2)=XX(2)+HINC
      BCKB=1.
      GO TO 1815
1809  Y1MID=XX(2)-YCM1
      PRINT 1809,Y1MID
1809  FORMAT(24H COMPONENT 1 HALF WIDTH=,E16.8)
      XX(1)=XCM2
      XX(2)=YM2TRU
      BCKB=1.
      HINC=.1
1815  CALL CALCBB(2,XX,BHALF,G)
      BCK2=((-1.)*BHALF)-B2HALF
      ABCK2=ABS(BCK2)
      IF(ABCK2.LT..010)GO TO 1820
      IF(BCK2.GT.0)GO TO 1811
      IF(BCK3)1812,1812,1814
1812  XX(2)=XX(2)-HINC
      BCKB=-1.
      GO TO 1815
1820  Y2MID=XX(2)-YCM2
      PRINT 1821,Y2MID
1821  FORMAT(24H COMPONENT 2 HALF WIDTH=,E16.8)
      PRINT 128
      PRINT 128
      PRINT 128
      PRINT 128
```

```
C COMPARISON WITH EXACT B(X,Y)
      WRITE (7,147)
147   FORMAT(35H33333**********33333**********33333)
      PRINT 128
      PRINT 128
      BDIFF=
      BSQDIF=
      XLINCR=.2
      YLINCR=.2
      SMAREA=.04
      DO 711 I=1,41
      XX(1)=((-1.)*XL)+((I-1)*XLINCR)
      DO 711 J=1,41
      XX(2)=((-1.)*YL)+((J-1)*YLINCR)
      CALL CALCBB(N,XX,BBAR,0)
      X=XX(1)
      Y=XX(2)
C NOTE BBAR IS NEGATIVE BBAR REALLY ON RETURNFROM CALCBB,SO *ADD* TO
C B(X,Y),NOT SUBTRACT
      BDIFF=BDIFF+((B(X,Y)+BBAR)*SMAREA)
      BSQDIF=BSQDIF+(((B(X,Y)+BBAR)**2)*SMAREA)
      WRITE(7,714) X,Y,BDIFF,BSQDIF
714   FORMAT(2(F4.1),2(E16.8))
711   CONTINUE
71    CONTINUE
      PRINT 712,BDIFF
712   FORMAT(41H THE TOTAL DEVIATION OF BHAT FROM BEXACT=,E16.8)
      BDNORM=BDIFF/64.
      PRINT 720,BDNORM
720   FORMAT(38X,11HNORMALIZED=,E16.8)
      PRINT 713,BSQDIF
713   FORMAT(49H THE TOTAL SQUARED DEVIATION OF BHAT FROM BEXACT=,E16.8)
      BSNORM=BSQDIF/64.
      PRINT 721,BSNORM
721   FORMAT(38X,11HNORMALIZED=,E16.8)
      PRINT 128
      PRINT 128
C
C
C
C
C
C
C
C
C
C
C COMPARISON WITH BTRID(X,Y)
      WRITE(7,7147)
7147  FORMAT(35H44444**********44444**********44444)
      PRINT 128
      PRINT 128
      PRINT 128
      BDIFF=
      BSQDIF=
      XLINCR=.25
      YLINCR=.25
      SMAREA=(.25)**2
```

```
      DO 7710 I=1,11
      XX(1)=(I-1)*XLINCR
      DO 7711 J=1,11
      XX(2)=(J-1)*YLINCR
      CALL CALCBB(N,XX,BBAR,G)
      X=XX(1)
      Y=XX(2)
C NOTE BBAR IS NEGATIVE BBAR REALLY ON RETURNFROM CALC33,SO *ADD* TO
C B(X,Y), NOT SUBTRACT
      BTDIFF=BTDIFF+((BTWID(I,J)+BBAR)*SMAREA)
     *BTSQDF=BTSQDF+(((BTWID(I,J)+BBAR)**2)*SMAREA)
      WRITE(7,7714) X,Y,BTDIFF,BTSQDF
7714  FORMAT(2(F4.1),2(E16.8))
7711  CONTINUE
7710  CONTINUE
      PRINT 715,BTDIFF
715   FORMAT(43H THE TOTAL DEVIATION OF BHAT FROM BTWID=,E16.8)
      BTDNRM=BTDIFF/(2.5**2)
      PRINT 722,BTDNRM
722   FORMAT(20X,11HNORMALIZED=,E16.8)
      PRINT 716,BTSQDF
716   FORMAT(48H THE TOTAL SQUARED DEVIATION OF BHAT FROM BTWID=,E16.8)
      BTSNRM=BTSQDF/(2.5**2)
      PRINT 723,BTSNRM
723   FORMAT(37X,11HNORMALIZED=,E16.8)
      PRINT 128
      PRINT 128
C
C
C
C
C
C
C CHECK FOR SYMMETRY ABOUT Y AXIS,IE,ARE SOURCES MIRROR IMAGES OF EACH
C OTHER
      ISYM1=0
      DO 1000 IX=1,31
      XX(1)=(IX-1)/10.
      DO 1001 IY=1,31
      XX(2)=(IY-1)/10.
C BHAT1 AND BHAT2 ARE NEGATIVES OF THEIR RESPECTIVE BBARS
C BUT ONLY THEIR DIFFERENCE IS IMPORTANT HERE
      XX(1)=XX(1)*(-1.)
      CALL CALCBB(N,XX,BHAT2,G)
     *ABDIFF=ABS(BHAT1-BHAT2)
      IF(ABDIFF.LT..001)GO TO 1008
      ISYM1=ISYM1+1
1008  IF(XX(2))1010,1010,1011
1010  XX(2)=XX(2)*(-1.)
      GO TO 1011
1001  CONTINUE
1000  CONTINUE
      PRINT 1006
1006  FORMAT(40H SYMMETRY CHECK,REFLECTION SYMMETRY ABOUT Y AXIS)
      IF(ISYM1.LE.10)GO TO 1004
      PRINT 1005,ISYM1
1005  FORMAT(52H ASYMMETRY WAS FOUND BETWEEN THE 2 SOURCE COMPONENTS,
```

```
     & 7H ISYM1=,I4,//////)
      GO TO 1019
1014  PRINT 1017
1017  FORMAT(50H NO SIGNIFICANT ASYMMETRY WAS FOUND BETWEEN THE 2 ,
     & 17HSOURCE COMPONENTS,//////)
1019  DUMMY=1.
C
C
C
C
C
C
C
C
C
C
C
C
C
C
C
      PRINT 128
      PRINT 128
C CHECK REFLECTION SYMMETRY FOR EACH SOURCE THRU THE COMMON AXIS
      ISYM2=0
      DO 1020 IY=1,31
      XX(2)=(IY-1)/10.
      DO 1021 IX=1,31
      XX(1)=(IX-1)/10.
1031  CALL CALCBB(N,XX,BHAT1,G)
      XX(2)=(-1.)*XX(2)
      CALL CALCBB(N,XX,BHAT2,G)
      ABDIFF=ABS(BHAT1-BHAT2)
      IF(ABDIFF.LT..001)GO TO 1028
      ISYM2=ISYM2+1
1028  IF(XX(1))1030,1021,1021
1030  XX(1)=XX(1)*(-1.)
      GO TO 1031
1021  CONTINUE
1020  CONTINUE
      PRINT 1026
1026  [illegible] REFLECTION SYMMETRY THRU X AXIS)
      IF(ISYM2.[illegible] TO 1[illegible]
      PRINT 1025,ISYM2
1025  FORMAT(27H ASYMMETRY WAS FOUND,ISYM2=,I4,//////)
      GO TO 1029
1024  PRINT 1027
1027  FORMAT(35H NO SIGNIFICANT ASYMMETRY WAS FOUND,//////)
1029  DUMMY=1.
      PRINT 128
      PRINT 128
C
C
C
C
C
C
C
C
110   CONTINUE
```

```
C
      PRINT 1032
 1032 FORMAT(13H PROGRAM STOP)
C
      END
```

```
      SUBROUTINE CALCFG(N,X,F,G)
      COMMON VREAVG(25,25),VIMAVG(25,25),TTUU(25),TTVV(25),UUN(25),
     & VVM(25),NUMAX,NVMAX
      DIMENSION G(2),X(2)
      N=2
      PI=3.1416
      TPI=2.*PI
C F IS -OBJ(X,Y)
      F=0.
      G(1)=0.
      G(2)=0.
      DO 101 I=1,NUMAX
      DO 101 J=1,NVMAX
C     PRINT 302,UUN(I),TTUU(I),VVM(J),TTVV(J),VREAVG(I,J),VIMAVG(I,J)
302   FORMAT(2X,F10.6,5X,F10.6,5X,F10.6,5X,F10.6,10X,E16.8,5X,E16.8)
      FAC=2.*TTUU(I)*TTVV(J)
      ARG=((UUN(I)*X(1))+(VVM(J)*X(2)))*TPI
      F=F-(FAC*((VREAVG(I,J)*(COS(ARG)))+(VIMAVG(I,J)*(SIN(ARG)))))
      G(1)=G(1)+((TPI*FAC*UUN(I))*((VREAVG(I,J)*(SIN(ARG)))-
     & (VIMAVG(I,J)*(COS(ARG)))))
      G(2)=G(2)+((TPI*FAC*VVM(J))*((VREAVG(I,J)*(SIN(ARG)))-
     & (VIMAVG(I,J)*(COS(ARG)))))
101   CONTINUE
100   CONTINUE
      RETURN
      END
```

```
LEVEL  21                    CALC*3      195   DATE = 80313          07/43/ 1

      SUBROUTINE CALC*3(N,X,F,G)
      COMMON VREAVG(25,25),VIMAVG(25,25),TTUU(25),TTVV(25),UUN(25),
     & VVN(25),NUMAX,NVMAX
      DIMENSION G(2),X(2)
      N=2
      PI=3.1416
      TPI=2.*PI
      F=0.
      G(1)=0.
      G(2)=0.
      DO 101 I=1,NUMAX
      DO 101 J=1,NVMAX
C     PRINT 802,UUN(I),TTUU(I),VVN(J),TTVV(J),VREAVG(I,J),VIMAVG(I,J)
802   FORMAT(2X,F10.6,5X,F10.6,5X,F10.6,5X,F10.6,10X,E16.8,5X,E16.8)
      FAC=2.*TTUU(I)*TTVV(J)
      ARG=((UUN(I)*X(1))+(VVN(J)*X(2)))*TPI
      F=F-(FAC*((VREAVG(I,J)*(COS(ARG)))-(VIMAVG(I,J)*(SIN(ARG)))))
101   CONTINUE
103   CONTINUE
      RETURN
      END
```

APPENDIX C

Program B

```
      DIMENSION L(07),M(07)
      DIMENSION Z(07,07)
      DIMENSION ZZ(07,07),ZZZ(07,07)
      DIMENSION VR1(30),VI1(30)
      DIMENSION CR(30),CI(30)
      DIMENSION TDATA(30),T(30)
      DIMENSION A(30)
      DIMENSION VR(25),VI(25),VBR(25),VBI(25)
      DIMENSION BR(100),BI(100)
      DIMENSION TUSET(30)
    1 VREAL(U)=(2./W)*(COS(2.*PI*U))*EXP(((-1.)*PI/W)*(U**2))
      VIMAG(U)=0*U
C
C
    1 W=10.
      N=7
      PI=3.1416
      POWCK=10.**70
      READ 1,XL,UMIN,DELTAU
1     FORMAT(3(E16.8))
      PRINT 8,XL,UMIN,DELTAU
8     FORMAT(4H LX=,E16.8,5X,5HUMIN=,E16.8,5X,7HDELTAU=,E16.8)
      READ 2,(TDATA(J),J=1,N)
2     FORMAT(E16.8)
      PRINT 9,(J,TDATA(J), J=1,N)
9     FORMAT(3H T(,I2,2H)=,E16.8)
      PRINT 6
6     FORMAT(////////////)
      PRINT 85
85    FORMAT(20X,14HAVERAGE VALUES,/)
C     THE 'Z MATRIX' IS THE INTEGRATION 'I MATRIX'
      UONE=UMIN
      UTWO=UONE+DELTAU
      DO 3 J=1,N
      T(J)=TDATA(J)
      TUSET(J)=T(J)
      SUMVR=0
      SUMVI=0
      MN=T(J)/DELTAU+.1
      DO 4 INCRU=1,MN
      IF (UONE)1111,1112,1111
1112  UONE=.000001
1111  IF(UTWO)1113,1114,1113
1114  UTWO=.000001
1113  SUMVR=SUMVR+(((VREAL(UTWO)+VREAL(UONE))/2.)*DELTAU)
      SUMVI=SUMVI+(((VIMAG(UTWO)+VIMAG(UONE))/2.)*DELTAU)
      UONE=UONE+DELTAU
      UTWO=UTWO+DELTAU
4     CONTINUE
      VR1(J)=SUMVR/T(J)
      VI1(J)=SUMVI/T(J)
      PRINT 180,J,VR1(J),J,VI1(J)
180   FORMAT(4H VR(,I2,2H)=,E16.8,15X,3HVI(,I2,2H)=,E16.8)
3     CONTINUE
      PRINT 5
      TNI=1./(2.*XL)
      RCHK=((-1.*UMIN)/TNI)+.5
      NCHK=RCHK
```

CALCULATES AVERAGE VALUES OF V(u) IN EACH

EVALUATE NYQUIST INTERVAL

```
LEVEL  21                    MAIN          198  DATE = 80325          13/27/46

      CHK=RCHK-NCHK                                  CHECK IF DOMAIN EXTENSION IS NECESSARY
      IF(CHK.LE..005)GO TO 851
C     RANGE EXTENSION                                DOMAIN EXTENSION IS REQUIRED
      NITOT=(((-2.*UMIN)/TNI)+1.)+.995
      NMAX=NITOT
      PRINT 853,NITOT
853   FORMAT(7H NITOT=,I4)
      D=.5*((NITOT*TNI)+(2.*UMIN))
      UMINEW=UMIN-D
      PRINT 891,UMINEW
891   FORMAT(8H UMINEW=,E16.8,/////)
      UMIN=UMINEW
C     DATA SET MODIFICATION BY EXTENSION
      NPLUS1=N+1
      DO 890 I1=2,NPLUS1
      I1MIN1=I1-1
      VR(I1)=VR1(I1MIN1)
      VI(I1)=VI1(I1MIN1)
      T(I1)=TDATA(I1MIN1)
      TUSET(I1)=T(I1)
890   CONTINUE
      VR(1)=0
      VI(1)=0
      NPLUS2=NPLUS1+1
      VR(NPLUS2)=0
      VI(NPLUS2)=0
      T(1)=D
      TUSET(1)=T(1)
      T(NPLUS2)=D
      TUSET(NPLUS2)=D
      GO TO 850
851   D=0                                            DOMAIN EXTENSION WAS NOT REQUIRED
      NITOT=(((-2.)*UMIN)/TNI)+.995
      NMAX=NITOT
      PRINT 853,NITOT
      NPLUS2=N
      DO 852 IL=1,N
      VR(IL)=VR1(IL)
      VI(IL)=VI1(IL)
852   CONTINUE
850   NCT=1
      NST=1
      TSUM=0
      DO 600 NTNI=1,NITOT                            START OF REFORMULATION SECTION
      PRINT 951,TBIT,TSUM                            TO PUT AVG. VALUES OF V(u)
951   FORMAT(6H TBIT=,E16.8,8H   TSUM=,E16.8)        AND Z MATRIX IN TERMS
      UU=TNI                                         OF NYQUIST INTERVALS
602   IF(T(NCT).GE.UU)GO TO 601
      A(NCT)=T(NCT)/TNI
      UU=UU-T(NCT)
      PRINT 954,UU,A(NCT),T(NCT),NCT
954   FORMAT(4H UU=,E16.8,9H  A(NCT)=,E16.8,8H T(NCT)=,E16.8,4HNCT=,I4)
      IF(NCT.GE.NPLUS2)GO TO 605
      NCT=NCT+1
      GO TO 602
601   A(NCT)=UU/TNI
      PRINT 954,UU,A(NCT),T(NCT),NCT
605   NSTOP=NCT
```

```
LEVEL  21                    MAIN              199 DATE = 80325          13/27/46

      VBR(NTNI)=0
      VBI(NTNI)=0
      DO 670 N2INIT=1,NITOT
      Z(NTNI,N2INIT)=0
670   CONTINUE
      PRINT 952,NST,NSTOP
952   FORMAT(18H ENTERING 701 LOOP,6H  NST=,I4,8H  NSTOP=,I4)
      DO 701 NJ=NST,NSTOP
      VBR(NTNI)=VR(NJ)*A(NJ)+VBR(NTNI)
      VBI(NTNI)=VI(NJ)*A(NJ)+VBI(NTNI)
11    N2=1
      NN=(1-NITOT)/2
      NNCHK=NST-NJ
730   UN1=UMIN+TSUM+(TUSET(NJ)/2.)
      PIT=PI*TUSET(NJ)
21    A1=((2.*PI)*((NN/(2.*XL))-UN1))
      ALFA=PIT+A1
      BETA=PIT-A1
      AL=XL*ALFA
      BL=XL*BETA
      SIGN=1.
      SM=AL+BL
      NODD=3
C
C
      POW12=0
5     IF(POW12.LE.POWCK)GO TO 50
      POWAL=1.
      POWBL=1.
      DO 799 INCNT=1,NODD
      POWAL=POWAL*(AL/INCNT)
      POWBL=POWBL*(BL/INCNT)
799   CONTINUE
      POWER=(POWAL+POWBL)/NODD
      GO TO 25
50    POWER=(((AL)**NODD)+((BL)**NODD))/NODD
      POW12=POWER
      SIGNCK=1.
      IF(NODD.LT.54)GO TO 22
      IF(POWER)23,23,24
23    SIGNCK=-1.
      POWER=POWER*(-1.)
24    POWRLN=ALOG(POWER)
      DO 651 LNFACT=2,NODD
      XLNFAC=LNFACT
      POWRLN=POWRLN-(ALOG(XLNFAC))
651   CONTINUE
      POWER=EXP(POWRLN)*SIGNCK
      GO TO 25
22    DO 650 IFACT=2,NODD
      POWER=POWER/IFACT
650   CONTINUE
C
C
25    SIGN=SIGN*(-1.)
      SMINCR=SIGN*POWER
      SM=SM+SMINCR
      AINCR=ABS(SMINCR)
```

VBR IS AVG. VALUE OF V(t) IN A N/QUIST INTERVAL, REAL PART

VBI GIVES THE IMAG. PART

= Z MATRIX

CALCULATE $\sum_{r=0}^{R} \frac{(-1)^r}{(2r+1)(2r+1)!}\left[(\alpha L_x)^{2r+1} + (-L_x)^{2r+1}\right]$

WHERE THE MAGNITUDE OF THE R^{TH} TERM IS LESS THAN .001

```
LEVEL  21                    MAIN          200 DATE = 80325          13/27/46

      IF(AINCR.LE..001)GO TO 7
      NODD=NODD+2
      GO TO 5
7     Z(NTNI,N2)=(SM/PIT)*A(NJ)+Z(NTNI,N2)
      ZZ(NTNI,N2)=Z(NTNI,N2)
      IF(N2.EQ.NITOT)GO TO 60
      N2=N2+1
      NN=NN+1
      GO TO 21
60    TSUM=TSUM+TUSET(NJ)
700   CONTINUE
702   PRINT 80,(NTNI,JN2,Z(NTNI,JN2), JN2=1,NITOT)
80    FORMAT(3H I(,I2,1H,,I2,2H)=,E16.8)
      RRCHK=T(NSTOP)-UU
      IF(RRCHK.GT..001)GO TO 680
      NCT=NCT+1
      NST=NSTOP+1
      GO TO 600
680   TSUM=TSUM-TUSET(NJ)
      T(NSTOP)=T(NSTOP)-UU
      NST=NSTOP
C     NOTE THAT NCT REMAINS THE SAME HERE SINCE THE CURRENT
C     T OLD INTERVAL STRADDLES THE NEW TNI INTERVAL
600   CONTINUE
      PRINT 6
      PRINT 610,(J,VBR(J),J,VBI(J), J=1,NMAX)
610   FORMAT(5H VBR(,I2,2H)=,E16.8,10X,4HVBI(,I2,2H)=,E16.8)
      PRINT 6
C     LINEAR SYSTEM SOLUTION FOLLOWS
777   PRINT 800
 800   FORMAT(24H LINEAR SOLUTION FOLLOWS,//)
70    CALL MINV(Z,NMAX,D,L,M)
      LLL=1
      CALL GMPRD(Z,VBR,CR,NMAX,NMAX,LLL)
      PRINT 90,(J,CR(J), J=1,NMAX)
90    FORMAT(4H CR(,I2,2H)=,E16.5)
      CALL GMPRD(Z,VBI,CI,NMAX,NMAX,LLL)
      PRINT 91,(J,CI(J), J=1,NMAX)
91    FORMAT(4H CI(,I2,2H)=,E16.8)
      PRINT 6
      PRINT 611,((J1,J2,Z(J1,J2), J1=1,NMAX), J2=1,NMAX)
611   FORMAT(3H Z(,I2,1H,,I2,2H)=,E16.8)
      CALL GMPRD(Z,ZZ,ZZZ,NMAX,NMAX,NMAX)
      PRINT 6
      PRINT 611,((J1,J2,ZZZ(J1,J2), J1=1,NMAX), J2=1,NMAX)
      PRINT 6
      PRINT 6
      NX=81
      PRINT 501,NX
501   FORMAT(23H NUMBER OF X INTERVALS=,I4)
      DO 502 NXX=1,NX
      BR(NXX)=0
      BI(NXX)=0
502   CONTINUE
      NXX=1
506   X=(-4.+(.1*(NXX-1)))
      DO 503 NNX=1,NMAX
      NINT=((1-NMAX)/2)+(NNX-1)
```

CALCULATES INVERSE MATRIX FOR Z

SOLVES FOR REAL AND IMAG PARTS OF EXPANSION COEFFICIENTS OF

MINV, GMPRD ARE FROM THE SCIENTIFIC SUBROUTINE PACKAGE FOR THE

CALCULATES VALUES OF B(X)

```
      XFAC1=COS((PI*NINT*X)/XL)
      XFAC2=SIN((PI*NINT*X)/XL)
      BR(NXX)=(CR(NNX)*XFAC1)-(CI(NNX)*XFAC2)+BR(NXX)
      BI(NXX)=(CI(NNX)*XFAC1)+(CR(NNX)*XFAC2)+BI(NXX)
503   CONTINUE
      BMAG=SQRT((BR(NXX)**2)+(BI(NXX)**2))
      PRINT 504,X,BR(NXX),X,BI(NXX),X,BMAG
504   FORMAT(4H BR(,F6.3,2H)=,E16.8,10X,3HBI(,F6.3,2H)=,E16.8,10X,
     & 5HBMAG(,F6.3,2H)=,E16.8)
      IF(NXX.GE.NX)GO TO 505
      NXX=NXX+1
      GO TO 506
505   PRINT 6
      STOP
      END
```

REFERENCES

1. Addleman, M., Differential VLBI Between the Quasar OJ 287 and *Viking Orbiter 1* (M.I.T.: Cambridge, MA, 1978), S.M. Thesis.

2. Bracewell, R. N., The Fourier Transform and Its Applications, McGraw-Hill Book Co., 1978.

3. Counselman, C. C., "Radio Astrometry", Annual Revue of Astronomy and Astrophysics (Annual Reviews, Inc.: Palo Alto, CA, 1976) V.14, pp.197-214.

4. Fomalont, E. B., "Earth-rotation Aperature Synthesis". Proceedings of the IEEE (IEEE: New York, 1973), V.61, No. 9, pp.1211-1218.

5. Gourevitch, S., Private communication regarding the tracks in the u-v plane for an interferometer incorporating elements on satellites.

6. Harwel Subroutine Library, United Kingdom Atomic Energy Authority Research Group Report AERE-R.7477, M. J. Hopper (ed.), 1973.

7. Herring, T., Private communication.

8. Hildebrand, F. B., Advanced Calculus for Applications, Prentice-Hall, Inc., 1976.

9. Kaplan, W., Advanced Calculus, Addison-Wesley Publishing Company, Inc., 1952.

10. Knight, C. A., Robertson, D. S., Rogers, A. E. E., Shapiro, I. I., Whitney, A. R., Clark, T. A., Goldstein, R. M., Marandino, G. E., and Vandenberg, N. R., "Quasars: millisecond-of-arc structure revealed by very-long-baseline interferometry", Science, (AAAS: Washington, D.C., 1971), 5172, pp.52-54.

11. Kraus, J. D., Radio Astronomy, McGraw-Hill Book Company, 1966.

12. Marsden, J. and Weinstein, A., Calculus, Benjamin/Cummings Publishing Company, Inc., 1980.

13. Moran, J. M., "Radio Observations of Galactic Masers", Frontiers of Astrophysics, E. H. Avrett (ed.) (Harvard University Press: Cambridge, MA, 1976), pp.385-437.

14. Rogers, A. E. E., "Theory of Two Element Interferometers", Methods of Experimental Physics, M. L. Meeks (ed.) (Academic Press: New York, 1976, V.12, Part C pp.138-157.

15. Shapiro, I. I., "Estimation of Astrometric and Geodetic Parameters", Methods of Experimental Physics, M. L. Meeks (ed.) Academic Press: New York, et al., 1976), V.12, Part C, pp.261-276.

16. Shapiro, I. I., and Knight, C. A., "Geophysical Applications of Long-Baseline Radio Interferometry", Earthquake Displacement Fields and the Rotation of the Earth, A. E. Beck, et al, (ed.) (D. Reidel Publishing Co.: Dordrecht, Holland. 1970), pp.284-301.

17. Swenson, G. W. and Mathur, N. C., "The Interferometer in Radio Astronomy", Proceedings of the I.E.E.E., (IEEE: New York, 1968), V.56, No.12, pp.2114-2129.

18. Thompson, A. and Bracewell, R.N., "Interpolation and Fourier Transformations of Fringe Visibilities", The Astronomical Journal (American Institute of Physics: New York, 1974), V.79, No.1, pp.11-25.

19. Treinish, L. A., Interpretation of differential very long baseline interferometric observations of quasars and spacecraft. (M.I.T.: Cambridge, MA, 1978), S.M. Thesis.

20. Whitney, A. R., Precision Geodesy and Astrometry via Very Long Baseline Interferometry (M.I.T.: Cambridge, MA, 1974) Ph.D. Thesis.

21. Wijwardhana, R., private communication suggesting index contraction in order to put the four index problem into a form amenable to standard matrix calculations.